

ROADMAP • OPEN ACCESS

## The 2022 magneto-optics roadmap

To cite this article: Alexey Kimel *et al* 2022 *J. Phys. D: Appl. Phys.* **55** 463003

View the [article online](#) for updates and enhancements.

You may also like

- [DIRECT NUMERICAL SIMULATION OF RADIATION PRESSURE-DRIVEN TURBULENCE AND WINDS IN STAR CLUSTERS AND GALACTIC DISKS](#)  
Mark R. Krumholz and Todd A. Thompson
- [Wearable multichannel haptic device for encoding proprioception in the upper limb](#)  
Patrick G Sagastegui Alva, Silvia Muceli, S Farokh Atashzar *et al.*
- [NEW YOUNG STAR CANDIDATES IN THE TAURUS–AURIGA REGION AS SELECTED FROM THE WIDE-FIELD INFRARED SURVEY EXPLORER](#)  
L. M. Rebull, X. P. Koenig, D. L. Padgett *et al.*



The Electrochemical Society  
Advancing solid state & electrochemical science & technology

### 242nd ECS Meeting

Oct 9 – 13, 2022 • Atlanta, GA, US

Presenting more than 2,400  
technical abstracts in 50 symposia



**ECS Plenary Lecture  
featuring  
M. Stanley Whittingham,**  
Binghamton University  
Nobel Laureate –  
2019 Nobel Prize in Chemistry



Register now!



## Roadmap

## The 2022 magneto-optics roadmap

Alexey Kimel<sup>1</sup> , Anatoly Zvezdin<sup>2</sup> , Sangeeta Sharma<sup>3</sup>, Samuel Shallcross<sup>3</sup>, Nuno de Sousa<sup>4</sup> , Antonio García-Martín<sup>5</sup> , Georgeta Salvan<sup>6</sup> , Jaroslav Hamrle<sup>7</sup> , Ondřej Stejskal<sup>7</sup> , Jeffrey McCord<sup>8</sup> , Silvia Tacchi<sup>9</sup> , Giovanni Carlotti<sup>10</sup>, Pietro Gambardella<sup>11</sup> , Gian Salis<sup>12</sup>, Markus Münzenberg<sup>13</sup> , Martin Schultze<sup>14</sup> , Vasily Temnov<sup>15</sup> , Igor V Bychkov<sup>16</sup>, Leonid N Kotov<sup>17</sup>, Nicolò Maccaferri<sup>18,19</sup> , Daria Ignatyeva<sup>20,21,22,†</sup> , Vladimir Belotelov<sup>20,21,22,†</sup> , Claire Donnelly<sup>23</sup> , Aurelio Hierro Rodriguez<sup>24,25</sup>, Iwao Matsuda<sup>26</sup>, Thierry Ruchon<sup>27</sup> , Mauro Fanciulli<sup>27,28</sup> , Maurizio Sacchi<sup>29,30</sup> , Chunhui Rita Du<sup>31,32</sup> , Hailong Wang<sup>32</sup> , N Peter Armitage<sup>33</sup>, Mathias Schubert<sup>34,35</sup>, Vanya Darakchieva<sup>35,36</sup>, Bilu Liu<sup>37</sup> , Ziyang Huang<sup>37</sup>, Baofu Ding<sup>37,38</sup>, Andreas Berger<sup>39,41,\*</sup>  and Paolo Vavassori<sup>39,40,41,\*</sup> 

<sup>1</sup> Institute for Molecules and Materials, Radboud University, Heyendaalseweg 135, Nijmegen 6525 AJ, The Netherlands

<sup>2</sup> Prokhorov General Physics Institute of the Russian Academy of Sciences, Moscow 119991, Russia

<sup>3</sup> Max-Born-Institut für Nichtlineare Optik und Kurzzeitspektroskopie, 12489 Berlin, Germany

<sup>4</sup> Donostia International Physics Center (DIPC), Donostia-San Sebastián 20018, Spain

<sup>5</sup> Instituto de Micro y Nanotecnología IMN-CNM, CSIC, CEI UAM+CSIC, Isaac Newton 8, E-28760 Tres Cantos, Madrid 28760, Spain

<sup>6</sup> Institute of Physics, Chemnitz University of Technology, Chemnitz 09107, Germany

<sup>7</sup> Institute of Physics, Charles University, Ke Karlovu 5, Prague 12116, Czech Republic

<sup>8</sup> Institute for Materials Science, Kiel University, Kaiserstraße 2, Kiel 24143, Germany

<sup>9</sup> Istituto Officina dei Materiali del CNR (CNR-IOM), Sede Secondaria di Perugia, c/o Dipartimento di Fisica e Geologia, Università di Perugia, I-06123 Perugia, Italy

<sup>10</sup> Dipartimento di Fisica e Geologia, Università di Perugia, I-06123 Perugia, Italy

<sup>11</sup> Department of Materials, ETH Zurich, Hönggerberggring 64, Zurich CH-8093, Switzerland

<sup>12</sup> IBM Research-Zurich, Säumerstrasse 4, Rüschlikon 8803, Switzerland

<sup>13</sup> Institute of Physics, University of Greifswald, Greifswald 17489, Germany

<sup>14</sup> Institute of Experimental Physics, Graz University of Technology, Petersgasse 16, Graz 8010, Austria

<sup>15</sup> LSI, Ecole Polytechnique, CEA/DRF/IRAMIS, CNRS, Institut Polytechnique de Paris, Palaiseau F-91128, France

<sup>16</sup> Department of Radio-Physics and Electronics, Chelyabinsk State University, Chelyabinsk 454001, Russia

<sup>17</sup> Syktyvkar State University, Syktyvkar 167000, Russia

<sup>18</sup> Department of Physics, Umeå University, Linnaeus väg 24, 901 87 Umeå, Sweden

<sup>19</sup> Department of Physics and Materials Science, University of Luxembourg, 162a avenue de la Faiencerie, 1511 Luxembourg, Luxembourg

<sup>20</sup> Russian Quantum Center, Moscow 121353, Russia

<sup>21</sup> V.I. Vernadsky Crimean Federal University, Simferopol 295007, Russia

<sup>22</sup> Faculty of Physics, Lomonosov Moscow State University, Moscow 119991, Russia

<sup>41</sup> Guest editors of the roadmap to whom any correspondence should be addressed.

\* Authors to whom any correspondence should be addressed.

† Publisher's note. Whilst IOP Publishing adheres to and respects UN resolutions regarding the designations of territories (available at [www.un.org/press/en/](http://www.un.org/press/en/)), the policy of IOP Publishing is to use the affiliations provided by its authors on its published articles.



Original content from this work may be used under the terms of the [Creative Commons Attribution 4.0 licence](https://creativecommons.org/licenses/by/4.0/). Any further distribution of this work must maintain attribution to the author(s) and the title of the work, journal citation and DOI.

- <sup>23</sup> Max Planck Institute for Chemical Physics of Solids, Noethnitzer Strasse 40, 01187 Dresden, Germany
- <sup>24</sup> Departamento de Física, Universidad de Oviedo, 33007 Oviedo, Spain
- <sup>25</sup> CINN (CSIC-Universidad de Oviedo), El Entrego, Spain
- <sup>26</sup> The Institute for Solid State Physics, The University of Tokyo, Kashiwa 277-8581, Japan
- <sup>27</sup> Université Paris-Saclay, CEA, CNRS, LIDYL, 91191 Gif-sur-Yvette, France
- <sup>28</sup> LPMS, CY Cergy Paris Université, Cergy-Pontoise, France
- <sup>29</sup> Sorbonne Université, CNRS, Institut des NanoSciences de Paris, INSP, Paris F-75005, France
- <sup>30</sup> Synchrotron SOLEIL, Saint-Aubin, B.P. 48, 91192 Gif-sur-Yvette, France
- <sup>31</sup> Department of Physics, University of California, San Diego, La Jolla, CA 92093, United States of America
- <sup>32</sup> Center for Memory and Recording Research, University of California, San Diego, La Jolla, CA 92093, United States of America
- <sup>33</sup> Department of Physics and Astronomy, The Johns Hopkins University, Baltimore, MD 21210, United States of America
- <sup>34</sup> Department of Electrical and Computer Engineering, University of Nebraska-Lincoln, Lincoln, NE 68588, United States of America
- <sup>35</sup> Department of Physics, Chemistry and Biology (IFM), Linköping University, Linköping SE-581 83, Sweden
- <sup>36</sup> NanoLund, Lund University, SE-221 00 Lund, Sweden
- <sup>37</sup> Shenzhen Geim Graphene Center, Tsinghua-Berkeley Shenzhen Institute and Institute of Materials Research, Tsinghua Shenzhen International Graduate School, Tsinghua University, Shenzhen 518055, People's Republic of China
- <sup>38</sup> Institute of Technology for Carbon Neutrality/Faculty of Materials Science and Engineering, Shenzhen Institute of Advanced Technology, CAS, Shenzhen 518055, People's Republic of China
- <sup>39</sup> CIC nanoGUNE BRTA, Tolosa Hiribidea 76, Donostia-San Sebastián, 20018, Spain
- <sup>40</sup> IKERBASQUE, Basque Foundation for Science, Plaza Euskadi 5, 48009 Bilbao, Spain

E-mail: [a.berger@nanogune.eu](mailto:a.berger@nanogune.eu) and [p.vavassori@nanogune.eu](mailto:p.vavassori@nanogune.eu)

Received 1 April 2022, revised 8 August 2022

Accepted for publication 30 August 2022

Published 28 September 2022

## Abstract

Magneto-optical (MO) effects, viz. magnetically induced changes in light intensity or polarization upon reflection from or transmission through a magnetic sample, were discovered over a century and a half ago. Initially they played a crucially relevant role in unveiling the fundamentals of electromagnetism and quantum mechanics. A more broad-based relevance and wide-spread use of MO methods, however, remained quite limited until the 1960s due to a lack of suitable, reliable and easy-to-operate light sources. The advent of Laser technology and the availability of other novel light sources led to an enormous expansion of MO measurement techniques and applications that continues to this day (see section 1). The here-assembled roadmap article is intended to provide a meaningful survey over many of the most relevant recent developments, advances, and emerging research directions in a rather condensed form, so that readers can easily access a significant overview about this very dynamic research field. While light source technology and other experimental developments were crucial in the establishment of today's magneto-optics, progress also relies on an ever-increasing theoretical understanding of MO effects from a quantum mechanical perspective (see section 2), as well as using electromagnetic theory and modelling approaches (see section 3) to enable quantitatively reliable predictions for ever more complex materials, metamaterials, and device geometries. The latest advances in established MO methodologies and especially the utilization of the MO Kerr effect (MOKE) are presented in sections 4 (MOKE spectroscopy), 5 (higher order MOKE effects), 6 (MOKE microscopy), 8 (high sensitivity MOKE), 9 (generalized MO ellipsometry), and 20 (Cotton–Mouton effect in two-dimensional materials). In addition, MO effects are now being investigated and utilized in spectral ranges, to which they originally seemed completely foreign, as those of synchrotron radiation x-rays (see section 14 on three-dimensional magnetic characterization and section 16 on light beams carrying orbital angular momentum) and, very recently, the terahertz (THz) regime (see section 18 on THz MOKE and section 19 on THz

ellipsometry for electron paramagnetic resonance detection). Magneto-optics also demonstrates its strength in a unique way when combined with femtosecond laser pulses (see section 10 on ultrafast MOKE and section 15 on magneto-optics using x-ray free electron lasers), facilitating the very active field of time-resolved MO spectroscopy that enables investigations of phenomena like spin relaxation of non-equilibrium photoexcited carriers, transient modifications of ferromagnetic order, and photo-induced dynamic phase transitions, to name a few. Recent progress in nanoscience and nanotechnology, which is intimately linked to the achieved impressive ability to reliably fabricate materials and functional structures at the nanoscale, now enables the exploitation of strongly enhanced MO effects induced by light–matter interaction at the nanoscale (see section 12 on magnetoplasmonics and section 13 on MO metasurfaces). MO effects are also at the very heart of powerful magnetic characterization techniques like Brillouin light scattering and time-resolved pump-probe measurements for the study of spin waves (see section 7), their interactions with acoustic waves (see section 11), and ultra-sensitive magnetic field sensing applications based on nitrogen-vacancy centres in diamond (see section 17). Despite our best attempt to represent the field of magneto-optics accurately and do justice to all its novel developments and its diversity, the research area is so extensive and active that there remains great latitude in deciding what to include in an article of this sort, which in turn means that some areas might not be adequately represented here. However, we feel that the 20 sections that form this 2022 magneto-optics roadmap article, each written by experts in the field and addressing a specific subject on only two pages, provide an accurate snapshot of where this research field stands today. Correspondingly, it should act as a valuable reference point and guideline for emerging research directions in modern magneto-optics, as well as illustrate the directions this research field might take in the foreseeable future.

**Keywords:** magneto-optics, magnetic characterization methods, magneto-optical effects, magnetic materials, modern experimental methods, theoretical description and modelling, magnetic microscopy

(Some figures may appear in colour only in the online journal)

---

## Contents

1. Introduction: perspective on recent advances in magneto-optics	5
2. Magneto-optics: quantum mechanical description and predictions	7
3. Magneto-optics: electromagnetic theory and modelling	9
4. Spectroscopic magneto-optical (MO) characterization	11
5. Higher order magneto-optics effect	13
6. Kerr microscopy	15
7. Probing magnons in the frequency domain: Brillouin light scattering (BLS)	17
8. MOKE measurements of spin and orbital currents in nonmagnetic semiconductors and metals	20
9. Generalized magneto-optical (MO) ellipsometry (GME)	23
10. Ultrafast magneto-optics	26
11. Ultrafast magneto-optics and magneto-acoustics with exchange magnons	29
12. Magnetoplasmonics	32
13. All-dielectric magneto-optical metasurfaces (ADMOMSs)	35
14. Characterization of 3D magnetic nanostructures	38
15. Magneto-optics with free electron lasers (FELs)	41
16. Magneto-optics with light beams carrying orbital angular momentum (OAM)	43
17. Probing spintronics systems using nitrogen-vacancy (NV) centres in diamond	46
18. Time-resolved THz polarimetry of quantum materials	48
19. THz electron paramagnetic resonance (EPR) magneto-optical (MO) generalized spectroscopic ellipsometry (GSE) for spin characterization in materials	50
20. Giant magneto-optical (MO) Cotton–Mouton (CM) effect in 2D materials	53
References	58

## 1. Introduction: perspective on recent advances in magneto-optics

Alexey V Kime<sup>1</sup> and Anatoly K Zvezdin<sup>2</sup>

<sup>1</sup> Institute for Molecules and Materials, Radboud University, Heyendaalseweg 135, Nijmegen 6525 AJ, The Netherlands

<sup>2</sup> Prokhorov General Physics Institute of the Russian Academy of Sciences, Moscow 119991, Russia

### Status

The discovery of M Faraday, who showed that linearly polarized light experiences polarization rotation upon propagation through a magnetized medium, prompted J C Maxwell to suggest electromagnetic origin of light and inspired P Zeeman to discover the splitting of spectral lines in an applied magnetic field. Hence in the 19th century, magneto-optics played a key role in both the development of electrodynamics and foundations of quantum mechanics.

The Faraday rotation emerges due to a difference in velocity of right and left-handed circularly polarized light propagating through a medium in the direction of its magnetization. This inequality implies different refraction coefficients for the light waves of opposite helicities and, according to the Kramers–Kronig relations, different absorptions of the waves known as magnetic circular dichroism (MCD). In quantum mechanics, the difference emerges due to the Zeeman splitting of quantum states of charged particles in external magnetic field. The splitting is proportional to the ratio  $q/m$ , where  $q$  is the charge and  $m$  is the mass of the particle. Hence, the magneto-optical (MO) effects are the most pronounced in the spectral ranges where light interacts with electrons, but much weaker if the optical properties are dominated by interaction of light with the lattice.

The development of experimental magneto-optics in the 20th century was inextricably linked with the development of light sources (see figure 1). The invention of laser played in this development the decisive role. For instance, laser sources allowed to boost the sensitivity of MO measurements (see section 8), explore MO phenomena beyond the approximation of linear optics and obtain conceptually new techniques to explore otherwise optically inaccessible magnetism at buried interfaces, antiferromagnetism and multiferroicity [1]. Synchrotrons are another important development that allow sufficiently intense and polarized x-ray radiation to perform MO measurements in the range of electronic transitions from 2p to 3d-shell (L-edge) and from 3d to 4f-shell (M-edges). As the shells are nearly not affected by crystal fields, x-ray MCD (XMCD) practically facilitates a probe of magnetism with elemental specificity, which is especially powerful in application to complex alloys and heterostructures [2]. Short wavelengths are another advantage of x-ray radiation that pave a direct path to MO imaging at the nanoscale.

## Current and future challenges

As the conventional theory of magneto-optics is based on the interaction of light with electronic resonances, MO properties of media are often assumed to be fully defined by their chemical composition. The recent development of patterning and nanofabrication changed this paradigm and revealed a possibility of many-fold enhancement of MO phenomena in photonic crystals and plasmonic structures which host photonic resonances [3, 4] (see sections 12 and 13). Aiming to achieve the largest possible enhancement of the MO phenomena stimulates the search for ways to increase the quality factor and decrease the losses of the artificially created photonic resonances.

The development of sources of terahertz (THz) light stimulated MO measurements in the range of low energy excitations in Dirac materials [5] and multiferroics (see sections 18 and 19). In magnetic semiconductors and metals, THz magneto-optics is a contactless and ultrafast probe of their magneto-transport properties [6].

State-of-the-art lasers can produce light flashes with duration well below 100 fs and an ultrashort laser pulse is practically the shortest stimulus in magnetism. Such pulses and pump-probe technique opens up the poorly understood field of ultrafast magnetism (see sections 10 and 11). The interest to the field is continuously fuelled by its potential to impact magnetic recording, spintronics and magnonics technologies as well as by counter-intuitive experimental observations. Magnetism is essentially a quantum mechanical phenomenon, but with the help of the so-called macrospin approximation magnets can be modelled as classical objects, which obey the laws of classical mechanics and thermodynamics. In strongly non-equilibrium states this approximation fails and description of magnetic phenomena becomes challenging (see section 2). Consequently, the development of the field of ultrafast non-equilibrium spin dynamics heavily depends on progress in experimental research. However, interpretation of MO transients in the strongly non-equilibrium state is a subject of hot debates [7].

Although one of the unique functionalities of lasers is to provide coherent radiation, this fact has been rarely employed in MO measurements. For instance, using coherence of light from a laser source and its diffraction on domain patterns in iron garnets, it is possible to observe domain wall displacements on distances much shorter than the wavelength of light [8]. Coherent nature of light from lasers is employed to generate beams with optical orbital angular momentum (OAM), which allow to observe such novel MO effects as magnetic helicoidal dichroism (section 16). Very recent breakthroughs in the development of intense sources of coherent polarized light in the extreme ultraviolet (XUV) and x-ray ranges has initiated the development of novel experimental techniques (see section 15). For instance, lensless imaging of magnetic nanostructures by x-ray spectro-holography has recently allowed observing picosecond nucleation of topologically protected



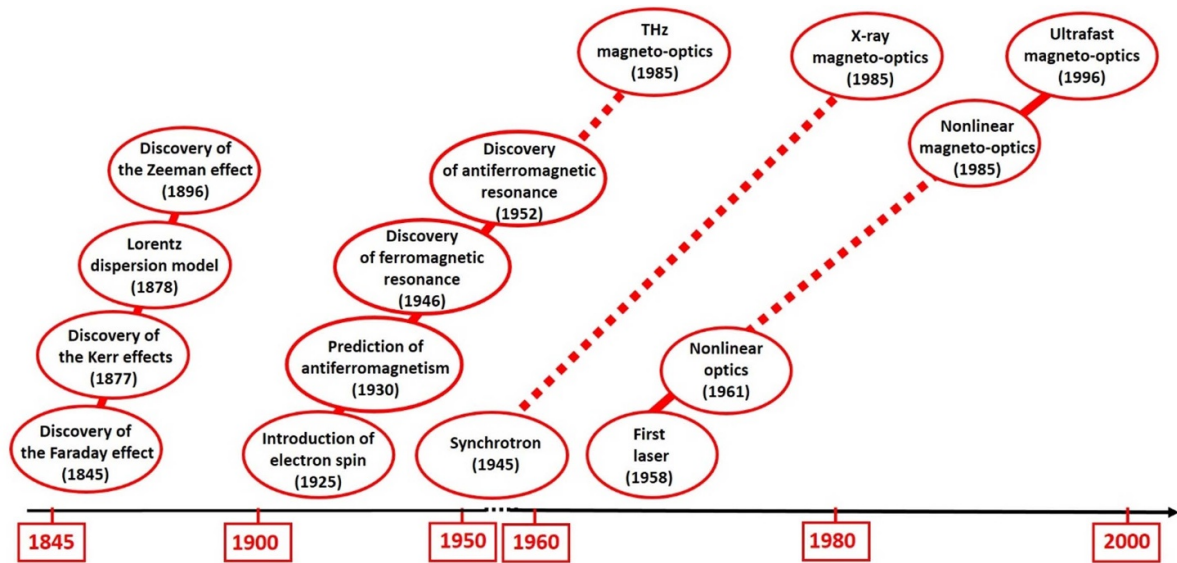


Figure 1. Roadmap of the key developments in magneto-optics in the past.

non-collinear spin textures [9]. Apart from large-scale facilities, recent progress on high-harmonic generation (HHG) in noble gases promises to provide sources of sub-fs coherent and tunable soft x-ray (SX) pulses for table-top MO measurements with unprecedented time and space resolution.

Further developments of microscopy technique, such as those based on the MO Kerr effects (MOKEs) (section 6), Brillouin light scattering (BLS) (section 7) and magnetic susceptibility of nitrogen vacancies (section 17), towards combination of the best possible spatial and temporal resolutions can eventually lead to ever faster and denser magnetic memory. Time-resolved ultrafast MO nanoscopes, such as the scanning near-field optical microscopes, operating at the length and time-scale of the exchange interaction, will inevitably enable a breakthrough in fundamental understanding of ultrafast magnetism.

### Advances in science and technology to meet challenges

In the past a lot of attention was paid to the problem of enhancement of light-spin coupling with the help of magneto-photonic and/or magneto-plasmonic structures, which practically play the role of optical cavity. Increasing the quality factor and decreasing the losses in these photonic and plasmonic structures has long been a task at the forefront of MO research. Recently, a conceptually new approach was proposed to enhance the coupling using all-dielectric magnetic metasurfaces, which exhibits much higher transparency (30% in resonance and 70% out of resonance) than plasmonic structures and superior quality-factor (section 13). Alternatively, the recently emerged field of cavitronics aims at the enhancement with the help of mechanical resonators [10]. It is believed that the efficient means of light-spin coupling will be beneficial for quantum technologies. Regarding the fact that the size

of the resonator is defined by the wavelength of light, it is anticipated that the first breakthroughs in single spin–single photon coupling are the easiest to achieve in the THz spectral range.

Further development of MO techniques in THz, XUV and x-ray spectral ranges will allow to improve the sensitivity of the measurements. In this way, THz, visible, XUV and x-ray magneto-optics will provide four complementary views on the same ultrafast phenomenon. It is expected that obtaining the complete experimental information will stimulate further close collaboration of theory and experiment aimed at the development of new approximations and conceptually novel theoretical approaches to describe ultrafast magnetism. Interpretation of ultrafast MO transients can also benefit from the on-going rapid developments of theoretical and computational methods for multiscale modelling of non-equilibrium dynamics of essentially quantum systems.

### Concluding remarks

MO effect demonstrated by M Faraday in 1845, even today remains one of the simplest and, at the same time, the most powerful tool for characterization of magnetic materials. The MO techniques are an appealing solution not only for read-out, but also for control of spins in data storage, spintronics, magnonics and quantum computing. While first discovered in the visible spectral range, over the course of time magneto-optics has been expanded to THz and x-ray spectral range and allowed to obtain new information about magnetic media, which is not accessible otherwise. Although in thermodynamic equilibrium magneto-optics of magnets seem to be well understood, experiments with ultrashort pulses especially in XUV and x-ray spectral range pose new challenges for theory and urges us to develop new frameworks beyond the conventional approximations.

## 2. Magneto-optics: quantum mechanical description and predictions

Sangeeta Sharma and Samuel Shallcross

Max-Born-Institut für Nichtlineare Optik und Kurzzeitspektroskopie, 12489 Berlin, German

### Status

Magneto-optics have long been employed as a probe of the magnetic ground state of materials (see section 4), however it is with the advent of ultrafast laser induced spin dynamics that this technique has assumed the prominence it currently holds. Transient MO response functions represent the *only* route to investigate magnetic order at the attosecond to picosecond time scales of ultrafast spin dynamics (the experimental situation is reviewed in section 11, with dedicated sections on free electron lasers (FELs) and time resolved THz spectroscopy presented in sections 14 and 17, respectively). This field, in turn, offers a paradigm shift from charge to spin based technologies that, given the pressing demands placed on memory and computer power by modern society, is likely to underpin the electronic technologies of the future. That it is possible to efficiently manipulate spins at ultrafast speeds was first demonstrated in [11] in which the elemental magnet Ni was shown to suffer a loss of moment upon laser excitation at sub-picosecond timescales. Several theoretical explanations were provided for this remarkable finding; spin-orbit coupling (SOC) [12, 13], transfer of spin moment to orbital degrees of freedom [14], and super-diffusive currents [15]. Several of these were experimentally contested [15–17], however the lack of quantitative comparison between experiment and theory has held back progress in identifying fundamental mechanisms. Such quantitative comparison, the bedrock of progress in the physical sciences, had to wait until the first *ab-initio* simulations of ultrafast phenomena [13]. These works appeared to confirm the dominance of SOC at early times, setting a material intrinsic limit of 10 s of femtoseconds on ultrafast spin manipulation, a paradigm that was dramatically upended by the discovery of the optically induced inter site spin transfer (OISTR) [18], revealing *local* spin manipulation to be limited in time only by the laser pulse duration.

Collaborative progress between experiment and theory relies on a common set of observables, however while MO experiments are founded on the measurement of response functions the natural variables of quantum simulation are time dependent magnetization and current densities. Recent advances have brought experiment and theory closer together both through the direct simulation of transient response functions [19], aiding the interpretation of complex spectral information for magnetic alloys, and the simulation of angle-resolved photoemission spectroscopy (ARPES), yielding information of quasi-particle band shifts [20].

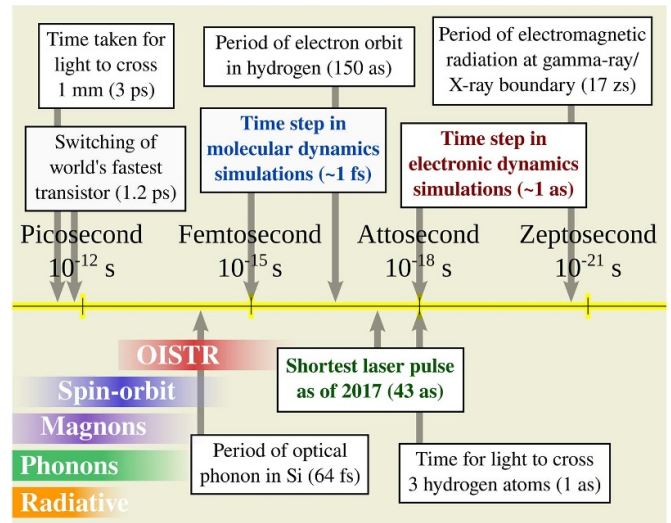


**Figure 2.** Time scales of various processes involved in ultrafast spin dynamics. Fundamental physical processes are indicated by the colour bars, with characteristic times given by the text boxes.

### Current and future challenges

Despite tremendous progress in the simulation of spin dynamics and magneto-optics, present state-of-the-art theory is restricted in key aspects that require several future developments (see figure 2) to bring first principles simulations closer to experiments:

- Phenomena at large time and length scales:* A plethora of interesting physical effects occur on spatial and time scales that cannot currently be addressed by time-dependent density functional theory (TD-DFT); (1) the coupling (and control) of spin dynamics by lattice excitations e.g. prepared phonons, (2) radiative effects, (3) mesoscopic spin structures such as skyrmions, domain walls (section 6 presents the experimental situation of characterizing complex magnetic structures via spatiotemporal Kerr imaging), long wavelength magnons and spin waves (SWs) (see section 7 for a review of BLS, a key tool to characterize complex SW textures), and (4) spin decoherence. All of these require fundamental methodological extension of the *ab-initio* approach, as described below.
- Many-body effects:* Reduced screening in two dimensional materials implies a profound role for excitonic effects in the early time dynamics. Present *ab-initio* theory, however, treats excitonic effects only in the static limit for weak pulses. To capture spin and charge dynamics in two-dimensional (2D) materials exciton dynamics must be treated on the same footing as the dynamics of free carriers. For periodic solids this will involve solving Maxwell's equation together with the TD-DFT electronic system. At the same time, excitonic effects play a significant role in shaping MO response functions, and the systematic inclusion of excitonic effects remains an outstanding challenge in their simulation.



- (c) *Emergent phenomena*: Emergent variables such as the exchange interaction and temperature form a natural description for later time (picosecond scale) phenomena such as all optical switching (AOS) in e.g. GdFeCo. On the other hand, few femtosecond timescale dynamics reveals a different physical regime characterized by profound spin-charge coupling such as exhibited by the OISTR effect. A key unresolved question is thus how and at what time scales do emergent spin variables and their interactions (such as can be described by the Landau–Lifshitz–Gilbert type approaches) emerge from the underlying dynamical electronic structure. Bridging these two time regimes and their distinct theoretical methodologies can be expected to offer new insights into the origins of remarkable effects such as AOS. Such hybrid approaches may also provide a promising route for the exploration of fundamental early time physics in novel devices involving transport (section 9 reviews the situation for the measurement of spin and charge currents via the MOKE), such as the so-called OGMR effect (OISTR induced giant magnetic resistance) in which the OISTR effect [18] would switch the magnetic order of a multilayer from ferromagnetic (FM) to antiferromagnet (AFM), thereby enacting a transient spin-filter.
- (b) *Long length scales*: Modern computer power limits the spatial scales accessible to simulation to system sizes of the order of 100 s of atoms [23]. Treating phenomena of longer length scales *ab-initio* will require a dynamical extension of the recently proposed ‘long-range ansatz’ [24], in turn necessitating a density function theory for the long-range dipole–dipole interaction term.
- (c) *Experimental magneto-optics for anti-ferromagnets*: as magneto-optic techniques measure total moment, these techniques cannot be used to probe the spin dynamics of AFM. Linear dichroism or the Voigt effect can in principle be used to study such systems and a future in-depth analysis of such transient response functions in the context of AFM spin dynamics is highly desirable [25].

### Concluding remarks

After more than two decades of being led by experiment, the extension of state-of-the-art quantum simulations to the field of ultrafast spin dynamics has resulted in a fruitful partnership between theory and experiment. This has already yielded profound progress: the prediction and experimental confirmation of new ultrafast phenomena [18], the ability to decode complex transient spectral information, and the beginnings of an understanding of the impact of laser light on quasi-particle band properties [20]. *Ab-initio* understanding of the light–matter interaction and ultrafast spin and charge dynamics remains, however, limited to very early times and short (unit cell scale) lengths. Complex magnetic structures and their dynamics, whose experimental measurement is currently the subject of intense activity as reviewed in sections 6 and 7, thus represent a key unsolved challenge for *ab-initio* theory, and the extension of the domain of simulation to the time and length scales at which such textures exist would enable a rich future collaboration between theory and experiment.

### Advances in science and technology to meet challenges

- (a) *Long time scales*: Currently TD-DFT can describe light–matter interaction only of the electronic system, which in solids limits the useful simulation time to approximately the first 100 fs. Extension to longer times requires coupling spin dynamics to additional degrees of freedom: (1) the nuclei degrees of freedom [21] and (2) Maxwell’s equations to include radiative effects [22].

### 3. Magneto-optics: electromagnetic theory and modelling

Nuno de Sousa<sup>1</sup> and Antonio García-Martín<sup>2</sup>

<sup>1</sup> Donostia International Physics Center (DIPC), Donostia-San Sebastián 20018, Spain

<sup>2</sup> Instituto de Micro y Nanotecnología IMN-CNM, CSIC, CEI UAM+CSIC, Isaac Newton 8, E-28760 Tres Cantos, Madrid 28760, Spain

#### Status

Theoretical modelling of electromagnetic fields (EFs) in nano-scale optical systems is inherently a challenge that has been subject to a continuous effort leading to a variety of tools and techniques. This complexity is, of course, increased for resonant systems, as the details of the EF in the vicinity and the interior of the nanostructure completely determines its optical response. In absence of MO activity, the tensor can, in most cases, be fully regarded as a scalar  $\epsilon(\mathbf{r})$  [26]. In presence of MO activity, the *dielectric tensor*  $\overleftrightarrow{\epsilon}(\mathbf{r})$  needs to be considered in full:

$$\overleftrightarrow{\epsilon}(\mathbf{r}) = \begin{pmatrix} \epsilon_{xx}(\mathbf{r}) & \epsilon_{xy}(\mathbf{r}) & \epsilon_{xz}(\mathbf{r}) \\ \epsilon_{yx}(\mathbf{r}) & \epsilon_{yy}(\mathbf{r}) & \epsilon_{yz}(\mathbf{r}) \\ \epsilon_{zx}(\mathbf{r}) & \epsilon_{zy}(\mathbf{r}) & \epsilon_{zz}(\mathbf{r}) \end{pmatrix}.$$

The appearance of off-diagonal elements give rise to the first (linear) manifestation of the MO activity whereas higher-order effects influence all (off-diagonal and diagonal alike). In the most common case of linear response we would have ( $\epsilon_{xx}(\mathbf{r}) = \epsilon_{yy}(\mathbf{r}) = \epsilon_{zz}(\mathbf{r})$  and  $\epsilon_{ji}(\mathbf{r}) = -\epsilon_{ij}(\mathbf{r})$  for  $i \neq j$  [26].

The nature of MO, sharing magnetism and photonics alike, makes its modelling somehow dependent on the final goal. One can use the optical response either to bring forth magnetic properties, as is traditionally happening in MO ellipsometry (see section 9) or to enhance the MO signal itself (see section 12). On the other hand, the non-diagonal elements in  $\overleftrightarrow{\epsilon}(\mathbf{r})$  reflect that the MO activity permits an external modification of the optical behaviour. This has been used to develop modulators and isolators since long ago but now, with resonant optical elements in the nanoscale, a new dimension has been reached. Therefore, the modelling needs to describe the geometry of the MO material and the region where the optical EF is localized.

**Multilayered (thin) films.** In this case, the material is disposed in layers where variations of the material and/or the localization of the EF occur only in one direction, and the propagation direction of the optical wave has a non-zero component along it. Here Transfer matrix techniques are enough to obtain accurate results [27]. Inclusions of MO material in a non-active one (or vice-versa) can be treated using an effective medium before performing the transfer matrix formalism, to obtain the required homogeneous in-layer material. This is valid as

long as the inclusions are non-interacting and/or the spacing is not commensurate with the optical wavelength (e.g. photonic crystals).

**Multilayered periodic nanostructures.** In this case, the distance between the elements is a key factor and thus it must be properly considered. For that reason, an expansion in a basis formed by plane waves is considered by many the best approach. This lies at the core of scattering matrix and rigorous coupled-wave or scattering matrix methodologies that needed to be adapted to cope with the requirements imposed by  $\overleftrightarrow{\epsilon}(\mathbf{r})$  (e.g. fast Fourier factorization techniques to keep reasonable computational time and memory resources) [28–30].

**Isolated (non-periodic) structures.** For this case the most used methodologies are based on space-time discretization to solve Maxwell's equations using finite element methods (FEMs) [31], finite difference time domain (FDTD) [32], discrete (or coupled) dipole approximation (DDA/CDA) or T-matrix methods [33, 34]. In all cases, the system, after discretization, turns into a complex system of equations whose solution is tackled by a different mathematical approach depending on its size. Each method poses its advantages and shortcomings. FEM can tackle proficiently any kind of geometry, and virtually with any  $\overleftrightarrow{\epsilon}(\mathbf{r}, \omega)$ , but the discretization scheme itself (tetrahedral) lead to undesired anisotropies. FDTD can solve the whole frequency spectrum, as it involves the time evolution of a given pulse, based on a parameter fitting of  $\overleftrightarrow{\epsilon}(\mathbf{r}, \omega)$  to be able to efficiently cope with the temporal evolution. This turns into a weakness when diagonal and off-diagonal elements are very different, as the error in the parametric fitting can be of the order of the MO elements themselves. DDA/CDA and T-matrix are very similar and consider that each discretization volume behaves as a point multipole (in many cases, keeping only the lowest dipole is already enough). This has advantages over FEM and FDTD since the background medium needs no discretization at all [34]. However, it has shown difficulties to cope with geometries with large anisotropies (e.g. very elongated needles or very flat disks or flakes).

#### Current and future challenges

The unprecedented development of experimental techniques, particularly in the nanoscale, brings with it structures and devices with a great deal of complexity, both in the geometry and in the composition of the system. These will be the cornerstone of future technologies, and modelling MO capabilities with enough accuracy to be predictive is paramount. It should not be forgotten that this field feeds from state-of-the-art magnetic technologies and optical elements, where multi-scale approaches are normally a must. These include the very challenging topics of interactions between spintronics and optics, the interplay of optical and acoustic resonances mediated by

the MO effect, THz MO or topological effects (see sections 10, 11, 16, 18 and 20).

The coexistence of different aspects that might lead to anisotropies, e.g. simultaneously MO and chiral, ‘magneto-chiral’, structures, are currently experiencing lots of attention. For such cases there is a competition between the purely optical (geometrical) dichroism and the MO one, therefore the theoretical tools to be used must be well suited to address the ultimate source of a given effect. Good examples of these kinds of systems are topologically protected chiral systems or parity-time broken symmetric systems under MO effects.

A 2D materials and metasurfaces are special cases. A 2D materials are challenging for the phenomena developing in-plane and out-of-plane take place in very different length scales. The methods described above require a large number of discretization elements to *rigorously* tackle numerical computation of the MO (even only optical) response. In metasurfaces, the order is a key factor to understand the physical phenomena. Systems exhibiting order in the short-range but not in the long-range (e.g. hyperuniform systems [35, 36]) cannot, in certain situations, be treated neither imposing periodicity nor ignoring interactions via conventional effective medium approaches.

The actual challenge in MO modelling lies thus in efficient treatment of the multiscale nature of the systems that are nowadays of interest. Different regions with rapidly varying  $\overleftrightarrow{\epsilon}$  require efficient discretization approaches or clever definitions on the *tensorial polarizability*  $\overleftrightarrow{\alpha}$  of the interacting elements. Quantum as well as non-locality effects have been subject of intense consideration in the framework of optical devices. In the MO case, these effects have not been extensively considered so far, but it is foreseen that modelling of future MO devices must consider them.

### Advances in science and technology to meet challenges

Advances should consider the development of strategies able to cope with multi spatial (geometry and wavelength) and multi-temporal scales in the same framework. Additionally, cross-linking the different approaches would make it possible to diminish the inconveniences present in each of them individually. Solvers able to deal with extreme cases such as gaps 100 times smaller than the wavelength or aspect ratios equally

dissimilar must be common in the near future. One way is improving the efficiency of the mathematical solvers (brute force) for millions of unknowns. Another relies on combination of strategies, such as using FEM or FDTD for parametric modelling of a single complex structure and the T-matrix to account for interactions when the structure is the building block of a colloid. That approach has the advantage of the accurate solutions for isolated entities provided by the FEM/FDTD while discretization-free signal propagation of the T-matrix properly accounts for the interactions. FEM needs avoiding unrealistic anisotropies arising from the meshing strategy, easy to detect when the system has a well-defined symmetry, but able to jeopardize the whole structure when not. FDTD requires parametrization schemes to be able to obtain fitting errors much smaller than the MO-elements. DDA and T-matrix do not require meshing or discretizing the free-space, but need formalisms using very anisotropic point dipoles, inhomogeneous discretization and of weak non-localities.

Efficient methods for calculating the interaction of a large number of entities for complex systems in a multidimensional space will be necessary. Future efforts for ad-hoc MO models should allow for the development of methods that incorporate quantum mechanics effects into a precise calculation of the material properties and anisotropies in  $\overleftrightarrow{\epsilon}$ . These include non-localities for multi-material systems and suitable ways to translate quantum mechanical effects in the *magnetic* part to  $\overleftrightarrow{\epsilon}$ . Ideally, comprehensive methodologies encompassing advanced micromagnetic calculations together with a reliable modelling of the optical response, with efficient computing at its core, would pave the way towards real device simulations.

### Concluding remarks

MO modelling should evolve tightly linked to multiscale methodologies. Optics and magnetism should evolve similarly to avoid over- or under-description of one of the fields. The main focus must be on devices, but not forgetting fundamental aspects when developing new codes or theoretical approaches. The future is linked to multiphysical descriptions, together with highly efficient numerical codes. In that way, modelling will possess actual predictive capabilities.

## 4. Spectroscopic magneto-optical (MO) characterization

Georgeta Salvan

Institute of Physics, Chemnitz University of Technology,  
Chemnitz 09107, Germany

### Status

This section focuses on MO spectroscopic characterization methods operating from the near-infrared (NIR) to the ultra-violet spectral range, that allows for the assessment of the electronic transitions involving valence states. MO characterization methods in the THz and x-rays spectral range are discussed in the sections 19 and 14, respectively.

The Faraday rotation, MCD, and the MOKE are non-reciprocal effects that can be caused when the time-reversal symmetry is broken in magnetized media. The magnetization can either be induced by a magnetic field in the case of diamagnets, paramagnets, or magnetically ordered materials, or can arise spontaneously in the latter. A review of the microscopical mechanisms of the MO activity of various inorganic materials can be found, for example, in the section 1 or in the book of Zvezdin and Kotov [37]. The microscopic origin of MCD occurring in molecular materials is discussed thoroughly, e.g. for diamagnetic and paramagnetic porphyrinoid molecular systems in [38].

The spectroscopic methods based on MO effects measured in transmission geometry (Faraday rotation, MCD) profit from their higher magnitude compared to those observed in reflection geometry (MOKE). MCD spectroscopy became widely used for the assessment of the electronic structure of molecular systems (including diamagnetic and paramagnetic molecules) at room temperature (RT) and at moderate magnetic fields (below 1 T) in the chemistry community, the fact that boosted the development of commercially available spectrometers. The transmission measurements are, however, limited to transparent samples such as molecules dissolved in solutions or solid matrices, or organic as well as inorganic films on transparent substrates.

On the other hand, the application of MOKE spectroscopy in reflection geometry is usually associated with opaque samples. The reported Kerr rotation and Kerr ellipticity spectra are mostly acquired using home-built setups with a detection sensitivity down to  $0.001^\circ$ . Achieving such a high sensitivity with conventional white light sources requires the modulation of the light polarization (either before or after the reflection on the sample) that is realised mostly using photoelastic modulators, similar to the MCD spectrometers. Thanks to the excellent sensitivity of the current MOKE spectrometers the characterization of ultra-thin FM layers with thicknesses in the sub-nanometre range (e.g. [39]), thin paramagnetic and diamagnetic molecular layers (e.g. [40]), organic/FM heterostructures (e.g. [41], see figure 3), or superparamagnetic clusters in organic matrices (e.g. [42]) or other complex heterostructures became possible.

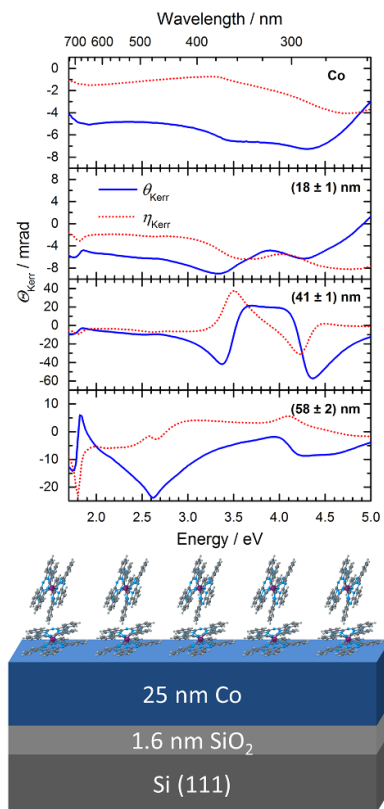


**Figure 3.** MOKE spectra of a Co film (top) and of thin films of the single molecule magnet TbPc<sub>2</sub> on Co/SiO<sub>2</sub>/Si recorded at RT in the paramagnetic state. The TbPc<sub>2</sub> film thickness is given in the legend of each graph. The continuous lines (blue) and dotted lines (red) represent the spectra of the Kerr rotation and ellipticity, respectively. (Bottom) Sketch of the samples. Reproduced from [41] with permission of The Royal Society of Chemistry.

### Current and future challenges

When MOKE spectroscopy is performed on complex systems such as multilayers on opaque substrates, the MO signal is not a simple superposition of the MO activity of the individual layers. Multiple reflections occurring at interfaces lead to interference effects (sometimes described as optical artefacts) that can dramatically influence the spectral lineshape. In order to assess the contribution of individual materials to the total MO signal, i.e. the material specific MO activity (described by the Voigt constant or the off-diagonal component of the dielectric tensor), the application of optical multilayer models and the knowledge of the energy dispersion of the optical constants (or diagonal components of the dielectric tensor) as well as of the layer thicknesses is necessary. Chemical interactions at interfaces that modify the electronic structure of the materials might complicate the numerical modelling (see [41]). Furthermore, higher-order effects might also bring a spectral contribution, as discussed in section 5. There have also been experimental attempts to disentangle the individual contribution in complex systems, for example by using magnetic field-dependent MOKE spectroscopy [43] or by exploiting

the representation of the Kerr effect in the complex rotation-ellipticity plane [44].

While MCD spectroscopy monitoring of time-dependent processes, such as molecular reactions, became available in commercial setups, real-time monitoring using MOKE spectroscopy on opaque samples is still rarely applied. As already mentioned, the MO activity in reflection is lower than in transmission and the spectral measurements are still too slow for real-time process monitoring. This is caused by the need of compromising between struggling for sensitivity using the combination of photoelastic modulation and single wavelength detection using photomultipliers. A further impediment might be the difficulty in the implementation of variable magnetic field sources in vacuum systems where processes such as film growth or thermal annealing of inorganic layers take place.

Another major challenge in the MOKE spectroscopic characterization resides in the lateral resolution of the state-of-the-art home-built spectrometers, that is in the range of millimetres. While MOKE microscopy performed either with white light or monochromatic sources is widely employed for magnetic domain imaging (see section 6), the possibility of performing MOKE spectroscopy with sub-micrometre lateral resolution would open new avenues in the characterization of, for example, magnetism in 2D materials and of inhomogeneous or micro-structured samples.

### Advances in science and technology to meet challenges

Thanks to the development of the numerical methods for optical multilayer models driven by the spectroscopic ellipsometry community alongside with the progress in the computing power, numerical simulations of the MOKE spectra or fitting of the experimental spectra will become more and more common. This will broaden the applicability range of the MOKE spectroscopy allowing, for example, to assess at the same time the intrinsic electronic and magnetic properties of individual components of multilayer structures as such or upon various processing methods such as thermally induced crystallization or upon application of strain or other external stimuli.

The development of compact *in situ* electromagnets for use in ultrahigh vacuum environments might offer a tool for real-time magneto-optic Kerr effect monitoring during growth processes (see e.g. [45]). The monitoring is still limited to single

photon energies, but spectroscopic measurements might be recorded while interrupting the growth.

A solution for the signal enhancement from samples with low MO activity might be provided by exploiting the interference effects occurring when dielectric layers with vanishingly low MO activity are combined with MO active layers. This method has already been exploited in MO storage media. A similar approach, based on embedding the MO active layer between two dielectric layers (called extreme anti-reflection enhanced MOKE), was recently demonstrated by MOKE spectroscopy and microscopy [46]. Another promising approach for the MO response enhancement relies on plasmonic resonances in Au films or nanostructures (see e.g. [47] and references therein or section 12).

Regarding the spectral MO measurements with (sub-)micrometre resolution, methods from other optical spectroscopies might also boost progress in magneto-optics if implementing magnetic field sources. For example, reflection difference spectroscopy at micrometre scale has already been performed with the sensitivity required for MOKE [48]. On the other hand, the newest imaging ellipsometers can be equipped for the measurement of the Müller matrix components containing information on the MO activity (see section 9 for more details on the ellipsometry relation to magneto-optics). A possible drawback related to the lower sensitivity of the current imaging ellipsometers compared with MOKE spectrometers could be overcome by using one of the MO signal enhancement approaches discussed above.

### Concluding remarks

MO spectroscopies in the NIR to ultraviolet spectral range offer access to the joint density of states involving valence states in various diamagnetic, paramagnetic, and magnetically ordered systems. The extraction of the individual MO response of materials and/or nanostructures in complex systems is challenging, but accessible via experimental and/or numerical simulation or fitting approaches. This response can be exploited for a better understanding of modifications induced by external stimuli (such as heat, light, strain, etc) to the electronic structure as well as to the structural, and magnetic properties of the individual components in complex heterostructures. Experimental developments that will allow performing MO spectroscopies with a (sub-)micrometre spatial resolution will pave new ways for the characterization of microstructured samples as well as of the novel aspects of magnetism in 2D materials.



## 5. Higher order magneto-optics effect

Jaroslav Hamrle and Ondřej Stejskal

Institute of Physics, Charles University, Ke Karlovu 5, Prague 12116, Czech Republic

### Status

The relation between the measured MO effect and magnetization direction can be separated into two subsequent steps. (a) The first step is a relation between magnetization direction and elements of the permittivity tensor  $\varepsilon_{ij}$ , which phenomenologically describes optical properties of the FM material. (b) The second step is a relation between the permittivity tensor  $\varepsilon_{ij}$  and the resulting MO effects. In the simplest approximation, both steps provide linear relations, resulting in a linear dependence between MO effect and the magnetization direction. However, both steps may contain also higher order (quadratic) terms, providing that relation between measured MO effect and magnetization is in general not linear anymore.

The magnetization direction can be understood as a small perturbation to optical properties of the FM material, described by the permittivity tensor  $\varepsilon_{ij}$ . Hence, its dependence on the relative magnetization components  $M_k$ ,  $M_l$  can be written in Taylor series as a sum of permittivity contributions [49, 50]

$$\varepsilon_{ij} = \varepsilon_{ij}^{(0)} + K_{ijk}M_k + G_{ijkl}M_kM_l,$$

where  $i, j, k, l = \{x, y, z\}$ , and  $\varepsilon_{ij}^{(0)}$ ,  $K_{ijk}$  and  $G_{ijkl}$  are second, third and fourth order MO tensor describing permittivity contributions independent on, linear to and quadratic to magnetization direction, respectively. The second order MO effects are proportional to the quadratic form of the magnetization, originating from permittivity contributions  $\varepsilon_{ij}^{(2)} = G_{ijkl}M_kM_l$ . Where  $\varepsilon_{ij}^{(2)}$  is the second-order contribution to the permittivity tensor. When diagonal permittivity,  $\varepsilon_{ii}^{(2)}$  depends on the magnetization direction, the corresponding MO effect can be detected by magnetic linear dichroism (MLD). When the off-diagonal permittivity term ( $\varepsilon_{ij}^{(2)}$ ,  $i \neq j$ ) depends on the magnetization direction, the MO effect can be detected by quadratic MOKE (QMOKE).

The quadratic MO effects are present not only in FMs, but also in AFMs. The ability of the second order MO effects to be sensitive to the spin-ordering of AFM (so called Néel vector) makes this effect one of the few techniques to detect spin-ordering in AFM. The general form of  $G_{ijkl}$  tensor depends on crystal symmetry. For example, in the case of FM cubic material possessing point symmetry (and considering that the length of magnetization vector is constant), only two independent parameters remain, called  $G_s$  and  $2G_{44}$  [51]. Determination of their spectra extends usual linear spectral magnetooptics (see section 4). The spectra of  $G_s$  and  $2G_{44}$  were determined for bcc Fe [51, 52] and Heusler compound  $\text{Co}_2\text{MnSi}$  [53] (figure 4). In both cases, the  $G$ -spectra were about  $10\times$  smaller compared to their linear-in-magnetization counterparts. Also, in both cases, there was a reasonable agreement between experimental spectra and those determined by *ab-initio* calculations based on

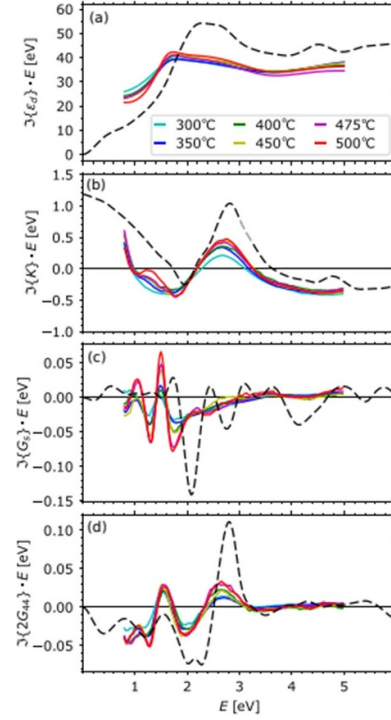


**Figure 4.** Imaginary part of permittivity spectra of Heusler compound  $\text{Co}_2\text{MnSi}$  prepared at different annealing temperatures, corresponding to different amount of  $L_{21}$  ordering (a)  $\varepsilon_d$  (permittivity of zeroth order in  $M$ ), (b) linear MO parameter  $K$ , (c) quadratic MO parameter  $G_s$ , and (d) quadratic MO parameter  $2G_{44}$ . Coloured full lines are the experimental spectra, black dashed lines are *ab initio* spectra. Reprinted from [53], with the permission of AIP Publishing.

Kubo formula, demonstrating validity of the linear response theory to describe MO effects quadratic in magnetization. Furthermore, the  $G$ -spectra on  $\text{Co}_2\text{MnSi}$  demonstrated nearly linear scaling of strength of  $G$ -elements with the amount of  $L_{21}$  crystallographic ordering, suggesting that QMOKE spectroscopy can be used to optically determine crystallographic ordering.

The relation between outgoing MOKE  $\Phi_s$  and  $\Phi_p$  for incident  $s$  and  $p$  light polarization, respectively, and off-diagonal permittivity elements  $\varepsilon_{ij}$  can be written as [54]

$$\begin{aligned}\Phi_s &= A_s (\varepsilon_{yx} - \varepsilon_{yz}\varepsilon_{zx}/\varepsilon_d) + B_s \varepsilon_{zx} \\ \Phi_p &= -A_p (\varepsilon_{xy} - \varepsilon_{xz}\varepsilon_{zy}/\varepsilon_d) + B_p \varepsilon_{xz}\end{aligned}$$

where  $\varepsilon_d$  is the diagonal permittivity and  $A_{s/p}$  and  $B_{s/p}$  are scaling optical factors between  $\Phi_{s/p}$  and permittivity elements, where  $A_{s/p}$  express scaling for polar geometry, i.e. part of MOKE even in the incidence angle  $\varphi$ ,  $A_{s/p}(\varphi) = A_{s/p}(-\varphi)$ , and  $B_{s/p}$  for longitudinal geometry (i.e. part of MOKE odd in the incidence angle,  $B_{s/p}(\varphi) = -B_{s/p}(-\varphi)$ ). Although one usually assumes, that relation between  $\Phi_{s/p}$  and off-diagonal permittivity elements is linear,  $\Phi_{s/p}$  also contains product of two off-diagonal elements,  $\varepsilon_{yz}\varepsilon_{zx}$  and  $\varepsilon_{xz}\varepsilon_{zy}$ , respectively. In the case both elements in the product are linear in magnetization, then this term provides quadratic-in-magnetization response, mimicking QMOKE originating from the second-order MO tensor

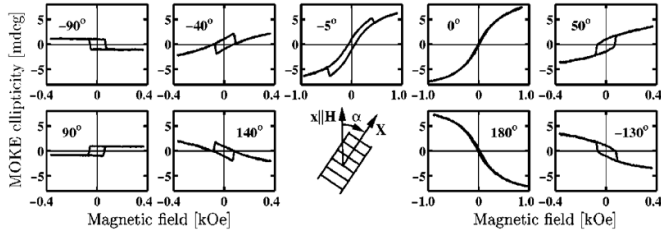


**Figure 5.** Magnetization loops of MOKE on vicinal structure Co/Au(322) at different sample orientations with in-plane applied field. The measured MOKE consists of vicinal MOKE, originating from a higher order term  $\varepsilon_{yz}\varepsilon_{zx}$ . The vicinal MOKE is linear in magnetization, however remarkably changes sign when sample is rotated by  $180^\circ$ . Reprinted (figure) with permission from [55], Copyright (2003) by the American Physical Society.

$\varepsilon_{ij}^{(2)} = G_{ijkl} M_k M_l$ . Hence, care is required to correctly interpret those contributions [51].

Another demonstration of higher order term  $\varepsilon_{yz}\varepsilon_{zx}$  is the vicinal MOKE (figure 5), originating from the vicinal interface of FM layer, where one off-diagonal permittivity term is linear in magnetization, whereas the other one is of structural origin due to low symmetry of the vicinal interface [55].

### Current and future challenges

In general, both the linear and quadratic MO effects can be employed either as a tool to study direction of magnetic ordering, or as a spectroscopy tool to provide insight into the electronic structure (see section 9). From the spectroscopic point of view, quadratic  $G$ -spectra of only two materials have been determined so far, both being cubic materials. In general, the measured MOKE may consist of several linear or quadratic contributions. Hence, several spectra must be measured at different magnetization and sample orientations, in order to separate different MO permittivity elements  $K_{ijk}$  and  $G_{ijkl}$ . However, such a separation procedure depends on crystallographic symmetry and surface orientations of FM material [56], which further complicates routine employment of QMOKE spectroscopy. Also, the symmetry analysis of cubic FM material without point symmetry (i.e. without inversion) predict a new quadratic term  $\Delta\Gamma$ , which would allow to detect absence of the point symmetry in FM materials by using optical methods [56], but has not been experimentally demonstrated yet.

Another challenge is to develop QMOKE spectroscopy for other classes of materials, establishing it as a standard spectroscopy tool. MO spectroscopy on AFM materials is limited now, mainly due to the inherent difficulty to manipulate spin-ordering direction in AFM materials, achieved for example by varying the temperature below and above Neel temperature [57, 58]. Furthermore, as new types of AFM ordering emerge (e.g. non-collinear spin ordering in  $\text{Mn}_3\text{Sn}$ ), the details of quadratic MO effects and their spectra in those systems are still to be understood [59].

Finally, one can employ inverse quadratic MO effect to manipulate Néel vector of AFM by pump-probe technique

[60] (see section 10), maybe even to induce selective magnetic precession of different elements. Also, one can envisage pump-probe system used to measure QMOKE spectroscopy in AFM. Here, the pump pulse will induce precession of atomic magnetic moments, which subsequently will be read by probe pulse, which photon energy will be varied, and hence reading QMOKE spectra.

### Advances in science and technology to meet challenges

Nowadays spectral ellipsometry is routinely used in both academia and industry to characterize quality of multilayer structures, with lateral resolution down to  $100\ \mu\text{m}$  and with possibility to measure and process spectra within few seconds. The MOKE spectroscopy can be established as a standard tool to quickly and cheaply characterize crystal quality of prepared FM films, having advantage of implicit sensitivity to FM material. The sensitivity to structural details of FM layer can be further enhanced by employing also QMOKE spectroscopy, as demonstrated in the case of  $\text{Co}_2\text{MnSi}$  [53] (figure 4). However, MOKE spectroscopy is currently not established as a routine tool to check crystal quality of FM layer.

To be able to measure QMOKE spectra in AFM materials, one needs to establish control of Néel vector, either statically or dynamically (precession). Control of Néel vector is clearly interesting also in other branches of physics, such as AFM spintronics or AFM spin dynamics [60]. Well-established inverse quadratic MOKE can contribute to achieve such a control.

Although it has been demonstrated that linear response theory (Kubo formula) well describes spectra of quadratic MO effects, their detailed origin and understanding within electronic band structure is elusive nowadays, as it is already complicated to detail the origin of linear MOKE in simple FM material [61]. It is a challenge to establish understanding of the origin of higher-order MO effects within electronic structure, key prerequisite to tune, optimize and finally better employ the effect (see section 2).

Another challenge is a detection (and eventually spectroscopy) of the third-order MO effects, which have been demonstrated to exist in bcc Fe [62] and fcc Ni [63], however any spectroscopy or *ab-initio* description of those MO effects is missing.

### Concluding remarks

MO effects have been used for a very long time to read and manipulate magnetization state as well as to investigate electronic structure of magnetic materials. Employing higher-order MO effects increases potential of those approaches, such as reading and writing of spin-order in antiferromagnetic materials or gaining higher sensitivity to selected quality of the crystallographic structure, such as crystallographic ordering or absence of point symmetry of the crystal.

## 6. Kerr microscopy

Jeffrey McCord

Institute for Materials Science, Kiel University, Kaiserstraße 2, Kiel 24143, Germany

### Status

Kerr microscopy is a method for the imaging of magnetic domains, which is strongly connected to other MO imaging methods like Faraday and Voigt effect microscopy [64, 65]. The physical origin of the Kerr effect (see section 4) is identical to the Faraday effect but is exhibited in reflection from a magnetized surface and thereby suitable for the analysis of metallic specimen. Kerr microscopy is a traditional technique [66] used by specialists in the field. Yet, during the last decade it has become a standard laboratory technique for the investigation of magnetic domain behaviour.

MOKE microscopy is based on the use of modified optical polarization microscopes or related setups using regular objective lenses, enabling flexible wide-field imaging from a centimetre to the micrometre scale (figures 6(a)–(c)). Consequently, wavelengths within the visible spectrum are normally applied, which restrict the attainable spatial resolution down to the 100 nm regime. Magneto-optics offer the chance to probe lateral dynamic magnetization response from the quasi-static down to the femtosecond timescale (figures 6(d)–(f)) using light emitting diodes [67, 68] and pulsed laser illumination sources [64, 69, 70]. In terms of temporal resolution, Kerr microscopy is at least comparable to current x-ray microscopy techniques.

In Kerr imaging the exact illumination conditions are of high importance as the three fundamental Kerr geometries, polar, longitudinal, and transverse MOKEs, must be adjusted carefully under microscopic conditions. They may contribute concurrently to the magnetic contrast, which impedes magnetic image interpretation. Likewise, higher order MO effects (see section 5) and the MO Gradient effect add to the magnetic image formation. The challenge has been partly overcome by advanced illumination schemes with simultaneous [64, 67] or sequentially alternating illumination schemes [68, 69], enabling the separation of the different Kerr effects for the MO image formation and the realization of quantitative Kerr effect micrographs [64, 67–69, 71]. With the increase of dynamic range and signal-to-noise ratio in current complementary metal-oxide semiconductor (CMOS) camera technology, imaging of the purely transverse Kerr effect with sensitivity only to the in-plane magnetization has become achievable [72]. This progress is supported by the revival of anti-reflection schemes [66] for achieving huge MO contrasts for even nanometre thick films [46]. This helps enabling analyser free domain imaging modes [46, 72].

By this, Kerr and MO microscopy offers unique benefits for the investigation of a large variety of spin systems, including also non-collinear AFMs [73] on a laboratory level.

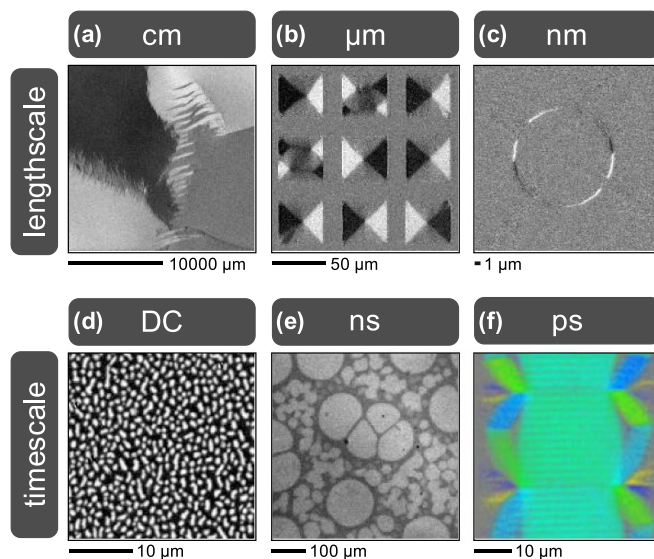


**Figure 6.** Exemplary Kerr microscopy images on different length and time scales. (a) Large view domain image from a mixed low anisotropy  $\text{Ni}_{81}\text{Fe}_{19}$  (40 nm) single film. (b) Variations from Landau domain structures in  $\text{Ni}_{81}\text{Fe}_{19}$  (50 nm) square elements. (c) Magnetic onion state in a 300 nm width  $\text{Co}_{90}\text{Fe}_{10}$  (0.8 nm)/ $\text{Ni}_{81}\text{Fe}_{19}$  (28 nm) ring structure. Reproduced from [64]. © IOP Publishing Ltd. CC BY 3.0. (d) Quasi-static domain image of skyrmion bubble formation in a  $\text{Co}_{40}\text{Fe}_{40}\text{B}_{20}$  (1.4 nm)/MgO thin film. (e) Single-shot dynamic domain evolution in a micrometre thick garnet layer (single shot imaging with 20 ns pulse width, MO Faraday contrast imaging). (f) Quantitative dynamic domain imaging of SWs in a  $\text{Co}_{40}\text{Fe}_{40}\text{B}_{20}$  (120 nm) film (excitation frequency of 3 GHz, time resolution of 7 ps). Reprinted from [69], Copyright (2017), with permission from Elsevier.

### Current and future challenges

Several challenges must be met to further enhance imaging for foreseen investigations in magnetism research, ranging from improving temporal and spatial resolution and alternative imaging modes for low MO contrast retrieval. Imaging of three-dimensional magnetic structures, integrating depth-selectivity, and material specificity known from MO magnetometry [44] would bring Kerr microscopy to the next level. Hereinafter, the most relevant challenges are specified.

Temporal resolution to image up to fast magnetization dynamics by stroboscopic imaging methods is standard for Kerr microscopy. Working merely for repetitive magnetic events, extending the imaging modes to fast single-shot imaging (figure 6(e)) of nonrepetitive events is nearly unexplored for time scales below the microsecond regime. Providing single-shot imaging for the regime of magnetization dynamics beyond that range would open a new field for the investigation of magnetization behaviour in magnetic materials and devices.

The spatial resolution in standard Kerr microscopy is mainly restricted by the optical diffraction limit, which scales with the wavelength and the numerical aperture of illumination and observation in the microscopic setup. The modes of illumination and observation are conversely fundamental to the

applied MO effects, while limiting the options for improving spatial resolution. Notwithstanding the demonstrated attainability of identifying isolated magnetic structures [74] below the fundamental resolution limit and determining magnetic domain wall positions with nanometre precession [75], imaging of details inside sub-micrometre structures is barely feasible. Related obstacles for the imaging of small magnetic structures are due to polarization effects occurring at the borders of structures. Correspondingly, Kerr microscopy and the setting of the MO effects work best for planar mirrorlike magnetic objects. Topography in three-dimensional (3D) magnetic structures (see section 14), e.g. to study novel magnetochiral effects [76], obscures the MO signals. This, together with the limited depth of focus in high-resolution optical microscopy and the abovementioned edge effects, leads to limitations for the application of Kerr microscopy for imaging of small 3D objects. The limits are enhanced by possible drift effects with the application of the traditional background subtraction technique [64, 66].

Similar arguments as laid out above are true for Faraday and Voigt microscopy, the latter also applicable for the imaging of domains in collinear AFMs that should not be mistaken with the regular birefringence imaging in magnetostrictive AFMs [77].

### Advances in science and technology to meet challenges

Spatiotemporal Kerr imaging beyond current state-of-the-art will involve adjustments on the overall mechanics, image detection, and the illumination source. Envisioned changes are laid out next.

The temporal resolution in Kerr microscopy can be imminently enhanced by the incorporation of improved pulsed laser systems, including pulse compression technologies, with sub-femtosecond resolution in laboratory experiments. Non-stroboscopic dynamic imaging modes to capture stochastic and chaotic processes would need to rely on the incorporation of high-power high-brilliance lasers with highly sensitive camera systems. Single-shot imaging of non-repetitive magnetization events in the below magnetic resonance regime, a so-far a blank spot in the imaging of magnetization dynamics, could be addressed with flexible diode lasers. All these incorporations may imply turning away from standard microscope setups

and an adaption of reflective microscope objective lenses. The latter would assist to advance into UV wavelength regimes, by which spatial resolutions well below a 100 nm appear achievable.

A general change in magnetic imaging schemes, like using full aperture illumination and by this dealing with all MO effects concurrently, could further improve the spatial resolution. Combining this with modes, where traditional sequential background imaging subtraction is not required, would be a major step forward to address the challenges pointed out above. The elimination of standard background subtraction would also be beneficial for single-shot dynamic imaging modes. This would further open the path to sophisticated imaging schemes like combining multiple levels of foci for the image construction of 3D magnetic structures.

Implementing novel imaging modes might lead to further improvements, which are not easily foreseen. Notwithstanding, combining it with other techniques or completely turning away from standard Kerr microscopy schemes involving near-field optical imaging techniques, relying on detection layers with magneto-optically active point defect spins (see section 17), or on completely new ways of using the regular MO effects might be the future of MO microscopy.

### Concluding remarks

With the still advancing developments, Kerr microscopy will remain one of the most important techniques for magnetic domain imaging. Based on optics it offers a straightforward access to investigations of ultrafast magnetic processes. Most challenging and reaching a fundamental limit is the restriction in spatial resolution, an obstacle that will be demanding to overcome. Despite this, with the latest improvements on illumination and detection side, applied Kerr microscopy has evolved during the last decade and will continue to make most valuable contributions to magnetism research.

With the on-going advances, the limitations of Kerr microscopy have not been reached so far. With future improvements regarding illumination and detection, MO imaging will continue to remain of pivotal importance for the investigation of magnetic phenomena on various time and length scales. With advanced and dynamic imaging modes, magnetism research in the laboratory will continue to benefit from Kerr microscopy, also in combination with and supporting other methods.



## 7. Probing magnons in the frequency domain: Brillouin light scattering (BLS)

Silvia Tacchi<sup>1</sup> and Giovanni Carlotti<sup>2</sup>

<sup>1</sup> Istituto Officina dei Materiali del CNR (CNR-IOM), Sede Secondaria di Perugia, c/o Dipartimento di Fisica e Geologia, Università di Perugia, I-06123 Perugia, Italy

<sup>2</sup> Dipartimento di Fisica e Geologia, Università di Perugia, I-06123 Perugia, Italy

### Status

As discussed in sections 6 and 11, time-resolved MOKE (TR-MOKE) can be exploited to investigate the dynamical properties of magnetic materials, including magnons that are the quantum-mechanical counterpart of spin waves. In an alternative approach, BLS can be used to probe SWs and map out their spectrum directly in the frequency domain [78]. In fact, in a BLS experiment a beam of monochromatic laser light is focused on the sample and the scattered light is frequency analysed by a high-resolution spectrometer. The scattering mechanism relies on the coupling, via MO coefficients, between the electric field of the incoming light and the periodic variation of the dielectric constant of the medium induced by the SWs [79]. BLS was applied in the field of magnetism already in the early 70s, when the advent of the tandem Fabry–Pérot interferometer (TFPI), developed by Sandercock, enabled the observation of light scattering from SW in opaque magnetic materials [80]. However, it has become the most powerful technique to investigate SWs in layered and patterned structures, only after the turn of the millennium, with the rising interest towards films, multilayers and magnetic nanostructures. Among the most recent and hot topics where BLS is providing fundamental contributions, it is worth mentioning here chiral materials with *Dzyaloshinskii–Moriya interaction (DMI)* [81, 82] as well as magnonic crystals and magnon waveguides where SW propagation can be controlled by a proper design of the sample geometry and composition [83–85]. BLS has several advantages over other techniques for the investigation of SWs: it is characterized by a high sensitivity down to the monolayer scale; it uses a compact experimental apparatus which can be also coupled with ultra-high vacuum chambers allowing *in-situ* characterization of ultrathin films; it operates directly in the frequency domain allowing the simultaneous detection of SWs between about 1 and 500 GHz; conventional BLS (figure 7(a)) offers the possibility to perform wave-vector resolved detection of thermal SWs, naturally present in the medium under investigation, and to measure the SWs dispersion relation, while micro-focused BLS (figure 7(b)) enables to operate as a scanning-probe technique with a spatial resolution of about 250 nm and the possibility for both phase- and time-resolved mapping of the SWs coherently excited by external transduction [86]. Thanks to the above characteristics, BLS is nowadays an indispensable and effective tool for research in nano-magnetism and in particular in emergent research topics

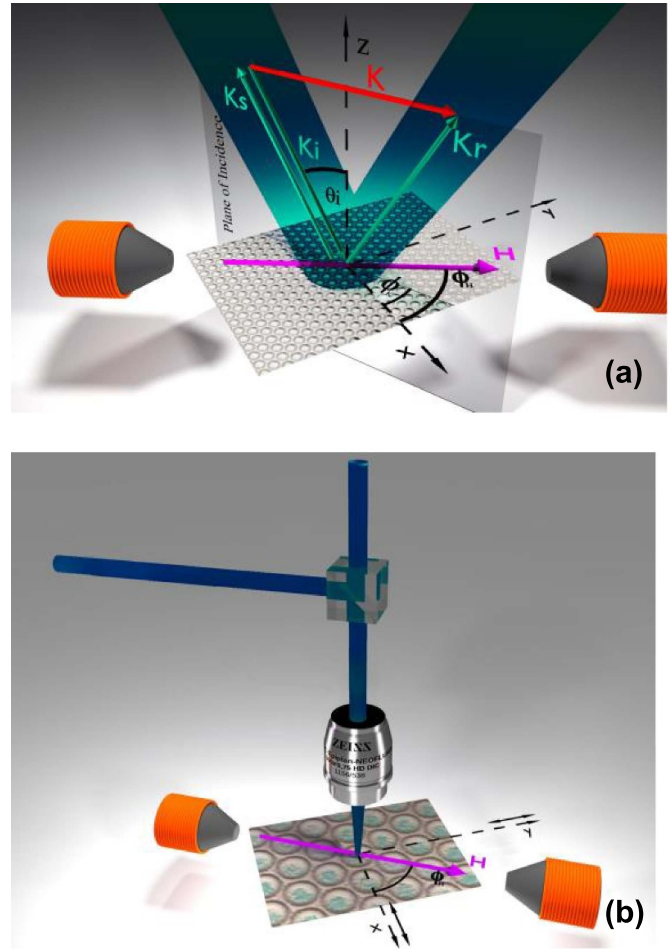


**Figure 7.** (a) Scattering geometry of the conventional BLS experiment in the so-called back-scattering configuration. The wave vector of the incident, reflected and scattered light is indicated, together with the in-plane direction of the applied magnetic field. The illuminated area of the sample has a typical diameter of 30–40  $\mu\text{m}$ . (b) Schematic drawing of the micro-BLS apparatus, where BLS is operated as a scanning-probe technique. The illuminated area of the sample has a typical diameter of 0.25–0.30  $\mu\text{m}$ .

such as magnon-spintronics [84, 85], chiral magnetism and topological spin structures [81, 82], Bose–Einstein condensation [87].

### Current and future challenges

As described in the previous paragraph, during the last two decades BLS has been adopted by several research groups all around the world, stimulated by the perspective of developing innovative devices for information and communication technology, where SWs are exploited as data carriers. With this technology, it is nowadays possible to conceive both analogic and digital devices operating up to several tens of GHz, with lateral dimensions of a few microns.



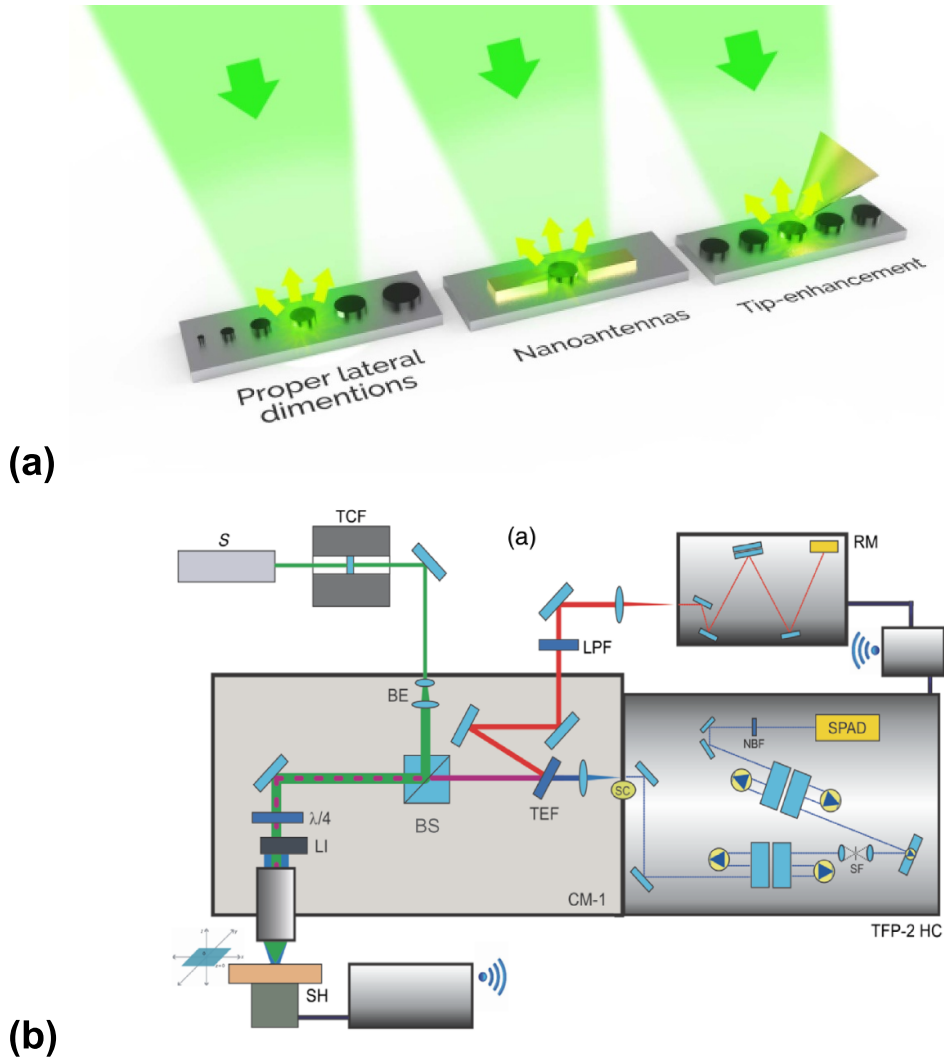


**Figure 8.** (a) Possible routes to achieve an enhancement of the BLS cross section from nanometric objects using plasmonic effects: realization of nanostructures made of low-damping plasmonic FM material (e.g. Ni) with the proper lateral dimensions, use of plasmonic gold nano-antennas to amplify the EF in the gap, tip-enhanced scattering using a gold tip. (b) Schematic picture of the integrated micro-BLS and micro-Raman setup consisting of a confocal microscope (CM-1), a TFPI (TFP-2 HC), and a Raman monochromator (RM). The sample is mounted onto a three-axes piezotranslation stage (SH) for mapping measurements. A polarizing beam splitter (BS) transmits the depolarized backscattered light through to the spectrometers. Immediately after, a short-pass tunable edge filter (TEF) transmits the quasielastic scattered light to the TFP-2 HC and reflects the deeply inelastic scattered light into the RM. Reproduced from [91]. CC BY 4.0.

Among the main challenges in the realization of such advanced magnonic devices one should include the scaling down, reaching high level of miniaturization and increasing the working frequencies [84–86]. Therefore, it will be crucial to efficiently observe the propagation of short-wavelength SWs with a proper spatial resolution, so that it is of utmost importance to further develop micro-focused BLS achieving a deeper lateral resolution and providing a sufficiently easy-to-use apparatus, also in terms of controlling software and automated sample positioning. These advances would also be beneficial to further application of BLS in the emerging field of chiral magnetism, where it has been established as the most powerful technique to quantify the interfacial DMI in magnetic films and multilayers [81, 82]. In this respect, a reduction of the acquisition time would represent a significant advance since ultrathin films have usually low signal and

one should limit the light power focused on the sample surface to avoid overheating. Also, it is expected that BLS will be able to give access to the dynamic eigenmodes of topological structures such as skyrmions, whose diameter is typically in the range 20–100 nm, provided that one may advance towards a further reduction of the lateral resolution of micro-BLS beyond the diffraction limit of light. Finally, driven by the perspective of lifting the operating frequencies of computing and communication devices beyond the GHz range, a remarkable current interest is towards short wavelength SW in, for instance, hybrid ferro- or ferri-magnetic/antiferromagnetic materials, where the THz regime can be achieved, as also discussed in section 11. SWs in such a frequency region have nanometric wavelengths, offering also good perspectives for the technological needs in terms of devices miniaturization.

## Advances in science and technology to meet challenges

In relation to the challenges outlined in the previous section, there are currently intense efforts to assist the adoption on BLS by more and more groups, achieving a fully automated operation of both conventional (i.e. wavevector-resolved) and micro-focused (i.e. spatial-resolved) BLS, as well as a better lateral resolution for the latter. To this respect, the recently established THATec-Innovation company [88], a spin-off of the University of Kaiserslautern, has developed useful software and hardware packages that are of great help in the conduction of BLS experiments, including the possibility of achieving phase and temporal resolution. The BLS lateral resolution is restricted by diffraction limit to about a half of the used wavelength, so that in the last years different groups have replaced the traditional green lasers with wavelength 514.5 or 532 nm by blue lasers with wavelength as low as 470 nm, achieving a better resolution and a higher scattering efficiency. This can be done at the price of optimizing optical coatings inside the interferometer to operate with a different wavelength. A further step to attain nano resolution would be to go beyond the diffraction limit in focusing the incoming light. A first attempt was made by Jersch *et al* [89] using a near-field optics, where the laser light was focused onto a tip of an atomic force microscope having a nanometre aperture and placed just few nanometres above the surface sample, achieving a spatial resolution of about 55 nm. However, this remained an isolated attempt, because of the extremely low signal strength. An alternative approach to consider in the near future could be the exploitation of plasmonic effects, as suggested in figure 8(a), using FM materials with low plasmonic damping (such as Ni), or the assistance of integrated plasmonic

(gold) nano-antennas or plasmonic tip [90] to produce an enhancement of the BLS signal from a selected nanostructure (see section 12).

Finally, in view of extending the operation frequencies to the THz regime, it could be useful to integrate the conventional BLS apparatus, based on the TFPI with a grating spectrometer usually exploited in Raman spectroscopy. Such an integration of micro-BLS and Raman apparatuses has been already exploited in bio-physics research, showing that this multimodal method enables the access to a wide spectral range, ranging from fractions of GHz to hundreds of THz (figure 8(b) [91]), and its extension to the research field of magnetism should be straightforward.

## Concluding remarks

In summary, during the last two decades BLS has become more and more popular for the analysis of the dynamical properties in nanomagnetic systems, given its unsurpassed capability in revealing SWs that is crucial for the emerging fields of magnonics and chiral magnetism. The considerable technical advances of the BLS experimental apparatus, including the possibility of micro-focusing and achieving phase and temporal resolution, with a high level of automation, have contributed to the widespread adoption of this technique. Further technical improvements, as overcoming the diffraction limit and reaching nanometric resolution are under development to keep pace with the miniaturization of nanomagnetic systems and devices. Moreover, extension to the THz range of frequencies would be desirable to assist the rise of operational frequencies of the next generation of devices for information and communication technology.

## 8. MOKE measurements of spin and orbital currents in nonmagnetic semiconductors and metals

Pietro Gambardella<sup>1</sup> and Gian Salis<sup>2</sup>

<sup>1</sup> Department of Materials, ETH Zurich, Hönggerberggring 64, Zurich CH-8093, Switzerland

<sup>2</sup> IBM Research-Zurich, Säumerstrasse 4, Rüschlikon 8803, Switzerland

### Status

Electric fields enable the generation and manipulation of spin and orbital magnetic moments in nonmagnetic conductors by means of SOC and orbital-selective processes. These effects are of great interest for both classical and quantum spin-based information processing in semiconductors as well as for the functioning of spintronic devices based on stacked magnetic and nonmagnetic materials, such as magnetic tunnel junctions, spin torque oscillators, and THz emitters. Owing to SOC, the orbital motion of electrons induced by an electric field can couple to the spin through two different mechanisms: spin-momentum locking of the conduction states, as in the Rashba and Dresselhaus effects, and spin-dependent scattering, as in the spin Hall effect. Whereas the former generates a uniform spin polarization or leads to coherent spin precession, the latter induces a spin current orthogonal to the direction of the primary charge current. Additional modulation of the electronic potential by strain, gate voltage, and stacking of different materials can be used to manipulate the spin orientation. Due to the interplay of spin diffusion and relaxation, both the Rashba and spin Hall effects induce a non-equilibrium accumulation of spins at the edges of a conductor, which can be probed directly through the MOKE [92–94] (figure 9(a) and sections 4, 6) or indirectly by spin torque and magnetoresistive effects [95].

Charge-to-spin interconversion processes have been extensively studied by MOKE in semiconductors with a direct band-gap and spin–orbit-split valence band states, such as the III–V and II–VI compounds [92, 93, 96]. Recently, MOKE investigations have been extended to nonmagnetic metals to probe the spin accumulation induced by the spin Hall effect [94, 97] and Rashba effect at a metal/oxide interface [98]. One can differentiate three regimes of Kerr rotation measurements: (quasi-) static, pump-probe, and noise spectroscopy. In the quasi-static case, the non-equilibrium spin polarization is observed as a function of a slowly varying magnetic field or electrical current. Transport of spins by drift or diffusion can be measured directly by spatially scanning a tightly focused probe beam with respect to a position where spin polarization is generated either electrically [99] or by optical orientation from a pump beam [96, 100], see figures 9(b) and (c). Using short laser pulses enables a time-resolved detection of spin transport that provides fundamental insight into spin decay mechanisms,  $g$ -factors, spin–orbit interaction, and hyperfine interaction with nuclear fields. Noise spectroscopy

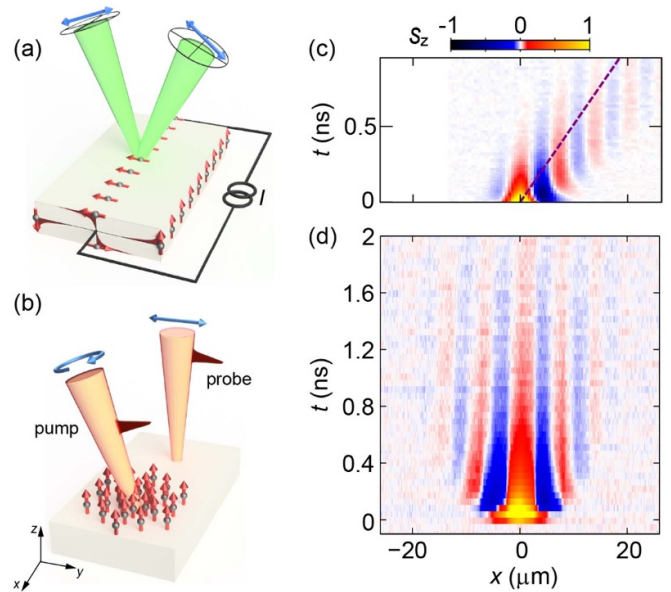


**Figure 9.** (a) Schematic of the spin Hall effect induced by electric field and optical detection of the spin accumulation. The shaded areas represent the spin accumulation profile. (b) Schematic of the spin accumulation induced by an optical pump and spin diffusion with momentum selected by relative position of pump and probe spots. Measurements of spin drift (c) and spin diffusion (d) in GaAs quantum wells where the spin–orbit interaction leads to a coherent precession of spin polarization resulting in oscillations of the out-of-plane spin component  $s_z$ . (c) and (d) Reproduced from [96], with permission from Springer Nature. Reprinted (figure) with permission from [100], Copyright (2016) by the American Physical Society.

performed by measuring at a high bandwidth the Kerr rotation of a continuous laser probe [101] also provides information on  $g$ -factors and spin dephasing times.

In addition to spins, MOKE is also a powerful tool to probe the electrically-induced orbital polarization due to the valley Hall effect and Berry curvature in 2D materials [102] and the orbital Hall effect in metals [103]. In the following, we discuss opportunities to further advance the use of MO techniques to probe charge-spin and charge-orbital interconversion processes and magnetic moment dynamics in nonmagnetic systems.

### Current and future challenges

Spin-momentum locking occurs at edges of 2D and 3D topological insulators and similarly in quasi-1D electron systems in the presence of spin–orbit interaction and magnetic field. In combination with proximitized superconductivity these material systems are also of interest for realizing Majorana zero modes. The direct observation of spin currents in such materials is an important scientific goal that will open new avenues for the generation and manipulation of spin polarization in topological systems. Further improvement of the sensitivity and spatial resolution in optical spin detection are needed to explore such effects. Polar MOKE (P-MOKE) is sensitive

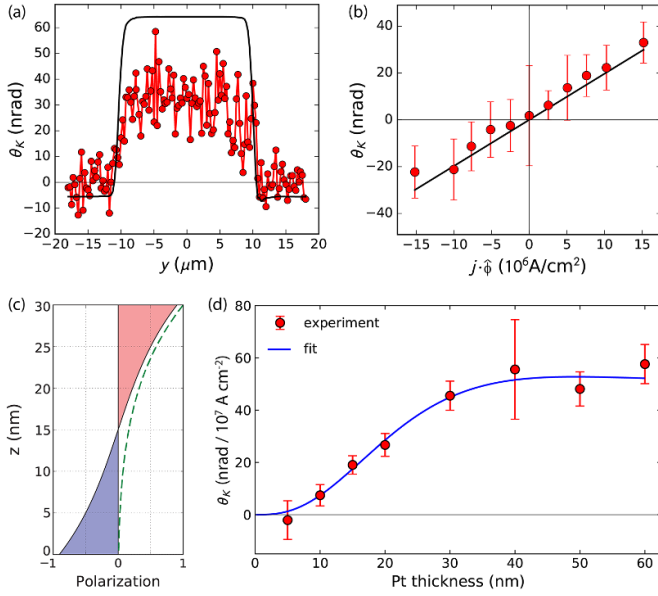


**Figure 10.** Kerr rotation  $\theta_K$  due to the spin Hall effect in Pt. (a) Line scan of  $\theta_K$  across a 20  $\mu\text{m}$ -wide, 15 nm-thick Pt wire at a current density  $j = 1.5 \times 10^{11} \text{ A m}^{-2}$  and (b)  $\theta_K$  as a function of  $j$ . The data points represent line scan averages; statistical error bars from averaging multiple line scans are indicated. The solid lines are linear fits to the data. Points left of the origin were measured with the reversed optical path,  $\hat{\phi}$ . (c) Depth profile of the calculated spin accumulation (shaded) in a 30 nm-thick wire for  $\lambda_s = 10 \text{ nm}$ . The dashed line represents the depth-dependent sensitivity of the MOKE. (d)  $\theta_K$  vs Pt thickness for  $j = 1 \times 10^{11} \text{ A m}^{-2}$ . The solid curve is a fit using a drift-diffusion model with  $\sigma_{xz} = 1880 \Omega^{-1} \text{ cm}^{-1}$  and  $\lambda_s = 11.4 \text{ nm}$  as free parameters. Reprinted (figure) with permission from [94], Copyright (2017) by the American Physical Society.

to the out-of-plane component of the spin polarization, but in some geometries also the in-plane spin component is of interest. For metals with spin polarization at the surface, this can be sensed with longitudinal MOKE (L-MOKE), but in semiconductors where polarized spins usually reside below the surface, the refraction of the beam along the sample normal suppresses the sensitivity to in-plane components. The development of methods to measure orthogonal spin components are therefore required. Furthermore, advances in combining high-bandwidth modulation of electric fields with synchronized detection of optical probe pulses will shed more light on the dynamics of spin current generation, also at the interface between nonmagnetic materials and FM metals.

In nonmagnetic metals, the spin and orbital accumulation generated by electric fields is usually detected indirectly through measurements of spin-orbit torques or magnetoresistance on an adjacent magnetic layer [95]. However, proximity effects, spin scattering, and interfacial SOC strongly influence the generation and relaxation of spins in magnetic heterostructures, preventing a precise determination of the spin and orbital conversion mechanisms and diffusion parameters in bare nonmagnetic metals. MOKE can overcome this problem, but investigations of metal systems remain challenging (see figure 10). The spin accumulation due to an applied

electric field  $E$  scales as  $s = \frac{\tau_s}{e\lambda_s} \sigma_{xy} E / e$ , with spin Hall conductivity  $\sigma_{xy} \approx 10^5 (1) \Omega^{-1} \text{ m}^{-1}$ , spin diffusion length  $\lambda_s \approx 1 - 10 \text{ nm} (1 - 10 \mu\text{m})$ , and spin relaxation time  $\tau_s \approx 0.1 - 1 \text{ ps} (1 - 10 \text{ ns})$  in 5d metals (III-V semiconductors) [92–94]. For typical  $E = 10^4 \text{ V m}^{-1}$ ,  $s$  is in the range of  $10^5 (10^2)$  spins  $\mu\text{m}^{-3}$  distributed over a distance  $\sim \lambda_s$  from the edge of the sample. This drastically limits the possibility of using P-MOKE to detect edge spins in metal systems. L-MOKE can be used to probe the surface spin accumulation, but with a lower sensitivity with respect to P-MOKE. In metals the probing depth is typically tens of nm, which complicates the measurement of the spin accumulation profile [94]. Additional complications arise from the large current density  $\sim 10^{10} - 10^{11} \text{ A m}^{-2}$  required to generate a sizable spin accumulation in metallic conductors, which causes Joule heating accompanied by thermoreflectance and mechanical drift.

### Advances in science and technology to meet challenges

The sensitivity of the Kerr rotation signal can be enhanced by engineering the interference of reflections from different layers or by embedding the spin-polarized region in an optical cavity [104]. The signal from spin noise measurements scales favourably with small spot sizes and by measuring noise correlations between two spatially separated detection spots also spin currents could be addressed [105]. Typically, in-plane spin components in semiconductors are made visible by letting spins precess in a transverse magnetic field. Alternatively, experiments with pump and probe beams on orthogonal surfaces (e.g. cleaved-edges of semiconductors) can access spins along different directions. Hexagonal 2D materials with broken inversion symmetry provide additional flexibility to generate spin and orbital magnetic moments by optical pumping and current injection. In such systems, the interplay of spin, orbital, and valley degrees of freedom can be tuned to an unprecedented extent by SOC, electrical gating, strain, and proximity effects, resulting in both edge and spatially uniform magnetization with relaxation time varying from ns to  $\mu\text{s}$  [102]. Another interesting application of MOKE would be to investigate the spin currents injected from quantum point contacts that exhibit a quantized spin-polarized conductance in a magnetic field. This requires optimization of the dopant profiles in semiconductor heterostructures during growth in order to obtain the target carrier densities under illumination. Cleaved-edge overgrowth of two quantum structures provide some of the cleanest quantum wires for such studies.

To detect electric field-induced spins and orbital moments in metals, different combinations of electrical and optical modulation schemes [94, 97] as well as MO ellipsometry (see section 9) can be used to improve the sensitivity of the measurements and reject spurious signals of thermal origin. Moreover, similar to semiconductors, the Hanle-effect can be employed to probe an in-plane spin polarization using P-MOKE by letting the spins precess about a magnetic field collinear to the current and develop a steady-state out-of-plane spin component [92, 93]. Distinguishing the Hanle effect from

magnetic-field induced artefacts, however, requires the Larmor frequency to be continuously varied up to  $\tau_s^{-1}$  and beyond, which in turns requires magnetic fields of several Tesla and/or cryogenic temperatures to increase  $\tau_s$ . Finally, quantitative measurements of the spin and orbital Hall conductivity also require precise calculation of the MO constants to separately extract the spin and orbital magnetization from the Kerr rotation [106].

### Concluding remarks

Taken together, steady-state and TR-MOKE measurements can greatly enhance the understanding of spin and orbital

currents generated by electric fields in quantum materials, topological systems, and spintronic devices. Pump-probe experiments performed with tunable photon energy and polarization further make it possible to selectively excite spin or orbital polarized carriers via optical selection rules in bulk as well as single-layer semiconductors, and follow their temporal evolution in response to electric and magnetic fields. Further improvements in sensitivity and spatial resolution would allow for extending MOKE investigations to a broader variety of phenomena, such as spin currents in quantum wires, edge states in topological insulators, orbital currents in metals and van der Waals heterostructures, and the chiral anomaly in Weyl semimetals.



## 9. Generalized magneto-optical (MO) ellipsometry (GME)

Andreas Berger

CIC nanoGUNE BRTA, Tolosa Hiribidea, 76, 20018 Donostia-San Sebastián, Spain

### Status

While both, conventional optical ellipsometry as well as ultrasensitive MOKE measurements had already been well-developed in the 1980s, it was the original study by Berger and Pufall [107] that demonstrated the viability of GME to experimentally determine the full plane-wave reflection matrix  $\mathbf{R}$  in a single experiment while achieving very precise results for its small MO components. The capabilities of this methodology were subsequently utilized by different groups to enable simultaneous optical and MO spectroscopy [108, 109] (see section 4), as well as MO vector magnetometry [109, 110].

Over the years, two dedicated experimental GME set-up types have been utilized and exhaustively tested, namely the original GME configuration using two nearly crossed polarizers, whose angle alignment is changed throughout the experiment (figure 11(a)) and the more recently developed T-MOKE ellipsometer design (figure 11(b)), in which the incoming arm polarizer is fixed and only the alignment of the elements along the reflected beam are being changed during the experimental measurement sequence [111]. Both designs have certain advantages and their respective performances have been tested in detail. However, other designs are certainly possible and ought to be tested to explore their achievable performance levels, in particular methodologies that utilize high frequency polarization modulation schemes, which should, at least in principle, have the potential to significantly reduce measurement times. In addition, integration of the GME methodology into commercial ellipsometers has been demonstrated [109].

Due to its very precise quantitative results, the GME method has been applied recently to investigate the effects of MO anisotropy [112], the impact of Quantum well states [113], and especially the magnetism of buried interface layers, which produce only rather small changes in MO signal levels but can nonetheless be very robustly detected [114]. Hereby, it is especially the GME enabled access to the full complex nature of the reflection matrix elements, which turns out to be of crucial importance [114]. Another strength of the GME methodology is its ability to separate true MO from false signals, given that the detected signal patterns exhibit specific symmetries, if they are indeed MO in nature [115]. This specific signal symmetry is also the reason, why different magnetization components can be so robustly separated from each other and make GME vector magnetometry so accurate, a fact that is apparent from the data shown in figure 12.

Certain aspects of the GME methodology have not been utilized so far and thus promise most significant advances in the future. One such example is its combination with ultra-fast experimental techniques, for which it promises to unambiguously disentangle optical from MO and thus magnetic

phenomena (see section 10). Another aspect that has not yet been utilized is the combined analysis of multiple data sets corresponding to different magnetic states. Such an approach should enable depth dependent materials analysis and magnetometry, which would be an extremely valuable tool, and would be reminiscent of the role conventional spectroscopic ellipsometry plays in determining the precise depth structure of multilayers. Such a capability would also be invaluable for spintronics, in particular transport-induced spin accumulation effects, which are very difficult to detect experimentally [94] and are normally only inferred from device performance data (see section 8). Thus, there is a wide bandwidth of scientific issues that would very much benefit from an extensive use and further development of GME.

### Current and future challenges

One of the two main challenges that have afflicted GME since its inception, and which have only marginally improved so far, is the issue of measurement time. In all dedicated experimental GME configurations, measurements are done as a function of applied field for a given optical element alignment, which is subsequently changed step-by-step. This leads to typical measurement times of about 30 min or more, which then corresponds to a full field-resolved sequence of GME-maps, of which some examples are shown in figure 12. While this measurement sequence and time is sensible for magnetization reversal studies, it is overly time consuming for other applications, in which only one magnetic state is explored. This problem is further compounded by the fact that not all optical element settings are equally useful for the GME data analysis, because the most relevant measurement points are *a priori* not known, given that the signal pattern itself depends on the sample properties, including its magnetic state. Only one serious attempt has been made so far to address this specific challenge, which led to the innovation of utilizing a diagonal GME-grid that contains more high-value data points [116], as illustrated in figure 12. However, this improvement, while meaningful was only modest in nature. Thus, novel pathways need to be explored to improve data acquisition and reduce measurement times by one or two orders of magnitude, which would allow for a far broader compatibility of this method with other measurements schemes, such as for instance time-resolved measurements, where complete measurements for a multitude of delay line settings are needed to achieve meaningful results (see section 10).

The other core challenge of the GME methodology is the complexity of its data analysis. While reflection matrix extraction is fundamentally straightforward, given that GME and T-MOKE ellipsometry approaches both have led to closed-form mathematical formulas [107, 111], which can be fitted by conventional software packages, implementations require some experience, because a multi-parameter phase space is being explored. So, corresponding expertise and skills have to be obtained, before GME data sets can be fully utilized. This data analysis complexity is even more relevant, when quantitative optical models need to be developed to analyse

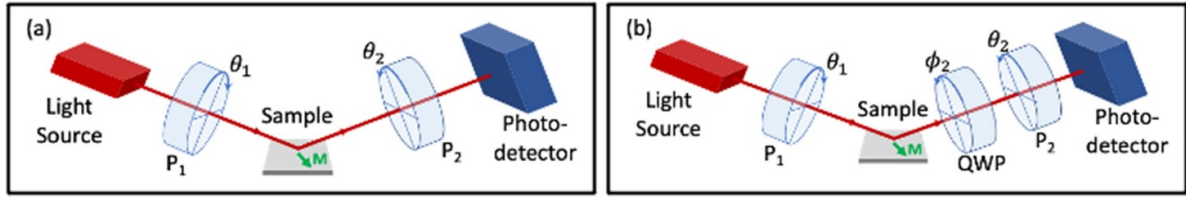


**Figure 11.** Schematic arrangements of experimental GME setups that have been utilized, namely (a) the conventional GME setup and (b) the more recently explored T-MOKE ellipsometry configuration; both detection schemes utilize a light source, which is a laser in most realizations, a linear polarizer  $P_1$  in the incoming beam, a second linear polarizer  $P_2$  in the reflected beam and a photodetector. The T-MOKE ellipsometry system in (b) furthermore contains a quarter wave plate QWP. In both approaches, a magnetic field sequence is applied to the sample to produce inverted magnetization states, whose signal difference at the photodetector is recorded for a sequence of optical element alignments. In (a), a series of polarization angle pair settings  $(\theta_1, \theta_2)$  for  $P_1$  and  $P_2$  is explored, while the methodology in (b) relies on a series of angle pair settings  $(\Phi_2, \theta_2)$  for QWP and  $P_2$ .

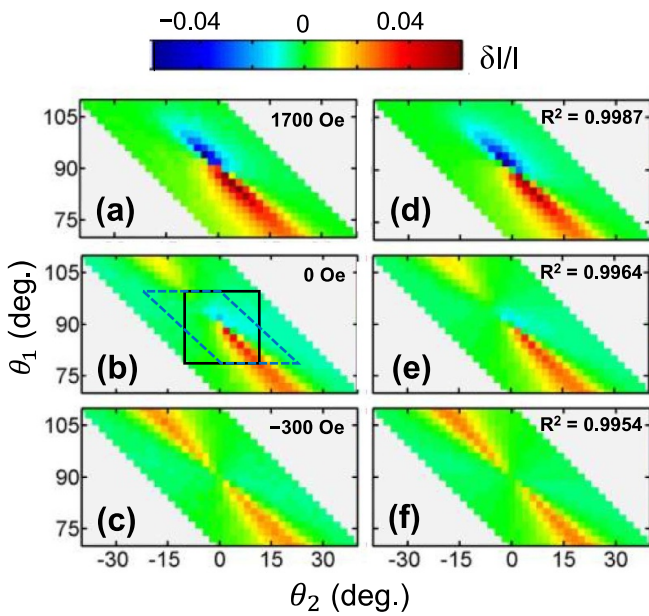


**Figure 12.** Experimental GME-data maps (a)–(c), measured for the same anisotropic sample at different applied field strengths, in comparison to their theoretical fit results (d)–(f), which are being employed to determine the complete reflection matrix  $\mathbf{R}$  of a sample and all the information contained in it. Figures (a) and (d) show results in which the longitudinal magnetization is largest, whereas the transverse magnetization behaviour is dominant in (c) and (f), visualizing the ability to separate magnetization components and conduct MO vector magnetometry with a single experimental setup. The legend on top applies to all sub-figures. (b) Indicates different data acquisition windows that are frequently used, namely square (black solid line) and diagonal (blue dashed line) shapes. Reprinted (figure) with permission from [112], Copyright (2015) by the American Physical Society.

reflection matrix data, which typically requires additional software implementations of such optical models, based on available matrix method approaches [117–120].

Other challenges, such as the integration of magnets into experimental ellipsometer set-ups and the further extension of the wavelength range that can be utilized for GME, are common challenges that affect basically all MO measurement techniques and thus, are not unique issues to be addressed by future GME developments alone.

### Advances in science and technology to meet challenges

Related to the challenge of reducing data acquisition times, there are presently three different pathways envisioned to achieve relevant improvements. The first and easiest to implement is the use of field modulation techniques, which have already been considered in some approaches [108, 111]. By using proper signal filtering and processing, improved sensitivities and reduced measurement times were demonstrated, which however did not constitute a complete breakthrough.

Very significant measurement time reductions should be achievable, if one were able to select the most sensitive experimental configurations only, which are however, dependent on the sample and thus the measurement results themselves. Thus, it will be necessary to develop data acquisition schemes that predict the most useful measurement configurations, based upon already acquired data in real time, using fast adaptive algorithms or artificial intelligence. Given the massive overdetermination of today's typical measurement sequences using about 400–500 optical element settings to determine the full reflection matrix, which itself contains only up to eight real-valued parameters, an improvement by an order of magnitude should in principle be achievable.

A completely different approach to significantly reduce measurement times would be the use of high frequency polarization modulation techniques, so that a very large number of detection conditions can be explored very fast. To receive the full benefit of the inherent advantages of GME, it will be necessary to facilitate a 2D scan of optical conditions, so that this approach will require 2 independent but synchronized modulation elements, as well as real-time signal sequence detection and processing. In principle, all optical components for such an approach exist, but have not been tested in a dedicated set-up to facilitate GME measurements, so that possible technical difficulties and resulting sensitivities are unknown to date.

A simplification of the GME data analysis is not really a scientific or technological challenge, but more related to the ability of the scientific community to develop broadly applicable and easy to use software modules that can address a wide variety of scientific topics in a reliable fashion.

## Concluding remarks

GME is an experimental technique that has wide-ranging capabilities, which have been only partially realized in the past two decades, leaving very substantial space for future instrumentation developments and even more so, for its application towards relevant scientific questions, including time-resolved phenomena. The most obvious ones are hereby the application of GME in ultrafast magneto-optics as well as for the detection and analysis of spin accumulation effects in spintronics. Further methodological advances will be very relevant as well,

not only to improve acquisition times, but also to break new ground in so far inaccessible areas, such as depth dependent magnetometry. A truly wide-spread usage of GME is quite possible, given that its equipment costs are very modest compared to other experimental techniques and its setups generally compatible with any kind of environmental condition. However, a future simplification of data analysis schemes or the development of a standard software package might be needed to achieve a broad acceptance by the relevant scientific community.

## 10. Ultrafast magneto-optics

Markus Münzenberg<sup>1</sup> and Martin Schultze<sup>2</sup>

<sup>1</sup>Institute of Physics, University of Greifswald, Greifswald 17489, Germany

<sup>2</sup>Institute of Experimental Physics, Graz University of Technology, Petersgasse 16, Graz 8010, Austria

### Status

Ultrafast magneto-optics started only 25 years ago with the discovery of ultrafast magnetization dynamics entering the sub-picosecond region by Beaurepaire *et al* [11]. The conceptually new tool were ultrafast lasers delivering intensive optical pulses lasting less than 50 fs [121]. This short flashes of light with durations competing the characteristic timescale of lattice dynamics allow to launch far from equilibrium excitations of a solids' spin system and permitted the development of concepts for probing the dynamics of both the electronic and the magnetic response of the system.

First experimental studies using this new tools observed surprisingly fast light-induced demagnetization events in bulk nickel. Fuelled by a number of follow up studies particular interest arose around the evolution of suspected transient states of the spintronic configuration. The experiments mark the onset of lively and opinionated debate reflecting the full complexity of the interplay between light, charges and spin in solids. One example is the controversy around the microscopic origin of the observations.

Might the observations be only due to transient modifications of the magneto optical constants or is 'real' spin physics on femtosecond timescales the underlying effect [122]? The debate was resolved and the observed effects identified to be indeed due to the latter over the last two decades [123]. This exemplifies the complexity of MO experiments with their non-trivial depth and polarization sensitivity as further detailed in sections 4 and 9 of this roadmap. But also reveals the broad range of possibilities offered by magneto-optics not only to detect but also to manipulate spins: ultrafast magneto-optics is more than an ultrafast magnetometer. It turned out to be a versatile tool for detection and manipulation of transient magnetic states on previously inaccessible timescales down to 1 fs ( $10^{-15}$  s) region. The impact of the laser pulse on the spin system depends on the exact excitation pathways, which offers many choices as exemplified in sections 1 and 2 of this roadmap and including probabilistic Joule heating as driver of ultrafast spin fluctuations and phase transitions [123] up to spin current excitations on nanometre length scales [124].

Additional control knobs are the excitation light-waves' time-varying properties (amplitude, polarization, instantaneous frequency) that can induce transient spin polarization effects in oxides [125] and metals [126, 127] (figure 13(b)). And the light field can create spin current and spin fluctuations via optical transitions that are creating hot electrons. These out-of-equilibrium electronic occupations in the correlated FM state decay into spin currents and, via Stoner excitations,

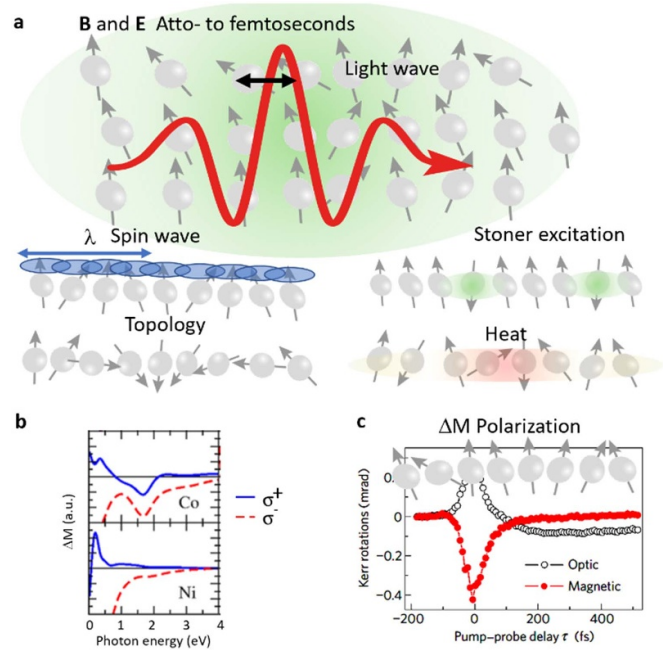


**Figure 13.** (a) Ultrafast and—strong optical waveforms can act on electronic degrees of freedom with their field transients in sub-femtosecond time intervals. The resulting non-equilibrium state can decay into a multitude of excitations of the spin system, from single spin excitation (Stoner excitations) to SW textures, from heating (FM phase transition) to the formation of complex spin structures. (b) In the presence of the laser field, a polarization induced magnetization can be found, consisting of spin and orbital moments [126]. (c) In ultrafast MO experiments, signatures of coherent coupling between the light field and the magnetic response have been observed [127].

into spin-wave excitations that have their inherent spatial and temporal dependencies in the nanometre—femtosecond time-space frame—and launch multi-time-and-lengths-scale dynamics linking the quasi-instantaneous response of individual carriers to orders of magnitude slower, macroscopic charge and spin transport processes. Observation of the entire transient phenomenology thus calls for MO methods that offer sufficient spatial (cf sections 6 and 14) and temporal resolution spanning a challenging dynamic range.

### Current and future challenges

A versatile and element specific approach to track the magnetic moment relies on M and L-edge core transitions [14]. Femtosecond slicing at synchrotron sources, laboratory based high harmonic generation (HHG) and the upcoming experiments at FELs (see section 15 of this roadmap) are generating an enormous amount of knowledge about the interplay of light, matter and the (transient) properties of the spin system on timescales competing with the period of even the fastest vibrational lattice excitations. This temporal resolution is linked to the duration of the light or x-ray pulses of such sources ranging from 25 femtoseconds to picoseconds and allows taking steps towards disentangling the influence of charge-relocations and lattice motion on the instantaneous magnetic



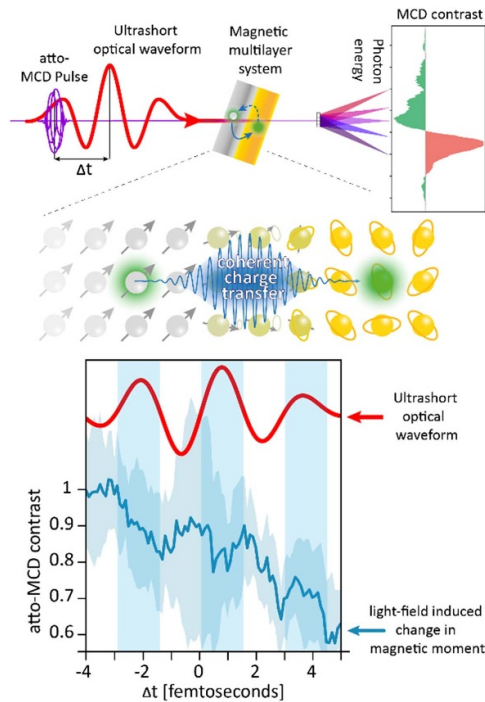


**Figure 14.** Circularly polarized attosecond XUV pulses addressing M-edge transitions in magnetic materials allow time tracking the early-time evolution of a samples' magnetic moment after an external optical stimulus (here a laser excitation pulse). Light-induced carrier separation in a layered material can result in charge and spin transport across an interface and cause a change in the magnetic moment of the individual layers as fast as the electronic excitation acts out. This allows for the fastest control of macroscopic magnetic moments observed to date.

moment. Most recently, experiments combining ultrafast laser sources and optimized HHG for attosecond pulse synthesis can granulate time into even finer increments and track and control the evolution of magnetic and electronic properties at the few-femtosecond timescale on which electron dynamics act out and before the lattice re-configures noticeably (figure 14) [128].

The required laser systems providing intense light fields lasting less than two cycles of the carrier wave at visible-infrared (VIR) and NIR wavelength are now commercially available and allow actual control of a samples electronic configuration via the oscillating electric field (i.e. 1–2 fs transient time) rather than through the much longer pulse duration defined by the intensity envelope. Such ultrafast optical waveforms can control electrons in spin-correlated systems within a single optical half-period (i.e. at hundreds of THz frequencies) and act on the electronic distribution before electronic correlations and dissipation destroy the initial coherence. This advance fuels the hope for the next generation of light-based spintronic applications that can be coherently controlled by a light wave (viz. switching between states without dissipation) and realize magneto-optic control at hundreds of THz to Petahertz clock rates. On the other side of the electromagnetic spectrum, in the (near) infrared region towards the THz gap (1–10 THz), new tools based on semiconductor quantum well

heterostructures, shift currents and spintronic THz emitters, studies are emerging where spin currents at the Fermi level are driven or selective phonon- spin and magnon excitations using few cycle and unipolar THz light pulses [129, 130].

### Advances in science and technology to meet challenges

The new experimental capacities in laboratories and at FEL and synchrotron sources propel the development of novel theoretical frameworks (see section 2) with the hope to trace back the rich phenomenology of magnetism to more universal microscopic concepts. Currently, even though there is a fairly good understanding of what goes on if we excite a ferromagnet with ultrafast laser pulses, the complexity of the multiscale challenge still sparks controversial discussions. A central aspect is the complexity of the correlated electronic state that couples to the spin states and the modification of this many-body state by the presence of EFs, heat and crystal strain. Further, since the exchange interaction between two configurations can be understood as a combination of Coulomb interaction and Pauli exclusion principle applied to the multi-electron state, it appears that transient out-of-equilibrium states can re-route the interaction pathways in the multi-spin state. This is the multi-dimensional analogy to the single electron Stoner excitations which are the prototype of a local spin excitation. As a corollary, more complex excitations or delocalized spin-waves can be regarded as a decay into Stoner superpositions.

SOC between magnetic and orbital moment poses additional challenges in understanding quickly evolving spin dynamics kicked off by an external stimulus. The coupling results in spin-mixing (Elliot-Yafet) of the two spin states with regard to the quantization axis, it is the origin of magnetic torque, spin-flips, spin-to charge conversion, coupling of the spin to lattice degrees of freedom and can result in complex spin-structure (symmetry-breaking interlayer DMI) with topological features.

To add complexity, spin-momentum can not only be transported via spin-excitation but also by charge transport. Charge currents can be spin-polarized due to a spin selective excitation mechanism or a spin selective interfacial filtering effect as additional source of spin-momentum transport which, owing to its different microscopic dependencies can be even more efficient in transferring momentum.

The above epitome symbolizes how the challenge in understanding a dynamical magnetic phenomenon lies in the most appropriate identification of the stimulus—and experiments with sufficient temporal resolution. What is excited?—What are the details of the process chain from photon absorption to the non-equilibrium electronic states in the system correlated to multi electron states and finally the conversion to information and heat? Generally, that corresponds to following the process from a non-thermal excited state still carrying the memory of coherence of the excitation field to the thermalized non-coherent stochastic and highly dynamic spin ensemble.



Exploiting this multi-scale wealth of couplings is a bulging reservoir of research challenges revolving around phase coherence and spin momentum control, spin-currents and spin torques, spin Hall effects, spatial spin topologies, phase transitions, vortex and topology control and spin caloritronic processes on the nanoscale, to name a few [131, 132]. With ultrashort and intense light fields, we anticipate novel ways to manipulate complex system correlations and the renaissance of a number of low-frequency spintronic functionalities at optical clock-rates. The switching of topological properties of transient light-matter states might become accessible in strong-field dressed systems as a new platform for spin-based information technology. And recent advances in light-wave electronics call for the integration of spin degrees of freedom in opto-electronic circuitry that is driven by ultrafast light-transients.

## Concluding remarks

Based on the profound understanding that decades of in-depth investigations of static and transient magnetic phenomena propelled by ever shorter light bursts have yielded, the ultrafast magnetism community now sets out to explore the new realm of coherent spintronics. Ultrafast light fields creating dynamic light-matter states as a new coordinate for system manipulation and the creation of function will allow exploring transient MO effects the manipulation of functional spin systems and correlated electrons. This novel regime of light-dressed material properties holds promise for novel functionality, more efficient and faster signal manipulation in spintronic applications, ultrafast and dissipation free state control and exciting new phenomena that to a large extent might be still beyond our current imagination.

## 11. Ultrafast magneto-optics and magneto-acoustics with exchange magnons

Vasily Temnov<sup>1</sup>, Igor V Bychkov<sup>2</sup> and Leonid Kotov<sup>3</sup>

<sup>1</sup> LSI, Ecole Polytechnique, CEA/DRF/IRAMIS, CNRS, Institut Polytechnique de Paris, Palaiseau F-91128, France

<sup>2</sup> Chelyabinsk State University, Department of Radio-Physics and Electronics, Chelyabinsk 454001, Russia

<sup>3</sup> Syktyvkar State University, Syktyvkar 167000, Russia

### Status

Whereas the majority of ultrafast time-resolved all-optical pump-probe experiments in magnetic materials probe the THz-frequency MO spectra (see section 18), the dynamics of ultrafast demagnetization (see section 10) and/or spatially homogeneous precession of magnetization vector (FM resonance, FMR), here we review some works on optically triggered excitation of SWs. SWs at nanometre wavelengths are dominated by exchange interactions and are called exchange magnons. Ultrafast optics is needed to (a) excite exchange magnons and (b) probe their dynamics using conventional TR-MOKE measurements [133–137], see figure 15.

A variety of time- and space-dependent excitation stimuli has been used to excite exchange magnons, all of them taking an advantage of the non-zero spatial overlap of their eigenmode functions with a spatially inhomogeneous excitation stimulus acting on the time scale that is shorter than the magnon oscillation period. The direct optical excitation (within  $\sim 10$  nm optical skin depth) [133, 134], injection of ultrashort pulses of spin-polarized electrons (within the spin diffusion length  $\sim 1$  nm) [135], combined action of laser-excited thermal and coherent acoustic phonons [136] or ultrashort acoustic pulses injected in the FM thin film (on ‘acoustic’ length scales) [137]. Whereas the majority of aforementioned experiments resulted in excitation of  $\sim 10$  GHz frequency magnons, only technically sophisticated experiments with ultrashort spin current pulses [135] in metal-ferromagnet multilayer structures have been shown to break the ultimate THz frequency limit. Generation of exchange magnons in the THz spectral range with different experimental metrologies would allow not only for establishing technologically relevant frequency and efficiency limits of ultrafast magnonic logics but also to investigate fundamental mechanisms in ultrafast magnetization dynamics [138–140] and reveal possible contributions of magnon excitation to ultrafast non-thermal magneto-elastic magnetization switching [141]. Moreover, investigations of exchange magnons provide a useful platform for quantitative spectroscopy of complex magnetic materials in terms of magnetic anisotropies, exchange stiffness and Gilbert damping parameter  $\alpha$  [134].

Optical detection of exchange magnons relies on various TR-MOKE configurations: different vector components of exchange magnons can be extracted from the

dynamics of time-resolved Kerr rotation or ellipticity signals (P-MOKE/L-MOKE) or intensity modulation (transverse MOKE). TR-MOKE signals average the spatially inhomogeneous magnon mode over the skin depth of probe radiation [134, 135]. Therefore, the detection efficiency of standing magnon modes with shorter-than-skin depth wavelengths rapidly decreases with the magnon order  $n$  rendering their detection extremely difficult [135].

### Current and future challenges

Leaving apart the technical issue with detection efficiencies, here we propose to improve the excitation efficiency of exchange magnons through understanding their generation mechanisms. Among all aforementioned excitation mechanisms of exchange magnons the ultrafast magneto-elastic with coherent acoustic phonons deserves special attention since (a) it does not rely on thermal effects and is energy-efficient for this reason, (b) could profit from independent optimization of acoustic and magnetic degrees of freedom and (c) allows for elegant analytical treatment of phonon–magnon interactions. A general theoretical analysis of Landau–Lifshitz–Gilbert equations accounting for exchange interactions suggests that excitation of exchange magnons is described by an equation of an externally driven damped harmonic oscillator:

$$\frac{d^2 s_z^{(n)}}{dt^2} + 2\alpha\omega_n \frac{ds_z^{(n)}}{dt} + \omega_n^2 s_z^{(n)} = A_n \int_0^L \varepsilon_{zz}(z, t) \cos(k_n z) dz,$$

where the time-dependent external driving force is determined by an arbitrary longitudinal strain pulse  $\varepsilon_{zz}(z, t)$  propagating inside the magnetic layer, magnon modes are described by cosine functions, and the prefactor  $A_n$  depends on the details of the experimental geometry, notably the magnitude and the direction of an external magnetic field, and material properties (magnetostriction coefficient) [142]. Being a simple analytical tool for experimental physicists, this equation highlights the importance of quantitative characterization of acoustic pulses injected in a FM layer. Whereas elastic boundary conditions need to be taken into account in order to quantify transmission and reflection coefficients at interfaces between the FM thin film and adjacent media, the precise determination of time-dependent acoustic transients inside the FM layer represents a technically solvable task. Given the intrinsic complexity of magneto-elastic interactions, which is often being reduced to the attempt to satisfy phase-matching conditions for phonon and magnon dispersion curves, one would need to identify the dominant property of acoustic pulses which would enable efficient generation of THz frequency exchange magnons.

The results of a simple simulation for the magneto-elastic generation of exchange magnons in a 30 nm nickel thin film by ultrashort unipolar acoustic pulses of different durations of 1, 2 and 3 ps (figure 16) answer this question. The magnetization dynamics (figure 16(a)) and their Fourier spectra (figure 16(b))

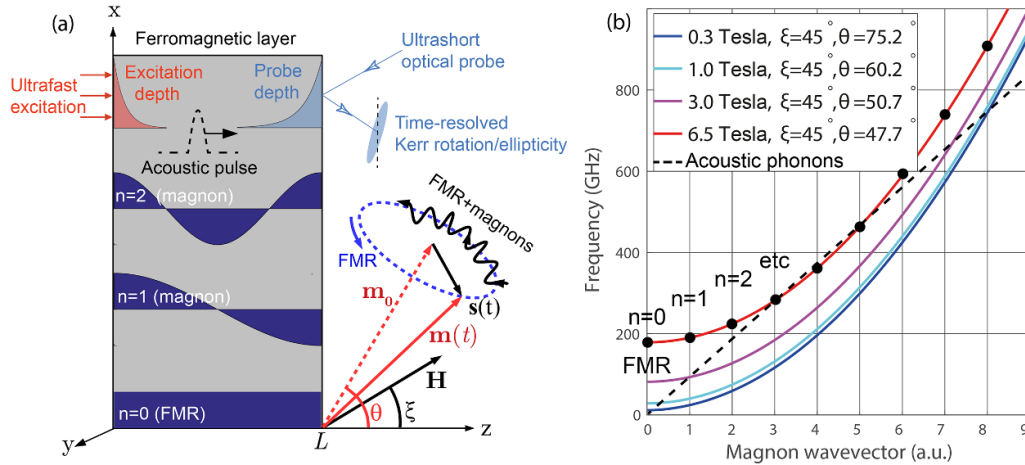


**Figure 15.** (a) Standing SW resonances  $n = 0$  (FMR),  $n = 1, 2$ , etc in FM thin films can be excited by various ultrafast excitation stimuli, including those propagating inside the material (acoustic pulses), and probed with ultrafast MO Kerr spectroscopy within the optical penetration (skin) depth of probe pulses. The resulting ‘local’ magnetization dynamics  $\mathbf{m}(t) = \mathbf{m}_0 + \mathbf{s}(t)$  represents a superposition of FMR and high-order magnon precessions around the stationary magnetization direction  $\mathbf{m}_0$ . The schematic illustrates a typical geometry with non-collinear magnetic field and magnetization vectors in FM thin films. (b) The amplitude and/or direction of an external magnetic field can be used to lift up the parabolic dispersion curves of exchange magnons, but also control their intersection (phase-matching) points with acoustic dispersion. Reprinted from [142], Copyright (2020), with permission from Elsevier.

strongly depend on the duration of acoustic pulses, presumably because of the difference in their spectral bandwidth. The first conclusion from these simulations is that only exchange magnons with frequencies *within the acoustic bandwidth* can be efficiently generated. Therefore, the first challenge of for THz magnonics would be to inject THz-frequency acoustic pulses in FM thin films. The second observation is that amplitudes of low-order magnon modes (vertical axis is truncated) are still much higher. The solution to this problem would be to generate sharp acoustic resonances at frequencies coinciding with those of the desired magnon modes. Therefore, from the perspective of ultrafast magneto-acoustics, the key (technical) parameter to boost the excitation of high-frequency exchange magnons is related to the spectrum of acoustic pulses injected in FM thin film.

The previous discussion assumes that magnon spectra in the THz spectral range are well-known. This assumption has been questioned recently by the incorporation of *inertial effects* in the magnetization dynamics [138, 139], leading to dramatically different magnon dispersions [140]. Figure 16(c) shows the anticipated theoretical dispersion relations for magnons with two distinct branches: precessional magnons (lower branch, discussed previously) and nutation magnons (upper branch), emerging as a consequence of magnetic inertia [140]. Simulations were performed for Gd-doped Py thin films, where the strong dependence of magnetic parameters (including exchange stiffness and Gilbert damping) on Gd-concentration was extracted from all-optical experiments with  $\sim 10$  GHz-frequency exchange magnons [134]. The scientific challenge of THz-frequency magneto-acoustic spectroscopy would target identifying unknown dispersion relations and Gilbert damping of magnetic excitations in complex magnetic materials in the THz-frequency range.

## Advances in science and technology to meet challenges

A promising way to tailor the efficiency of magneto-acoustic excitations is to design samples with desired acoustic properties. Previous efforts have shown that the use of freestanding nickel membranes, acting as an acoustic cavity, allowed for the *resonant enhancement* of the excitation amplitude of FMR-precession at GHz frequencies [143]. However, no fingerprints of magnon excitation with  $n > 0$  have been reported in these experiments, presumably because of a large (300 nm) thickness of a freestanding nickel film resulting in spectrally overlapping and thus indistinguishable magnon modes. Following this research line, experiments with thinner freestanding FM membranes and/or multilayers would provide better chances to isolate or individually tune frequencies of magnon and phonon resonances.

An alternative approach would be to design hybrid structures with integrated semiconductor superlattices, acting as acoustic transducers, which are capable of generating well-defined sharp acoustic transients in the THz frequency range [144]. Long-lived coherent longitudinal acoustic phonons at THz frequencies, observed in these experiments, could be injected in thin layers of magneto-strictive materials to resonantly excite individual spin-wave resonances.

Excitation of large amplitude magnon pulses represents another big challenge in the context of nonlinear magnetization dynamics and magnetization switching in FM nanostructures [139]. Whereas playing with shapes of FM nanostructures is definitely important, another engineering parameter is the strength of magneto-elastic coupling that can be increased in complex rare-earth based magnetic compounds such as Terfenol-D. Since doping generally changes

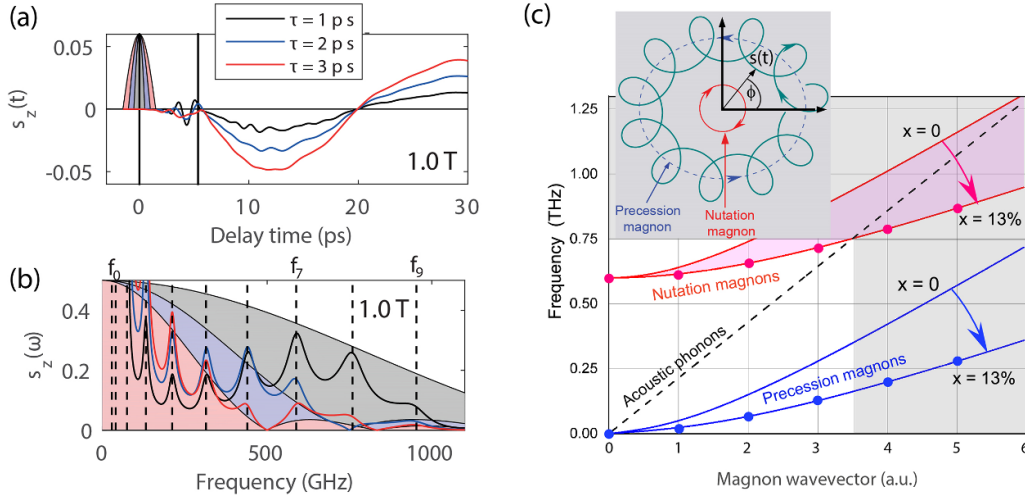


**Figure 16.** (a) Ultrafast magnetization dynamics driven by a single acoustic pulse traversing through a 30 nm thin layer of FM nickel shows that (b) nearly all exchange magnon modes within the acoustic bandwidth can be excited. Dashed coloured areas in (a) and (b) show temporal profiles and Fourier spectra of three distinct acoustic pulses with 1, 2, and 3 ps time duration, respectively. Reprinted from [142], Copyright (2020), with permission from Elsevier. (c) When experimentally accessible, THz-frequency magneto-elastic interaction spectroscopy could be used to quantify the phenomenon of the inertial magnetization dynamics [138, 139], which should manifest itself in the appearance of an upper (THz-)frequency band of nutation magnons [140]. Simulation performed for Gd-doped Permalloy thin films  $\text{Gd}_x\text{Py}_{1-x}$ , characterized through  $\sim 10$  GHz-frequency time-domain exchange magnon spectroscopy [134]. The inset shows an exemplary flower-like magnetization trajectory consisting of two magnon modes from different branches, which are precessing in opposite directions. Reprinted (figure) with permission from [140], Copyright (2021) by the American Physical Society.

not only the magneto-elastic but also magnetic properties [134], the design on an efficient magneto-elastic structure for high-frequency magneto-elastics becomes a multiparameter optimization problem.

An exciting perspective in high-frequency magneto-acoustics with quasi-monochromatic acoustic waves is provided through the potential application of transient grating (TG) geometry [145, 146] in the sub 100 nm range of periodicities using ultrashort x-ray free electron laser (XFEL) sources (see section 15). In an XFEL TG-pump—MO probe experiment on FM thin films one would expect  $\sim 100$  GHz frequency exchange magnons to be driven not only by Rayleigh surface acoustic waves but also with rather exotic Sezawa and pseudo-Sezawa modes [145].

## Concluding remarks

In conclusion, we have discussed a simple experimental configuration for generation and detection of high-frequency exchange magnons in FM thin films by different fs-laser-triggered optical stimuli. We focused on the magneto-acoustic excitation mechanism using ultrashort acoustic pulses, which

is not accompanied by unwanted thermal effects. The possibility to excite high-frequency exchange magnons appears to be limited by the spectral bandwidth of acoustic pulses injected in FM thin films. Possible strategies to tailor acoustic spectra rely on using free-standing FM membranes or hybrid multilayer structures incorporating semiconductor superlattices acting as THz-frequency opto-acoustic transducers.

The capability to tune magnetic resonances through acoustic resonances by applying external magnetic fields with experimentally feasible magnitudes of the order of 1 Tesla, as discussed in figure 16, provides a unique opportunity to quantify amplitudes and lifetimes of THz-frequency exchange magnons in complex magnetic materials. As an example, the impact of inertial effects on magnon dispersions could be identified in this kind of measurements.

Further theoretical analysis in high-frequency magneto-acoustics should help identifying the role of phase-matching conditions, magnetic and acoustic boundary conditions [137] in generating large-amplitude magnon precession in magnetostrictive materials. It is expected to facilitate the experimental studies targeting the magnon-assisted parametric [146] and nonlinear magnetoacoustic dynamics [147].

## 12. Magnetoplasmonics

Paolo Vavassori<sup>1,2</sup> and Nicolò Maccaferri<sup>3,4</sup>

<sup>1</sup> CIC nanoGUNE BRTA, Tolosa Hiribidea, 76, 20018 Donostia-San Sebastián, Spain

<sup>2</sup> IKERBASQUE, Basque Foundation for Science, Plaza Euskadi 5, 48009 Bilbao, Spain

<sup>3</sup> Department of Physics, Umeå University, Linnaeus väg 24, 901 87 Umeå, Sweden

<sup>4</sup> Department of Physics and Materials Science, University of Luxembourg, 162a avenue de la Faïencerie, 1511 Luxembourg, Luxembourg

### Status

As discussed in sections 1 and 3, the MO effects manifest in a magnetic-field-modulation of the polarization and intensity of reflected and transmitted light. Therefore, the integration of MO-active materials in nanophotonics is particularly appealing since light states are utilized as information carriers in a plethora of applications ranging from optical communications and sensing, to imaging and quantum technology. Indeed, MO nanomaterials are very promising as they would enable a reliable, active, and fast manipulation of light properties at the nanoscale for future nanophotonic applications (active photonic devices, GHz and even THz optical nanomodulators, MO memories based on magnetoplasmonic architectures, etc). In addition, MO effects break the symmetry of time inversion (Lorentz reciprocity). Therefore, yet another and most direct application to nanophotonics would be the implementation of nanoscale optical isolation in nonreciprocal nanoscale devices.

Unfortunately, ordinary magnetic materials with sufficiently strong MO effects in the frequency range of interest (VIS and NIR/mid-infrared (MIR)) do not exist and this has been the roadblock in both the miniaturization of optical isolators and the development of magnetically controlled nanophotonic devices. The lack of strong MO materials has unleashed extensive research on exploiting the peculiarities of optics at the nanoscale to enhance MO effects. Nanoscale optical effects have been exploited to slow down light to increase interaction time with the MO materials and to increase the electrodynamics that results in the optical and MO effects. A variety of structures have been scrutinized, such as FM [148] and hybrid FM/noble metal nanoresonators [31], plasmonic and photonic crystals [149, 150], and more recently hyperbolic and epsilon-near-zero metamaterials [151], which are promising in optical circuitry, especially for buffering, switching, and time-domain processing of optical signals. This intense search triggered and has been nursed by the dramatic and parallel advances in the sensitivity and spatio-temporal resolution of characterization methods and tools. For instance, the development of advanced ultrafast spectroscopy techniques to unveil the temporal dynamics of charges and spins in MO nanomaterials, will open a plethora of opportunities in a variety of research areas based on magneto-photonic

processes and their coherent control (see also sections 10, 11 and 18).

### Current and future challenges

One of the most investigated paths to boost the weak MO-induced modulation of light is to exploit the strongly enhanced electrodynamics produced by the excitation of localized plasmon resonances (LPRs), i.e. the collective oscillations of the quasi-free electrons to amplify the MO response in metallic nano-antennas. However, the generation of a large MO response comes at the price of a parallel enhancement of radiated light with the original polarization. This seemed an unsurmountable limit for the maximum achievable amplification of magnetic-field activated change in polarization and intensity of reflected and transmitted light.

There is an on-going search of materials that could allow reducing the losses (both radiative and ohmic) and increasing the MO activity. Challenges here come from the fact that in the VIS–NIR range it seems that there is not a better option than the metals conventionally utilized [152]. In the NIR–MIR range, insulating ferrimagnets (see section 13) and conductive oxides have been proposed as a better alternative to metals [153]. This lack of materials has also pushed the search for metamaterials, such as hyperbolic and epsilon-near-zero metamaterials. These systems are extremely versatile since they display hyperbolic (or indefinite) dispersion and show conductive or insulating properties depending on the spatial direction considered. They also look extremely promising for a plethora of applications, such as light-driven ultrafast information processing [154] and might become a key platform for ultrafast coherent MO recording. Finally, extensive efforts are currently devoted to broadening experimental and theoretical studies to the temporal domain (see sections 10 and 18), in particular on the sub-ps time range where non-thermal effects occurs, e.g. carrier–carrier scattering, the main mechanism involved in the charge-spin interaction below 100 fs (see upper panel in figure 17). In this framework, particularly interesting would be the study of plasmon dephasing (happening on the time scale of few tens of fs) on the spin dynamics in MO-active nanomaterials (see lower panel in figure 17). Only very recently people have started to explore ultrafast dynamics in nanoscale MO systems [155, 156].

### Advances in science and technology to meet challenges

A promising path recently proposed to circumvent the limitation posed by the parallel amplification of the light with the original polarization that is needed to produce the enhancement of MO activity in magnetoplasmonic nanoantennas, is to exploit hybridization of the dipolar mode induced by the incident light with dark modes in specially designed dimeric nanostructures. The underlying concept is illustrated in figure 18 for the magnetoplasmonic nanocavity reported in the literature [31]. The drawback of the proposed nanocavity structure



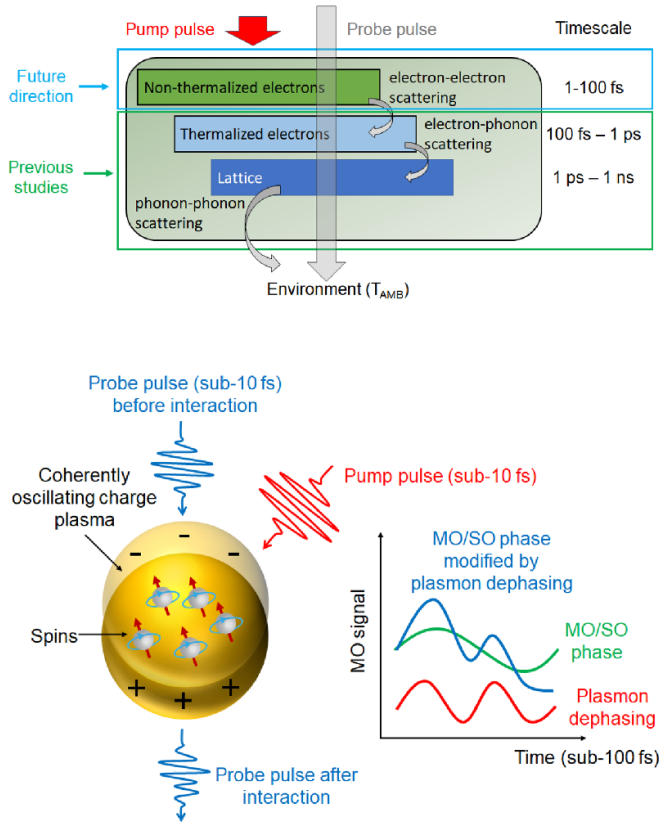


**Figure 17.** Ultrafast dynamics of non-thermal electrons in magnetoplasmonic nanostructures. Upper panel: schematics of current and future directions in ultrafast magnetoplasmonics. The study of non-thermal pathways in nanoscale magnetoplasmonic materials might represent a leap towards low-dissipative and ultrafast MO information processing. Lower panel: study of plasmon dephasing on the spin dynamics with sub-10 fs temporal resolution. After excitation with an ultrashort light pulse, plasmon dephasing by either radiative scattering by re-emission of a photon, or by electronic transitions induced by the absorption of the photon, can take place. How these effects can impact the MO response and spin dynamics on sub-ps timescale is still unknown and might open excellent opportunities for coherent manipulation of MO effects at the fs timescale. In the plot, we show a sketch of the possible modification that the plasmon phase can have on the spin dynamics of the system, e.g. a magnetic nanostructure, and this might also impact the spin-orbit interaction thus consequently the MO activity.

is its large footprint that reduces considerably the surface coverage of the MO-active material. Future research should focus on designs to increase the sharpness and strength of the resonances and allow for a substantially reduced footprint of the nanocavity. The sharpness of a resonance is determined by the damping of the plasmon due to radiative losses and dissipative effects. The exploitation of surface lattice resonances, namely the diffractive coupling in periodic arrays, is worth exploring since they are known to lead to a dramatic reduction of radiative losses [157]. A partial reduction of the dissipative losses can be achieved by using either magnetic garnets or noble metal/FM multi-layered nanostructures (e.g. Au/Co, Au/Fe, and Pt/Co), which bring the additional advantage of a quite high MO activity and a perpendicular magnetic anisotropy that allows their magnetic manipulation using a low magnetic

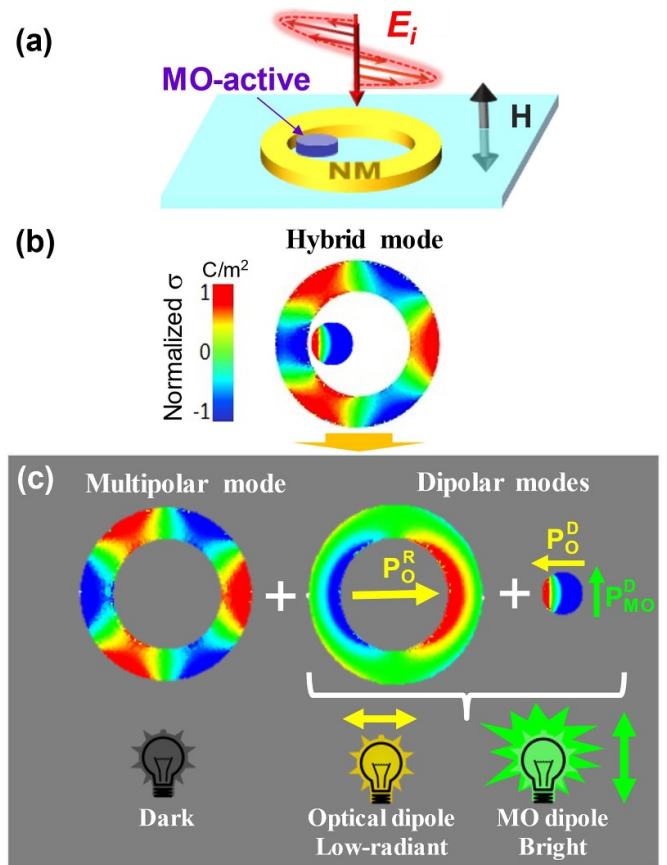


**Figure 18.** General concept of MO amplification exploiting dark modes illustrated for the case reported in the literature of a non-concentric nanocavity made of a MO-active disk inside a noble metal ring resonator, shown schematically in panel (a) [31]. The nanocavity supports the excitation of a hybrid multipolar mode in a specific wavelength range, shown by the normalized surface charge,  $\sigma$ , map in panel (b). Panel (c) displays the multimodal analysis of the hybrid mode, which shows that the excitation of this hybrid mode results in an enhanced optical dipole in the MO active material that generates a highly enhanced MO dipole. Whilst the MO dipole in the disk ( $P_{MO}^D$ ) is fully radiant, the radiation from the optical dipole ( $P_O^D$ ) is only marginally increased due to the destructive interference with a coexisting out-of-phase optical dipole in the ring ( $P_R^O$ ). This concept can be implemented both in reflection and transmission geometry. In the latter case, it provides exceptionally high figure of merit due to the very high transmissivity (>65%) [31].

field [158]. Notably, magnetic switching of plasmonic lasers using this type of multi-layered magnetoplasmonic nanostructures has been recently reported [159]. Similar approaches can be used also for multi-layered metal-dielectric hyperbolic metamaterials, which recently have been shown to display tuneable MO activity even if their building blocks are non-magnetic [151].

Finally, we foresee that exploring non-thermal pathways [160], where the intrinsic losses due to heating can be overcome by exploiting the dynamics of the electrons on sub-100 fs timescales, can open excellent perspectives in both the fundamental and applied aspect of ultrafast magnetoplasmonics. By exploiting the non-thermal dynamics of electron gas, we expect that novel plasmon-driven phenomena can

be discovered and controlled for the duration of the laser pulse (sub-10 fs), where the microscopic degrees of freedom, such as the spin, can be strongly coupled to the amplitude, frequency, and polarization of the plasmonic field (see also section 10). This direction is still unexplored in magnetoplasmonics and nanoscale magneto-optics and can become a rising research line in the upcoming years.

### Concluding remarks

We have briefly reviewed the current trends in magnetoplasmonics, highlighting recent advances in the field where MO enhancement can be achieved going beyond the exploitation of currently known LPRs. We have shown how plasmonic dark modes or hyperbolic dispersion of the materials used can

open future and exciting directions towards the development of novel nonreciprocal MO nanodevices. We have also given an overview of possible future directions to improve the performances of these architectures and provided a brief vision on the exciting opportunities arising from studying the fundamental properties of magnetoplasmonic systems at ultra-fast timescales. For instance, non-thermal electronic dynamics and sub-10 fs spin dynamics affected by plasmon dephasing are interesting directions to be explored by using state-of-the-art pump-probe spectroscopy techniques. They might unveil novel pathways to control spin dynamics in the non-thermal regime also with metallic nanostructures, thus overcoming the intrinsic limitations placed by ohmic and other losses, opening excellent opportunities towards plasmon-driven coherent MO activity.

### 13. All-dielectric magneto-optical metasurfaces (ADMOMSs)

Daria O Ignatyeva<sup>1,2,3</sup> and Vladimir I Belotelov<sup>1,2,3</sup>

<sup>1</sup> Russian Quantum Center, Moscow 121353, Russia

<sup>2</sup> V.I. Vernadsky Crimean Federal University, Simferopol 295007, Russia

<sup>3</sup> Faculty of Physics, Lomonosov Moscow State University, Moscow 119991, Russia

#### Status

All-dielectric nanostructures with magnetic constituents attract much research interest since, on the one hand, they have low optical losses and, on the other hand, provide advanced MO functionalities. Usually, the thickness of the nanostructure, as well as the lateral scales of their single elements, are subwavelength so it can be treated as a kind of metasurface whose overall optical response is determined mainly by its elements, ‘meta-atoms’. The meta-atoms provide localized optical resonances and their periodic array enriches the structure with the guided ones. Magnetization of the ADMOMSs modifies optical modes: either changes their field distribution or shifts their dispersion. As a result, the MO response of ADMOMS becomes significantly different from a smooth magnetic film: the MO effects get boosted and, moreover, some new MO effects might appear. It makes ADMOMS an interesting subject for basic research and quite promising for sensing and telecommunication applications.

Initially, ADMOMSs were proposed theoretically [161, 162] and were recently demonstrated on the basis of magnetic dielectrics arranged in periodic arrays of trenches or nanodisks [163–170]. Several unusual effects were shown to arise in ADMOMS. It is well-known that usually the MO effects associated with the in-plane magnetization component, such as transverse or longitudinal Kerr effects, are weak, especially in the transparent materials. One of the ways to overcome this is to use the specially-designed plasmonic nanostructures (see section 12) that introduce losses by their nature. The other approach demonstrated recently is based on the special properties of the optical eigenmodes excited in all-dielectric metasurfaces. The magnetization-induced shift of the transverse magnetic (TM) mode dispersion provides three orders of magnitude enhancement of the transverse MOKE up to 2% [163] in the material transparency region where the conventional effect is below 0.01%. Excitation of guided modes propagating at various angles to the light incidence plane and medium magnetization originates a novel MO intensity effect observed both in *p*- and *s*-polarizations whereas a smooth film produces no such effect for *s*-polarization [164] (figure 19(a)). Similar effect is observed if excitation of localized resonances provides an efficient gyromagnetic response [170]. Under the simultaneous excitation of the TM and transverse electric (TE) modes, longitudinal magnetic field mediates their coupling leading to significant growth of the longitudinal Kerr effect (up to 1°) even for small angles of incidence of less than 1° [165, 170] (figure 19(b)). The unique sensitivity of the ADMOMS

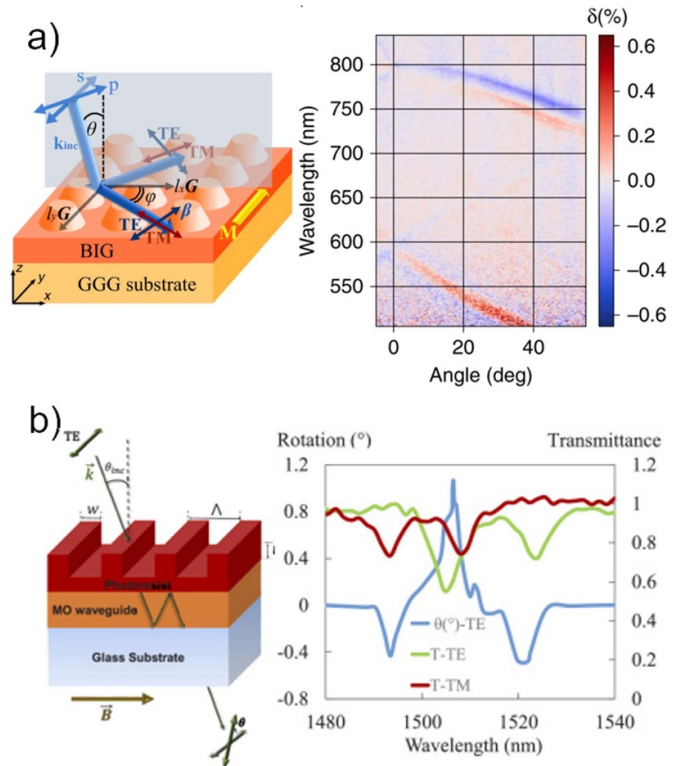


**Figure 19.** Unusual MO response of ADMOMSs. (a) Transverse magnetophotonic intensity effect observed in *s*-polarized light in 2D metasurface. This effect equals to zero for an unstructured smooth magnetic film. Reproduced from [164]. CC BY 4.0. (b) Significant enhancement of longitudinal MO effect at 0.4° angle of incidence. [Reprinted/Adapted] with permission from [165] © The Optical Society. This effect is several orders lower for a same smooth magnetic film.

to the in-plane magnetization component is a key feature for novel studies of the in-plane materials.

A notable enhancement of the Faraday effect is observed both in the cases of metasurfaces with guided [166] and localized [167] modes, that is important for various applications [174] including MO microscopy (see section 6), magnetometry [168], etc.

Moreover, the results of the first studies of the optically launched spin dynamics in ADMOMS are promising in the sense of optical excitation and probing of the quantized exchange SWs due to very high confinement and non-uniform distribution of the optical field within the magnetic structure [169]. Due to the local and non-uniform spin dynamics excitation, ADMOMSs open new horizons for the ultrafast optomagnetism (see section 10).

#### Current and future challenges

For practical applications, the MO devices working with high efficiency, i.e. providing 100% MO light modulation or 45° MO polarization rotation are highly desired. Although ADMOMS provided significant, several orders of magnitude enhancement of the MO effects [163–170], their absolute values are still rather small. The highest MO modulation

efficiency demonstrated in transmission [171] was higher than 10%, and in reflection was 20% [170, 171]. The highest MO polarization rotation observed in ADMOMS was  $1^\circ$  [165, 171]. Further optimization of the ADMOMS design is necessary to improve these values.

It is important not only to increase the MO effects but also to preserve a rather high level of basic signal. Although ADMOMS is nearly free of optical losses, the presence of the optical resonances usually reveals itself as the dips in the transmittance spectra. An interesting approach to overcome the decrease of the transmittance by using the phenomenon of electromagnetically induced transparency was proposed theoretically in [172].

Apart from that, ADMOMS were theoretically predicted to support bound states in the continuum (i.g. [32]). Such states provide infinite  $Q$ -factors in ideal structures that is interesting for a wide range of practical applications, including sensing and all-optical magnetization control. However, bound states in the continuum could be destroyed due to the presence of absorption and fabrication inaccuracies so that the techniques and materials of magnetic ADMOMS require further improvement to observe this interesting phenomenon.

Excitation of the localized modes associated with individual nanoresonators (figure 20(a)) was shown to increase the MO effects in ADMOMS [167, 170, 173]. Although recently 2D arrays of such resonators forming a metasurface were studied, this approach is interesting for the potential miniaturization of MO devices and going down to the level of single meta-atom magneto-optics. The studies considering a single magnetic meta-atom interaction with photons were not performed yet, but represent an efficient approach to reduce the lateral size of the addressed MO structure down to the sub-wavelength scale. Magnetic meta-atoms are also of prime importance for the opto-magnetic effects and might be crucial as highly localized sources of optically excited magnons. Studies in this direction have just started (figure 20(b)) [169].

## Advances in science and technology to meet challenges

ADMOMS require nanostructured magnetic dielectric materials with a high MO figure of merit which is the ratio of the MO activity to the absorption coefficient. Several types of ADMOMS were recently fabricated, and in each case a trade-off between the MO activity of the material, its absorption, and fabrication capabilities was achieved. For example, iron garnets are the most efficient materials combining high MO activity and low absorption. However, the technology of iron-garnet nanopatterning is rather complicated, so that fabrication of such structures is challenging [163, 164, 167]. On the other hand, ADMOMS could be fabricated using a composite material of magnetic nanoparticles embedded in a glass matrix, instead, as reported in [165, 166, 171]. This approach is easy and convenient for implementation, although such nanocomposite itself has rather low MO activity compared to the iron garnet. Significant restrictions are imposed on the spatial resolution of such structure. On the other hand,

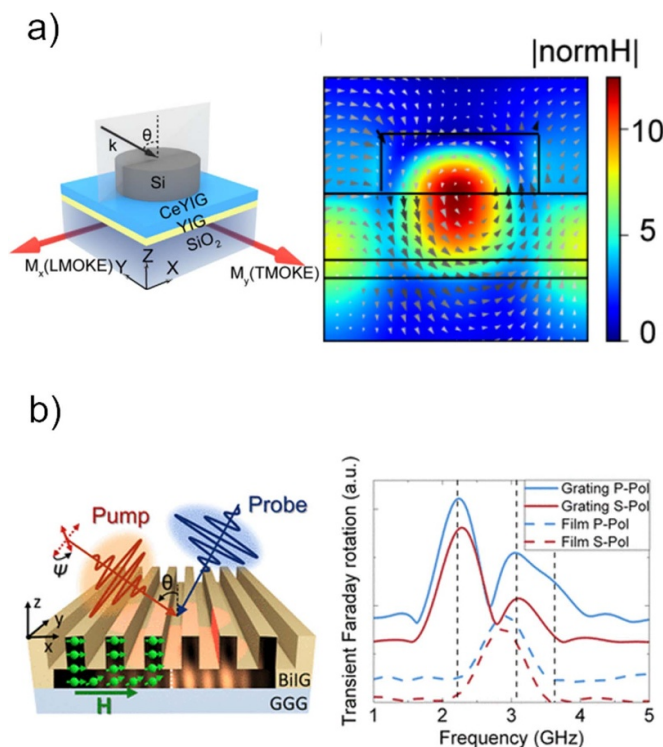


**Figure 20.** ADMOMS challenges and perspectives. (a) Localization of light in a single magnetic ‘meta-atom’ under excitation of magnetic dipole resonance of a nanodisk. [170] John Wiley & Sons. [Copyright © 2022 WILEY-VCH Verlag GmbH & Co. KGaA, Weinheim]. Grey arrows show intensity and direction of the electric field components. Intensity of magnetic field components is shown by colour. (b) Optical generation of multiple spin-wave resonances due to a localized action of a laser pulse. Reprinted with permission from [169]. Copyright (2020) American Chemical Society. Right figure shows that spin-wave spectra of ADMOMS has several resonances corresponding to the 3 lowest quantized spin-wave modes. At the same time the spin-wave spectra of the homogeneous film exhibits only one resonance corresponding to the uniform spin precession.

the technologies of Si deposition and nanopatterning are well developed nowadays, and recent works show that it can be applied to fabricate a nanostructure on the top of a smooth magnetic oxide film [170].

The other challenge is the requirement of precise nanostructuring. ADMOMS, in contrast to their plasmonic counterparts, are extremely sensitive to the geometrical parameters of the structure. High  $Q$  values, especially for the guided-wave-based and bound-states-in-the-continuum-based ADMOMSs having several nanometres-width optical resonances sensitive to even a few nanometres shift of the resonance position due to the inaccuracy. Fabrication inaccuracies may not only result in the additional scattering and metasurface operation efficiency decrease but also may be responsible for the complete destruction of the desired resonances.

Up to now, only ADMOMS with a periodical arrangement of a large number of ‘meta-atoms’ were studied. Intriguing possibilities open if one goes down to a single ‘meta-atom’ level, i.e. focus on the study of the MO or opto-magnetic response of a single nano-object. Such an approach requires

advances in the light focusing and precise positioning, and novel experimental approaches to the measurements of the MO effects at the nanoscale.

### **Concluding remarks**

All-dielectric magnetic metasurfaces attract the attention of the scientific community due to their ability to control the light

via an external magnetic field and to combine high transparency with enhanced MO response. ADMOMS demonstrate unusual MO properties that could not be found in smooth materials. Observed enormous enhancement of the MO effects in them is very promising for the device miniaturization and enriching their capabilities for sensing, magnetometry, light modulation, etc. Low optical losses and thermal heating, and a variety of optical modes with peculiar properties make ADMOMS important for potential opto-magnonic studies.



## 14. Characterization of 3D magnetic nanostructures

Claire Donnelly<sup>1</sup> and Aurelio Hierro-Rodriguez<sup>2,3</sup>

<sup>1</sup> Max Planck Institute for Chemical Physics of Solids, Noethnitzer Strasse 40, 01187 Dresden, Germany

<sup>2</sup> Universidad de Oviedo, Departamento de Física, 33007 Oviedo, Spain

<sup>3</sup> CINN (CSIC-Universidad de Oviedo), El Entrego, Spain

### Status

The recent advance of magnetic nanostructures to the third dimension promises an abundance of new physics, as well as a multitude of possibilities for applications [175]. In 3D space, the higher degrees of freedom allow for the formation of new spin textures, which range from singularity-containing domain walls [176] to higher order topological structures [177]. In addition, the patterning of 3D geometries, made possible by recent advances in 3D nanofabrication techniques [178, 179], offers new routes to tailoring the magnetic properties. The integration of curvature can induce effective anisotropy and chiral energy terms as well as automotive effects [180], while the patterning of chiral geometries allows for the direct imprinting of chiral spin textures [181]. In terms of applications, the move to 3D promises key increases in device density [182], as well as increased functionality, with prospects for green electronics.

One of the largest challenges facing the realization of the promises of 3D nanomagnetism has been the development of appropriate characterization techniques with which to visualise the 3D magnetization [183–185]. Indeed, most available imaging methods—including magneto-optics, which this Roadmap focuses on—are either planar or surface sensitive, and have been used in combination with micromagnetic simulations to gain an understanding of the 3D magnetization. Direct access to the magnetic configuration via slicing of the sample is prevented by the dependence of the magnetization on the geometry itself. Instead, a non-destructive, *tomographic* technique is required.

Tomography, as in the computed tomography (CT) scan in a hospital, is achieved by measuring transmission projections of a sample from many different orientations. For this, x-rays are used as they offer higher penetration depths than photons in the visible range. The combination of all the recorded projections using computer algorithms leads to the reconstruction of the scalar 3D structure of the sample. In the framework of 3D magnetic imaging, however, we map the magnetization *vector field*. For this, we make use of magneto-optics in the x-ray regime—in particular, we can obtain element-specific sensitivity to the magnetization by exploiting XMCD. By measuring in transmission, one therefore obtains a projection of the magnetization component parallel to the beam direction integrated through the sample. However, for vector tomography there is an additional complication: to probe all three components of the magnetization, a single tomographic rotation axis is not enough. Such an experiment requires at least two complementary tomographic datasets [183, 184], or

an alternative geometry such as laminography [185]. Finally, the internal magnetic configuration is recovered using a vector reconstruction algorithm (see figure 21).

A key advantage of the technique is that there is no need for prior knowledge of the sample, meaning that direct access to complex magnetization configurations is possible. In this way, first *direct* observations of textures within the bulk have been achieved, including Bloch point singularities [183, 184], skyrmion tubes [186], and magnetic vortex rings [187], as well as novel domain wall textures in patterned 3D structures [188] (figure 22).

### Current and future challenges

These demonstrations of 3D magnetic imaging have revealed the power of the technique to provide direct access to the 3D magnetization configurations, becoming an experimental window to new physics and sparking new directions of research. However, with each new direction, comes new challenges.

One such direction concerns the visualization of topological magnetic textures, such as skyrmions and vortices, as well as Bloch point singularities. The observation of the details of these features requires high spatial resolutions on the order of the exchange length. Indeed, the first observation of the presence of Bloch point singularities only had a spatial resolution of 100 nm [183]—meaning that although the texture surrounding the singularity could be resolved, the structure near the centre of the Bloch point remains elusive. As a result, imaging at *shorter lengthscales* is key.

In addition to their static configuration, their *dynamic* behaviour is crucial to painting the complete picture of these exotic spin textures. For example, in 3D nanowires, domain walls are predicted to propagate at ultra-fast velocities [176], reaching regimes in which SWs can be spontaneously emitted. Imaging of the *in operando behaviour* in three-dimensions, under the application of different excitations is therefore crucial to developing our understanding for fundamentals, and applied technologies.

There is also key interest in the 3D structure of *alternative materials*—both magnetic, and beyond. Following the recent demonstration of electric control of antiferromagnetic order [189], there is a growing need for enhanced knowledge of the static—and dynamic—behaviour of these elusive systems. Exploiting linear dichroic effects could lead to 3D imaging of antiferromagnetic systems, while combination with Bragg techniques could open the door to the visualization of ferroelectric domains.

### Advances in science and technology to meet challenges

One of the most promising upcoming technical advances involves the development of the next generation of synchrotron radiation sources, which promises to provide orders of magnitude higher coherent flux. This will allow to probe the weaker signals of alternative materials such as AFMs, but most importantly, it will strongly impact coherent diffractive

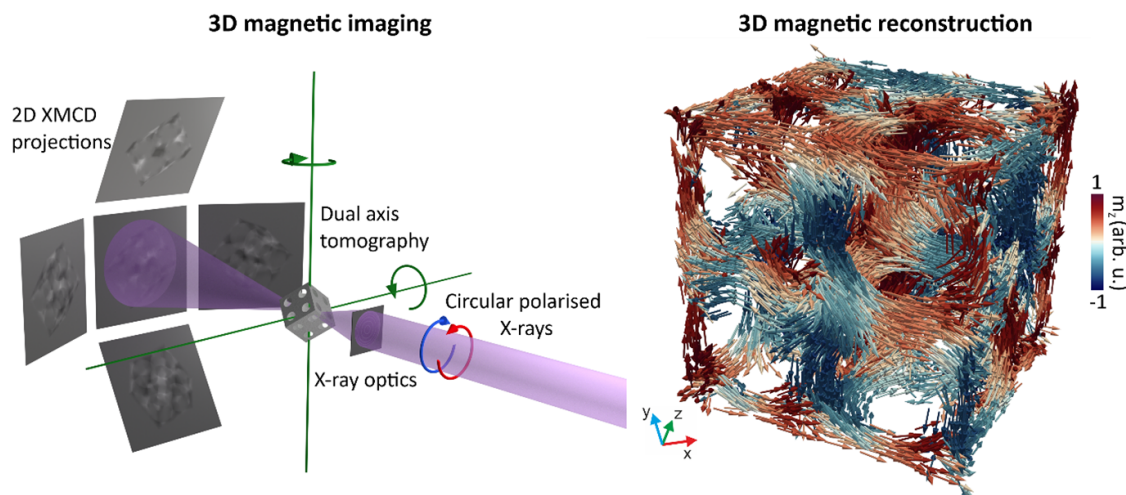


**Figure 21.** A 3D x-ray magnetic imaging requires the measurement of XMCD projections for a number of different orientations of the sample. These projections are then combined using a reconstruction algorithm to obtain a map of the magnetization vector field.

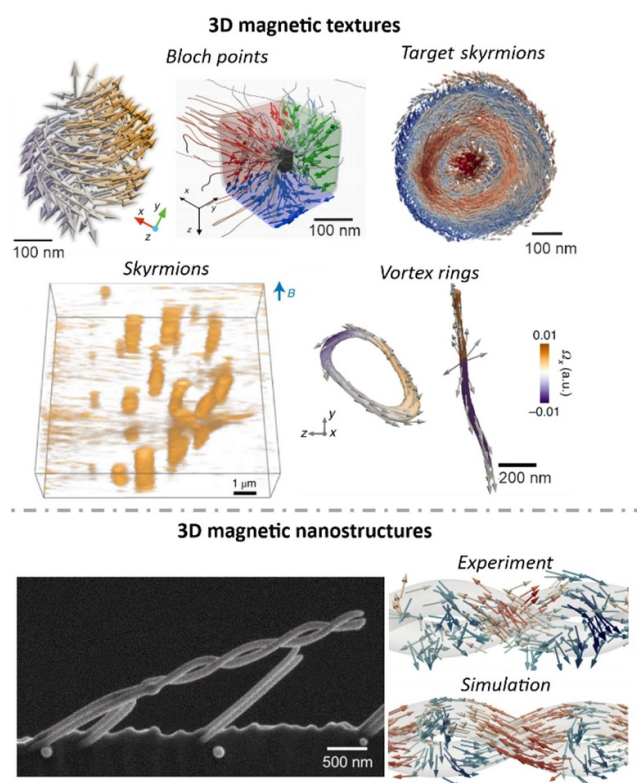


**Figure 22.** X-ray magnetic tomography and laminography have led to the mapping of 3D magnetic textures such as Bloch point singularities, skyrmion textures, and magnetic vortex rings within larger systems, while in patterned nanostructures new types of coupled domain walls have been observed. Reproduced from [183], with permission from Springer Nature. Reproduced from [184]. CC BY 4.0. Reproduced from [186], with permission from Springer Nature. Reproduced from [187], with permission from Springer Nature. Reproduced from [188]. CC BY 4.0. Reprinted with permission from [191]. Copyright (2020) American Chemical Society.

imaging techniques, where the spatial resolution is currently flux limited [183]. This increase in coherent flux will make it possible to reach key magnetic length scales. In this framework, we encounter new challenges: a fundamental limitation of XMCD is that it prevents the imaging of divergent magnetization structures [190], while different contrast mechanisms for imaging AFMs are required. We envisage that

by developing new reconstruction algorithms based on both XMCD and alternative contrast mechanisms such as x-ray magnetic linear dichroism (XMLD), the structure of divergent textures such as singularities, as well as topological antiferromagnetic textures, could be resolved.

The increase in flux will also allow for experiments to be faster, allowing for the advance to in operando measurements.

Typically, an experiment providing a mapping of coherent rotation modes and domain wall dynamics with pump-probe magnetic laminography requires over one week of beamtime [185]. As these experiments become faster, *in situ* imaging of dynamic behaviour as well as quasi static imaging under the application of a wider variety of excitations such as fields or currents will become possible. Technical advances in the sample environment will open the door to a wide variety of *in situ* measurements. For example, moving to pump-probe scanning transmission x-ray microscopy (STXM) opens the door to a wide range of excitation frequencies, while with the development of faster detectors and x-ray FELs (XFELs), stroboscopic imaging of ultrafast responses (see sections 10 and 15) could become feasible. These capabilities for four-dimensional imaging could also be extended to spectroscopic measurements. Indeed, by performing spectroscopic magnetic tomography, sum rule analysis could be used to resolve the orbital and spin moments in three dimensions, giving insight into SOC at the nanoscale.

Finally, four-dimensional imaging will bring very large datasets. Here, the move to advanced analysis will be crucial to the efficient interpretation of the magnetic behaviour, with recent implementation of analysis based on the

topology offering easy identification of relevant topological textures [184, 187]. With such Big Data(sets), we envisage that advanced tools based on machine learning will play a key role in exploiting the full potential of these techniques.

### Concluding remarks

With the advance to 3D magnetic imaging, we have a two-fold change of paradigm. First, the access to the third dimension represents a significant advance from 2D to 3D, bringing new configurations and textures that are not possible in planar systems, allowing for the full exploration and exploitation of the magnetization vector field. Secondly, this direct access to the 3D magnetization represents a new experimental approach in magnetism. Here, we experimentally access the magnetization in 3D directly with nanometre and picosecond spatial and temporal resolutions, with no prior assumptions. In time, we envisage that higher dimensional magnetic imaging will provide a new era of experimental micromagnetism, and that this type of measurement will direct our understanding of these complex material systems.

## 15. Magneto-optics with free electron lasers (FELs)

Iwao Matsuda

The Institute for Solid State Physics, The University of Tokyo,  
Kashiwa 277-8581, Japan

### Status

An XFEL is the linear accelerator-based light source that generates an ultrahigh brilliant x-ray with ultrashort pulse-width, spatial coherence, and tunable photon energy. After the designs and the pilot examinations from 1970s, today XFEL facilities are opened for users at various sites over the world [192–194]. At the XFEL beamlines, researchers carry out the state-of-the-art x-ray experiments of scattering, spectroscopy, imaging, and diffraction. The application ranges various academic fields of physics, chemistry, biology, and medical science. Nowadays, the XFEL beam has also become a significant probe to examine technical innovations in industry.

Photon energy of XFEL covers the wide range from vacuum ultraviolet to x-rays. An x-ray has been categorized in two regions: the hard x-ray (wavelength of 0.1 nm or shorter) and SX region (0.1 nm or longer). Typically, a beam of the hard x-ray is used for determining (atomic) structure of a material, while that of the SX is for examining the electronic states. In this article, I focus on magnetic spectroscopy, mainly in a region of SX that corresponds to the wavelength range around 10 nm and covers a region of the vacuum ultraviolet ray. The SX MO effects have allowed us to directly probe spin states that are responsible for magnetic or spintronic properties of a material [195–197]. Researchers have conducted measurements of the x-ray MO Kerr or Faraday effect (XMCD) when an XFEL beam is linearly (circularly) polarized.

### Current and future challenges

Interactions between light and magnetic materials make various MO responses, such as the MOKE and the Faraday effect, that are useful for experimental physics (see sections 4, 8, 9, and 11). Photon energy of the SX covers absorption edges of various elements and, thus, the MO measurement can be element-selective [198, 199]. Furthermore, optical performance of the XFEL beam allows us to make time- or spatially resolved experiments.

Figure 23 shows an example of such a (core-level resonant) MOKE experiment on the Co/Pt heterostructure at the SACLA soft XFEL beamline (SXFEL BL-1) [198]. The absorption spectrum shows features of the Co M-edge (absorption peak) and the Pt N-edge (Fano resonance) at  $h\nu = 60$  eV and  $h\nu = 72$  eV, respectively. The material shows the photo-induced ultrafast demagnetization (see section 10) and the time-resolved measurement successfully traces that a magnetic variation in the Co layer is much faster than that in Pt. The results demonstrate that the XFEL beam is a powerful tool to reveal nature of femtomagnetisms. Besides SXFEL, HHG of infrared-ray have also become a light source for element-specific MO experiments [199, 200]. Both the SXFEL and

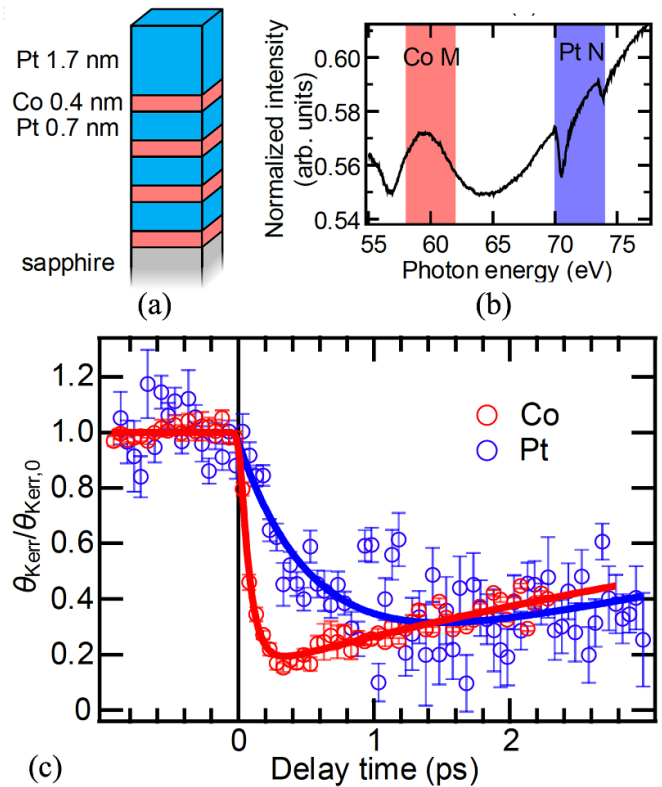


**Figure 23.** (a) The Co/Pt multi-layer sample (b) x-ray absorption spectra with indications of the Co M-edge and Pt N-edge regions, (c) element-selective MO Kerr responses with various delay time, taken at  $h\nu = 60$  eV (Co M-edge) and  $h\nu = 72$  eV (Pt N-edge) [198].

HHG sources cover the photon energy range of SX but individually have distinctive optical parameters. SXFEL has unique characters, such as ultrahigh brilliance, that exceed performance of the HHG radiation but the beamtime is severely allocated for users. Depending on the experimental conditions, varieties of the SX MO measurements can be carried out selectively at the SXFEL or HHG beamline.

In developing nanodevices, spatially resolved measurements of MO spectroscopy are significant to examine the magnetic (spin) states in a local region that determine the functionalities. There are two technical approaches with SXFEL. The one approach is held by scanning the SXFEL nanobeam, focused by a mirror, and the other approach is coherent diffraction imaging [194, 201]. Since an XFEL beam has a full spatial coherence, SX MO phenomena are expected to be combined with advanced imaging techniques, such as holography, ptychography, or tomography, in future. By detecting the local MO responses, these measurements with SXFEL allow us to acquire magnetic images in nanometre scale with element-selectivity and/or ultrafast temporal resolutions.

Today, XFEL MO experiments of magnetic dynamics and imaging are stably performed at the various facilities. The researchers have nowadays moved onto the *operando* measurements that trace evolutions of the local magnetic (spin) states in actual devices in real time. The novel approaches require precise controls of the sample environment, i.e. current



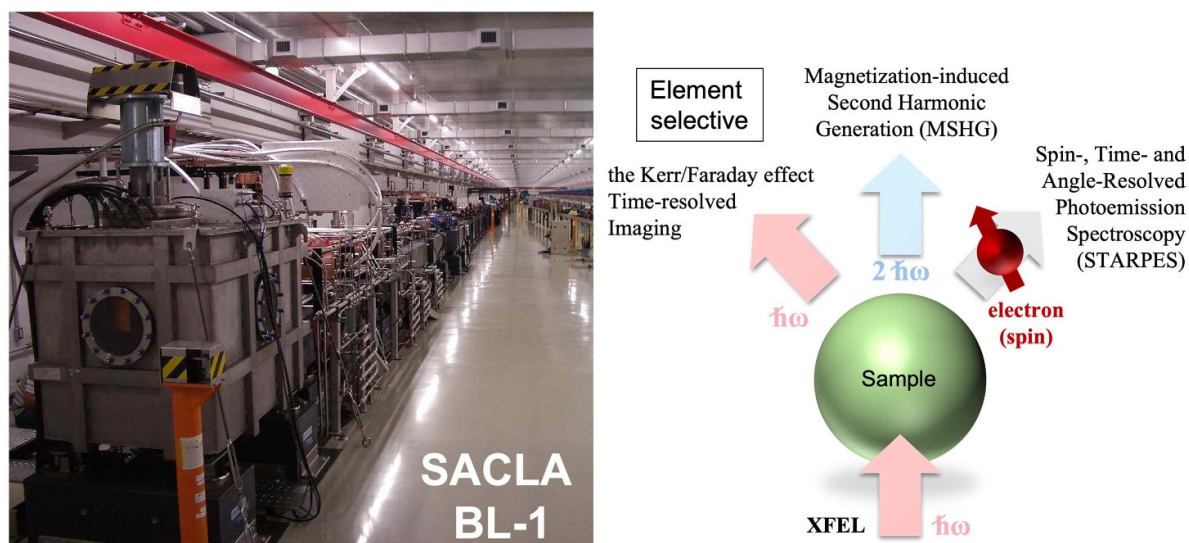


**Figure 24.** A photograph of the soft XFEL (SACLA BL-1) and future prospects of the usage.

injection, external EF, or local temperature. Furthermore, it is also necessary to measure the additional responses of the sample, such as (magneto)resistance, during the measurements with XFEL. Consequently, a large dataset in multi-dimensions is acquired after the XFEL beamtime and the big data should be examined with informatics to make systematic characterizations of a material and to discover hidden properties that may become useful in future.

### Advances in science and technology to meet challenges

In coming years, users will be able to choose two operation modes of XFEL, one mode with ultrahigh brilliance and a repetition rate of several 10 Hz (the conventional-type) or the other mode with the moderate brilliance and the MHz-frequency. The followings are my future prospects of MO research with these XFEL modes.

The ultrahigh brilliant XFEL beams opened research of the non-linear optical effect. In 2018, two independent groups observed the second harmonic generation (SHG), which is optical frequency conversion of producing a double field frequency, in SX region [202, 203]. The phenomena occur in a medium of broken inversion symmetry or at an interface. These SHG signals were enhanced when photon energy matched with the absorption edge of a material (the core-level resonance). The findings indicated that the x-ray SHG lies in the obtention of elemental or chemical information of a sample in the non-linear signals. The novel approach has already made progresses in material science today [204]. Thus, in the future this method should be extended to the magnetization-induced SHG (MSHG). It is expected that MSHG with SX selectively probes magnetization at an interface with element selectivity. Combining with the ultrashort pulse of XFEL, one should also

be able to trace the ultrafast spin dynamics across the interface that determine functionalities, such as spin torque, of spin devices.

To deal with light–matter interaction in the vacuum ultraviolet—to—x-ray region, it is significant to recall the photoelectric effect and photoemission spectroscopy that directly probes electronic states in materials. The XFEL with a high repetition rate (1 MHz) has provided performance of experiments of time- and ARPES (TARPES) that can trace temporal evolutions of electronic states during dynamic events, such as photo-induced transitions. Today, researchers can make spin-resolved ARPES, or SARPES, in the laboratory or at synchrotron radiation facilities and determine the spin-polarized band structure of a sample [205]. By introducing the SARPES technique in the XFEL facilities, it is expected that one can perform experiments of spin- and TARPES (STARPEs) [206]. The novel method would directly trace evolutions of electrons in magnetic or spintronic dynamics with information on spin orientations, carrier velocities, and scatterings.

### Concluding remarks

In magneto-optics, a polarization state of the probing light links with magnetic properties of a sample. With XFEL, the information can be element-selective and it can also be combined with nanometre-scale spatial and femtoseconds time-resolutions. In the future, non-linear MO effects will be examined and extended to the spectroscopy method to probe ultrafast spin dynamics across the selected interface. A measurement of STARPEs can be made with XFEL to trace temporal evolution of the spin-polarized electronic states in a material. It continues being highly useful to perform advanced MO experiments at XFEL facilities for material science (figure 24).



## 16. Magneto-optics with light beams carrying orbital angular momentum (OAM)

Thierry Ruchon<sup>1</sup>, Mauro Fanciulli<sup>1,2</sup> and Maurizio Sacchi<sup>3,4</sup>

<sup>1</sup> Université Paris-Saclay, CEA, CNRS, LIDYL, 91191 Gif-sur-Yvette, France

<sup>2</sup> LPMS, CY Cergy Paris Université, Cergy-Pontoise, France

<sup>3</sup> Sorbonne Université, CNRS, Institut des NanoSciences de Paris, INSP, Paris F-75005, France

<sup>4</sup> Synchrotron SOLEIL, Saint-Aubin, B.P. 48, 91192 Gif-sur-Yvette, France

### Status

Building on the discovery of the Faraday effect in 1846, the interplay of light with magnetic materials has ever since been strongly focused on *polarization*-dependent interactions (see section 1) especially uneven interactions with left and right circularly polarized beams (LCP and RCP). At the mesoscopic scale, suitable to Maxwell equations in optics, these effects appear as different values of the complex optical index for LCP and RCP, leading to polarization changes and differential absorption upon transmission through, or reflection off, the magnetic sample. In the paraxial approximation, i.e. when light beams are loosely focused so that their electric and magnetic fields remain transverse, LCP and RCP correspond to photons of opposite spin angular momentum (SAM). Indeed, the projection of the angular momentum (AM) of a light beam with a plane wavefront along its propagation axis  $z$ , reads  $S_z = \sigma \hbar$  per photon, where  $\sigma = \pm 1$  for LCP and RCP, and  $\sigma = 0$  for linear polarization. Light can also carry an OAM, as in the case of Laguerre–Gaussian modes that are indexed with two integers,  $(\ell, p) \in (\mathbb{Z}, \mathbb{N})$ , and show  $\ell$  intertwined spiralling wavefronts (figure 25). More precisely, along the azimuth  $\theta$ , the phase of the beam varies like  $\ell\theta$  and the projection of the AM, along the  $z$ -propagation axis, reads  $L_z = \ell \hbar$  per photon. In the paraxial approximation, the two kinds of AM simply add up, and the projection of the total momentum of the light beam is  $J_z = (\sigma + \ell) \hbar$  [207]. For tightly focused beams, interconversion between SAM and OAM has been observed, opening the field of spin–orbit interaction of light [207].

The strong analogy between SAM and OAM of light inspired the development of mirror applications in their own fields [208, 209], such as data multiplexing and transmission, entanglement, spectroscopy, matter manipulation including Bose–Einstein condensates and imaging. The rapidly evolving interest in OAM beams had a sparse overlap with magneto-optics, which remains strongly associated to SAM. However, this situation may evolve very quickly in view of recent theoretical and experimental work. In analogy with the results obtained for the electric-quadrupole interactions of OAM beams with atoms and molecules, it was predicted that the interaction of OAM beams with magnetic samples should depend on the value of  $\ell$  [210]. Indeed, it was experimentally demonstrated that the interaction vanishes in the

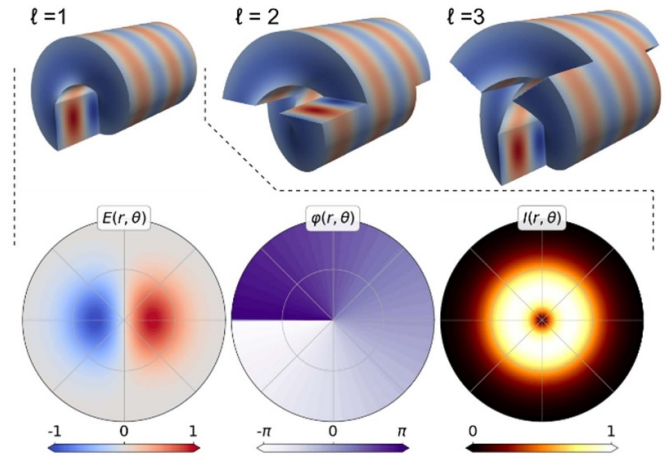


**Figure 25.** (Top line) 3D representation of the electric field amplitude for Laguerre Gaussian beams with  $\ell = 1$ ,  $\ell = 2$  and  $\ell = 3$ , showing one, two and three intertwined spirals, respectively. (Bottom, from left to right) Projection on a transverse plane of the electric field amplitude, phase and intensity for a Laguerre–Gaussian beam carrying a topological charge  $\ell = 1$ . As time passes, the field rotates about the centre.

electric-dipole approximation [211]. In a further study, van Veenendaal and Mc Nulty theoretically identified signatures of the absolute value of the OAM in the incoherent diffraction pattern from a magnetic vortex [212]. Neither prediction [210, 212] though, has been verified yet. Over the last two years, there has been a surge in publications that promote the use of OAM beams outside the visible range. Sirenko *et al* [213, 214] reported OAM-dependent transmission at THz frequencies in FM and antiferromagnetic oxides featuring collective magnetic excitations (figure 26), and attributed it to the coupling between the  $\ell$ -dependent longitudinal magnetic field of light and the sample magnetization (see also section 18). Vortex beam dichroism related to the total AM of THz radiation was further reported in [214]. Woods *et al* [215] showed that the reflection of an  $\ell = 0$  x-ray beam off an artificial spin-ice with a topological defect changes the OAM content of the outgoing beam. Finally, Fanciulli *et al* showed theoretically [216] and experimentally [217] that helicoidal dichroism, i.e. an effect dependent on the OAM value and sign, appears when light beams are reflected off non-homogeneous magnetic structures.

### Current and future challenges

This brief summary of the state-of-the-art shows that magneto-optics with OAM is just rising today, with only a few theoretical predictions and proof-of-principle experiments. It is interesting to note that three approaches are proposed, harnessing different features of such beams: (a) direct interaction through electric-quadrupole terms [210], (b) indirect coupling

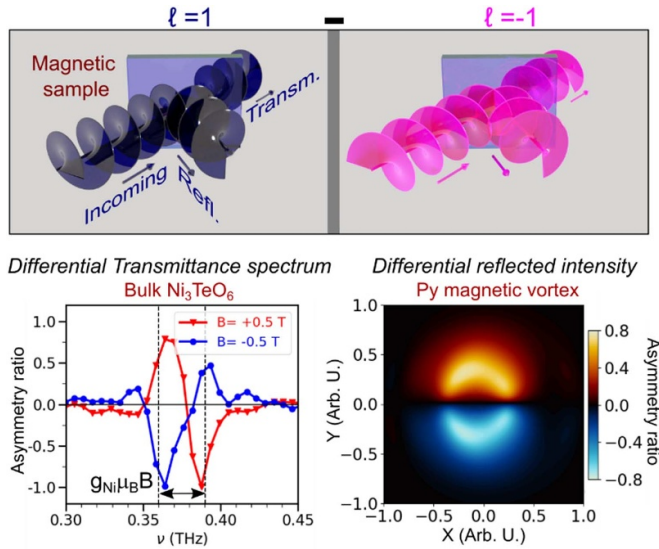


**Figure 26.** Examples of magnetic helicoidal dichroism expressed as asymmetry ratio  $[I(\ell = +1) - I(\ell = -1)]/[I(\ell = +1) + I(\ell = -1)]$ , where  $I$  is the spectrally/spatially resolved intensity for left/right panels. Left: experimental THz transmission in  $\text{Ni}_3\text{TeO}_6$  at the antiferromagnetic resonance (courtesy of A Sirenko) [214]. Right: calculated reflectivity from a permalloy magnetic vortex ( $\lambda = 23.5$  nm, Fe-3p resonance) [217].

between the light magnetic fields and the sample magnetization [213, 214], and (c) global interactions at the size of a magnetic structure, i.e. nanometres to microns [215–217].

**OAM-sensitive magnetic spectroscopy.** (see also section 4) A first objective of theoretical and experimental efforts should be to validate the predictions of [210], providing a smart access to electric-quadrupole transitions, free from the often dominating electric-dipole ones. This seminal work was focused on the K-edges of several materials, and a generalization to the L and M-edges would be highly desirable for applications. Also, it requires a strong focusing of the beam, down to a few nanometres, which remains a challenge today. The second spectroscopic approach [213, 214] exploits the longitudinal component of the light-induced magnetic field to alter the spectroscopic lines in the THz region ( $\lambda = 0.1\text{--}1$  mm). Here the challenge is to extend this approach to other spectroscopic regions (visible, UV, XUV), and decouple as much as possible SAM and OAM effects. This will also require theoretical efforts in order to gain in-depth understanding of the interactions. A development with high potential for applications is to master the analogue to the inverse Faraday effect, by which the sample magnetization may be manipulated by shining light beams of selected OAM values. It is worth stressing that the, in principle unlimited, OAM value of  $\ell\hbar$  per photon introduces a new parameter in the currently available toolbox for all-optical control of the magnetization, which may be combined with SAM and photon energy to provide extended capabilities in this domain.

**Spin-textures interactions with OAM beams.** In recent proof-of-principle works [215–217], it has been established that the OAM content of a light beam after reflection off a magnetically inhomogeneous structure strongly depends on its spin texture (figure 26). These works are just scratching the surface of a new kind of diagnostic for probing global spin textures, including antiferromagnetic ones [215]. However, the full microscopic modelling of the coupling between light and spins remains elusive. Also, the full balance of AM has not been established, the capability of altering the magnetization texture with OAM beams was not demonstrated, and a global approach for all kinds of magnetic textures, in reflection or transmission, is still missing. Overall, more theoretical work is clearly required.

These are the major challenges towards the full development of magneto-optics with OAM as a diagnostic tool, but also as a shaping tool for light and/or magnetic structures. The development of such tools being based on light pulses, it is naturally fit for applications in time-resolved experiments to study ultra-fast phenomena at the femtosecond time scale, as discussed in sections 10 and 15 of this Roadmap.

### Advances in science and technology to meet challenges

Addressing new challenges requires a continuing effort to develop and control reliable, stable and broadband tuneable sources of OAM beams. The above-mentioned breakthroughs relied on very specific sources, in the THz ( $\lambda = 0.1\text{--}1$  mm [213, 214]) XUV ( $\lambda = 20\text{--}25$  nm [217]) and X ( $\lambda = 1\text{--}2$  nm [215]) spectral ranges. Light sources covering the extreme ultraviolet to SXs range with selectable values of both OAM and SAM will be essential for envisaging new spectroscopic applications, notably those involving transition-metals and rare-earths based magnetic materials. Several topics need to be developed, such as the broadening of initially narrow spectra through non-linear effects, the optical parametric amplification with OAM, the design of broadband spiral phase plates or Fresnel zone plates, the protocols for producing OAM x-ray beams using high harmonic generation [218] and FELs [219]. All these objectives are within reach but require further experimental efforts.

The second advance is to develop, in these difficult spectral regions, efficient OAM mode sorters. This is a kind of a chicken-and-egg problem, as any controlled MO effect with OAM could serve this purpose. However, other approaches, mainly demonstrated in the VIR spectral regions are available and should be extended to the spectral ranges of interest for spectroscopies of magnetic materials.

Finally, theoretical advances are of the utmost importance to describe the OAM-matter interaction on firmer bases and to guide experimental work. In particular, a full description of the possible interactions at different size scales of homogeneous and structured magnetic material is highly desirable to clear the picture, especially at the microscopic level. It raises

fundamental questions about the treatment of OAM in light matter interaction, in parallel or concomitantly with SAM. In particular, non-paraxial beams, notoriously difficult to treat numerically, naturally lift the separation between OAM and SAM and introduce transverse angular momenta. Their coupling with magnetic materials has not been elucidated thus far.

### Concluding remarks

Magneto-optics with OAM light beams is an almost blank page, on which only a very few first proof-of-principle ideas were written. It is highly promising from both applied and fundamental perspectives. It carries the prospect of designing new

MO devices, sensitive to the OAM of light, as well as easing the creation and/or diagnostics of beams with OAM. Endless applications can be envisioned, from data encoding and processing to spectroscopy and magnetization control. It is also a testing ground for fundamental properties of structured light beams that may now be shaped within an optical cycle. These capabilities required the introduction of such notions as helicity, transverse angular momenta, SOC of light fields or superchiral fields. The interaction of such structured light beams with magnetic structures, due to their variety, could become a natural and precise test of these new fundamental concepts and advantageously serve the development of structured light spectroscopy.

## 17. Probing spintronics systems using nitrogen-vacancy (NV) centres in diamond

Hailong Wang<sup>1</sup> and Chunhui Rita Du<sup>1,2</sup>

<sup>1</sup> Center for Memory and Recording Research, University of California, San Diego, La Jolla, California 92093, United States of America

<sup>2</sup> Department of Physics, University of California, San Diego, La Jolla, California 92093, United States of America

### Status

Operation of conventional magneto-optic techniques mainly relies on the interaction between polarized light and magnetization, thus, the ultimate spatial resolution is set by the optical diffraction limit, which typically lies in the range of a few hundred nanometres (see sections 6 and 8). In addition, the field sensitivity of the conventional MO sensing tools is compromised by interference effects, unable to reach quantum regime to detect magnetic fields with significantly reduced magnitudes. Over the past decade, NV centres [220], optically active spin defects in diamond, have emerged as a new multimodal sensing platform with improved spatial resolution and field sensitivity to investigate the forefront research of magnetism, spintronics, and more broadly speaking the condensed matter physics. Many of the advantages of NV centres derive from their quantum-mechanical nature endowed with excellent coherence, controllable entanglement, and high fidelity of operations, enabling opportunities for outperforming the classical counterparts [220]. An NV centre is formed by a nitrogen atom adjacent to a carbon atom vacancy in one of the nearest neighbouring sites of a diamond crystal lattice, as shown in figure 27. The negatively charged NV state has an  $S = 1$  electron spin and naturally serves as a three-level quantum spin qubit system. To date, NV centres have been demonstrated to be a transformative sensing tool for exploring electrical, magnetic, and thermal features arising from a variety of material systems. Examples include nanoscale imaging of non-collinear spin textures [220, 221], optical detection of resonant SW modes [222, 223], non-invasive measurement of spin transport properties of proximate (anti)ferromagnets [223, 224], and many others [225]. A range of NV-based quantum sensing and imaging techniques such as NV confocal microscopy, NV relaxometry [222, 223], NV wide-field [225] and scanning magnetometry [221, 226, 227] have been developed and successfully applied to explore the intriguing science at the frontier of modern condensed matter physics. A unique advantage of NV-based quantum sensing techniques results from their capability to detect noncoherent fluctuating magnetic fields that are challenging to be accessed by the conventional magnetometry techniques. On another front, being single-spin qubits, NV centres offer an attractive platform to be compatible with other functional solid-state media to develop hybrid architectures for applications in emerging quantum information sciences and technologies. To date, NV-based quantum computing platform has been theoretically proposed and actively explored in this context [228–230].

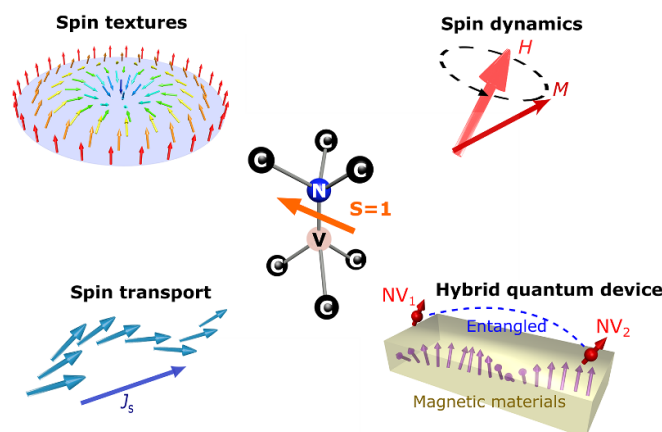


**Figure 27.** NV centres used for probing magnetic textures, spin dynamics, spin transport, and developing hybrid quantum devices.

### Current and future challenges

Despite these remarkable progresses, technical challenges remain to be addressed in order to push the performance of the current NV-based quantum technologies to the next level. The first one concerns spatial resolution which is mostly relevant to the practical applications. In the current state-of-the-art, NV centres are typically contained in single crystalline diamond substrates [225] in the form of NV ensembles for wide-field imaging measurements or in patterned diamond nanostructures [223] for single-spin addressment, as shown in figure 28. For NV ensembles, the spatial resolution is determined by the optical diffraction limit (see section 6) [225], while for scanning NV microscopy using patterned diamond cantilevers with individually addressable spin sensors [226], the spatial sensitivity is primarily set by NV-to-sample distance, which could ultimately reach the regime of tens of nanometres [221, 226]. To accommodate the ever-increasing requirements of modern scientific research, it is highly desirable to push the spatial resolution limit of NV quantum sensing techniques to the atomic length scale to reveal the microscopic features in a more detailed way.

The second challenge concerns the adaptability of NV centres to different experimental conditions. At present technological level, NV sensing and imaging measurements are mainly performed in a relatively low magnetic field range. Because the applied external magnetic field is coupled with NV electron spin resonance frequency, a major difficulty results from the significant energy loss with the increasing microwave frequency, which prevents the application of a large magnetic field in most existing NV measurements. Also, when temperature is below 100 K, the optical contrast of NV centres usually quickly degrades, which also restricts a broad application of NV-based sensing techniques.

The third challenge concerns the scalability of NV centres for implementing high-density, energy-efficient quantum processors [228, 230]. To date, the role of NV centres in quantum-computing remains peripheral. The major bottleneck results from the difficulty to access individual NV spin qubits in a scalable way and to identify appropriate interconnects to



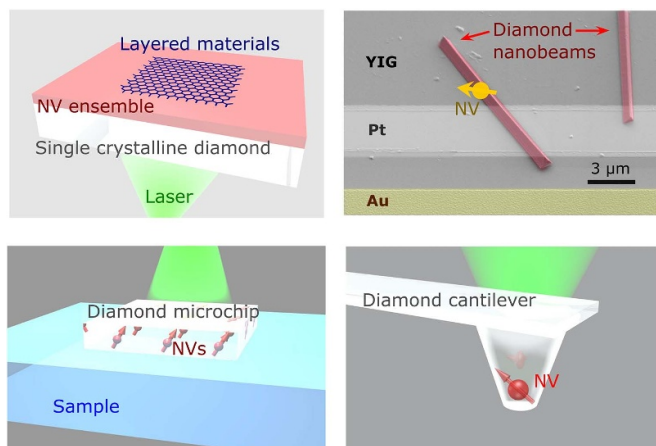


**Figure 28.** NV centres contained in a single crystalline diamond, diamond nanobeam, diamond microchip, and diamond cantilever for quantum sensing measurements. The top right panel is taken from [223]. Reprinted with permission from AAAS.

establish strong coupling between NV centres while maintaining their individual functionality [228, 230].

### Advances in science and technology to meet challenges

Scanning NV microscopy [221, 226, 227] represents the most advanced NV-based sensing/imaging technique in the current state-of-the-art. Further improvement of its spatial resolution relies on advances in diamond fabrication skills to create shallowly implanted NV centres in patterned diamond cantilevers to establish sub-nanometre scale proximity between NV single-spin sensors and materials studied. Meanwhile, it is worth mentioning that spin defects contained in other solid-state media such as silicon carbide and hexagonal boron nitride [229, 231, 232] also host the promise to achieve atomic scale quantum sensing and imaging. Over the past few years, tremendous research efforts have been devoted along this research direction [220, 229]. For instance, quantum sensing and wide-field imaging of local spin textures of proximate low-dimensional magnets in hexagonal boron nitride-based van der Waals heterostructures have been recently demonstrated [231, 232]. The spin-sensor-to-sample distance in the presented device structures could ultimately reach the atomic length scale, offering a new platform for implementing ultrasensitive quantum sensing of spin, charge, and thermal signals at the nanoscale.

In order to expand the magnetic field range of NV-based quantum sensing techniques, microwave engineering is required to develop high-frequency, low-loss microwave circuits for NV operation. The recent development of (sub)THz frequency microwave technologies promises to push the operational magnetic field range of NV sensing to the tens

of tesla regime. Meanwhile, the usage of [111] oriented diamond containing out-of-plane oriented NV centres could also partially address this issue especially for studying magnetic materials with spontaneous perpendicular anisotropy. To date, longitudinal NV spin relaxation time  $T_1$  has been investigated with the application of an external magnetic field up to 8 Tesla along the [111] axis of the diamond sample [233].

In current NV measurements, spin states of individual NV centres are mainly controlled by spatially dispersive microwave Oersted fields generated by electric currents in a proximate stripline or waveguide and optically detected by measuring the NV fluorescence [223, 225]. The electromagnetic crosstalk and Joule heat associated with this approach will inevitably lead to decoherence of NV spin qubits, imposing an inherent challenge to develop a high-density, scalable NV-based quantum operation platform. To address these issues, it is highly desirable to explore alternative strategies such as utilizing microwave magnetic fields generated by resonant nanomagnets [223, 230] and mechanical resonators [234] to achieve efficient control and readout of NV spin qubits. Coherent magnetic oscillations of the functional nanomagnets could be electrically excited by the spin-transfer torque, spin-orbit torque, or voltage-controlled magnetic anisotropy [223, 230]. We note that the magnetic stray fields generated by nanomagnets spatially decay in a much more rapid way due to the dipole interaction in comparison with the Oersted fields, significantly improving the scalability of NV spin qubits for implementing high-density quantum devices. To improve the adaptability of the NV centres to device integration, solid-state-based transducers [229, 230], e.g. SWs [223, 230], photons [229], and other interconnects have been actively explored to establish long-range NV–NV interaction beyond the conventional dipole–dipole coupling [228] regime, offering a new NV-based quantum operational platform for next-generation quantum information science and technological applications.

### Concluding remarks

In summary, NV centres with nanoscale spatial resolution and high field sensitivity hold significant potential for spintronics study and development of state-of-the-art quantum information sciences. As the rapid development of modern scientific research in material synthesis technologies, device fabrications, microwave engineering etc, we share the optimism that NV centres will be applied to a broad range of experimental conditions to detect multiple degrees of freedom of emergent condensed matter systems, adding valuable functionalities to the tool box of the existing magneto optic techniques. The dipole coupling between solid-state materials/devices and NV centres will also provide ample opportunities for developing functional quantum architectures, contributing to the advancement of novel information computing technologies.



## 18. Time-resolved THz polarimetry of quantum materials

N Peter Armitage

Department of Physics and Astronomy, The Johns Hopkins University, Baltimore, MD 21210

### Status

The linear response of a condensed matter system to electromagnetic waves can be characterized by its frequency dependent complex conductivity and/or its complex magnetic susceptibility. Although the THz is a natural frequency scale for many condensed matter systems, until recently many materials' [235] electromagnetic responses were unexplored in the THz range as these frequencies lie above what can be measured with conventional AC electronics and below that accessible with optics (photonics). However, in recent years, techniques such as time-domain THz have been developed that span this gap, creating scientific opportunities that were not widely available previously. Even more recently it has become clear that pairing time-domain THz spectroscopy (TDS) with dc magnetic fields uniquely leverages the capability of TDS as the capacity to measure a material's *complex* response function as a function of frequency, magnetic field, and polarization gives a very detailed look into its low energy phenomenon. These experiments and capabilities have some resemblance to those performed in THz ellipsometry (see section 19), but here the sensitivity to complex response functions is performed by directly measuring the phase relationships of two orthogonal  $E$  fields and not via measuring how elliptical polarization changes upon oblique reflection or transmission.

The reason these new experiments are so powerful are multifold. First is the simple matching of energy scales. The energy of excitation can be increased by putting systems in magnetic field and pushed into the THz range. The rough energy scale of excitations is  $eB\hbar/m$ , which for magnetic phenomena sets the energy scale for spin flip excitations (where  $m$  is the bare electronic mass). For electronic excitations, this energy is that of cyclotron motion where  $m$  is the particle mass. For a 10 T field, this corresponds to approximately 0.14 THz, although in many systems the actual excitations will be at larger frequencies due to magnetic anisotropy and larger  $g$ -factors (for magnetic excitations), and smaller masses (for many topological systems). Therefore with laboratory magnets, the relevant excitations are in the THz range. Second, an exceedingly important innovation has come in being able to discriminate the polarized THz response, such that the conductivity of the system or the magnetic response can be given in terms of right (R) and left (L) polarized light [235–238]. These are the 'polarization eigenstates' for many materials in magnetic field; a material's response is much more simply understood in terms of them. However, these responses are only accessible if one can measure the complex transmissions and polarization rotations for  $x$  and  $y$  polarized light (which

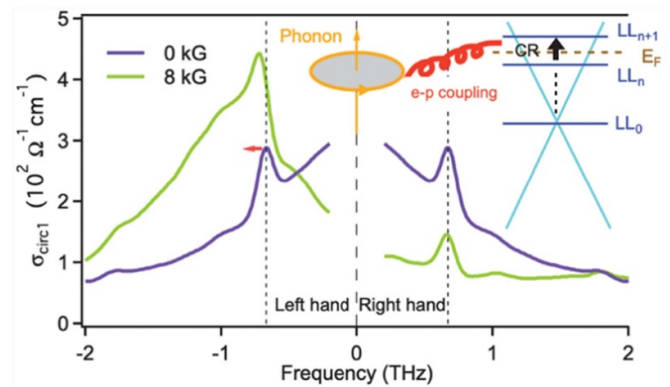


**Figure 29.** Comparing the optical conductivity of thin films of  $\text{Cd}_3\text{As}_2$  in 0 kG and 8 kG. The response of the material to L and R hand polarized THz light is given in terms of negative and positive frequencies. Reprinted with permission from [238]. Copyright (2020) American Chemical Society.

is then transformed to the R/L basis). Polarization resolved experiments using older phase insensitive Fourier transform infrared style experiments cannot resolve this information.

### Current and future challenges

A number of examples of the usefulness of these methods can be given. In figure 29, I show the THz spectra of a thin film of a Dirac semimetal  $\text{Cd}_3\text{As}_2$  [238]. At zero magnetic field, the data show a prominent zero frequency Drude peak from the free carriers, and two smaller sharp phonon derived peaks at 0.67 and  $-0.67$  THz. We have plotted the response of the system to L and R polarized THz light as negative and positive frequencies (this follows as R/L light can be seen to have  $e^{\pm i\omega t}$  time dependence). With applied field, the peak shifts to negative frequencies, which is consistent with electron-like charge carriers. More notably at finite field, the phonons become circularly polarized, as shown by a notable splitting in response to R- and L-hand polarized light. This splitting can be expressed as an effective phonon magnetic moment that is approximately 2.7 times the Bohr magneton, which is almost four orders of magnitude larger than *ab initio* calculations predict for phonon magnetic moments in nonmagnetic insulators. This exceedingly large value is due to the coupling of the phonons to the cyclotron motion and is controlled directly by the electron–phonon coupling. Although large in absolute scale, it is still a small effect in the THz spectra and would be unresolvable if the separate L and R complex responses could not be discriminated.

A particularly important advance is access to very large magnetic fields with polarization discrimination [239, 240]. As shown in figure 30, advances in TDS technology based on systems with electronically-controlled optical sampling (ECOPS) allows a full THz spectrum to be taken on ms time scales and hence coupled to pulsed magnets. ECOPS works by using two ultrafast optical pulse trains that are electronically modulated at frequencies up to 1600 Hz instead of a

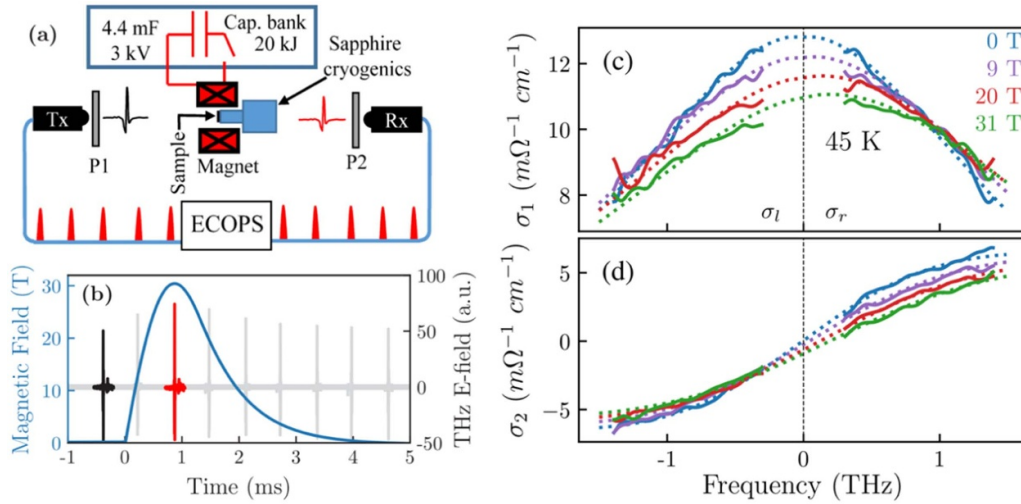


**Figure 30.** (a) Experimental schematic. A small pulsed magnet is incorporated with an ECOPS-based TDS system. Broadband THz optical pulses generated by the transmitter ( $T_x$ ) are linearly polarized (by P1) and focused through the sample in the magnet and directed through a second polarizer (P2) and detected by the gated receiver ( $R_x$ ). Parabolic collimating and focusing mirrors not shown. (b) The field profile of a 31 T magnet pulse (blue, left axis) is plotted along with the simultaneously measured THz electric field (right axis). (c) and (d) Experimentally measured optical conductivity from LSCO up to 31 T at 45 K. A clear cyclotron shift is observed, along with and broadening consistent with increasing scattering rate. Dashed lines show fits using a cyclotron model. Reprinted (figure) with permission from [241], Copyright (2021) by the American Physical Society.

mechanical delay. When synchronized to a pulsed magnetic field, the THz waveform can be recorded at multiple field values during a single pulse. Experiments were recently performed on the cuprate superconductor  $\text{La}_{2-x}\text{Sr}_x\text{CuO}_4$  (LSCO) up to 31 T [241]. As seen in figure 30, the low frequency Drude peak shifts slightly, but systematically to the positive frequency side, showing the existence of hole like carriers. The peak shift is linear in magnetic field revealing a hole mass of  $4.9 m_e$ . Because the shift is small, again, such information can only be gained by the ability to discriminate the response to R and L polarized light.

### Advances in science and technology to meet challenges

Going forward, it is essential to increase both the accessible maximum magnetic fields and the accessible low temperatures that are compatible with pulsed magnetic fields and these TDS spectrometers. Current pulsed setups coupled to ECOPS go to  $\sim 35$  Tesla, but it is likely that fields up to 60 T are possible. Fields this high would be useful for cuprate superconductors [241] (to quench magnetic field at even lower temperatures), and quantum magnets [242, 243]. Lower temperatures are also important as current cryostat designs for pulsed field systems keep the sample in vacuum and hence are limited to temperatures of  $\sim 10$  K. The use of these systems for many quantum magnets is limited therefore, because many systems have exchange constants on this order of energy. One would like to perform experiments in a superfluid helium bath, in which temperatures of 1.2 K are easily obtainable.

Experiments on quantum magnets to such temperatures at high fields are important because other magnetic spectroscopic measurements such as inelastic neutron scattering are currently limited to less than 14 T. This puts such high field THz spectroscopy in a unique position. It is also important to further increase the precision of measurements of Faraday rotation. Preliminary work indicates that fibre coupled TDS systems with two detection channels for measuring two orthogonal THz polarizations simultaneously can resolve Faraday rotations of approximately 1 millidegree or less [244]. This is an approximately two orders of magnitude advantage over previous schemes that used a fast rotating or manually rotated polarizers [236]. It opens up the possibility to perform precision experiments of the extremely small polarization rotations that have been resolved in the MIR range in materials like ruthenates and cuprates and have been interpreted to be a sign of spontaneous time-reversal symmetry breaking in those systems [245, 246].

### Concluding remarks

Time-domain THz experiments in magnetic field give vast opportunities. The ability to measure the polarized response with real and imaginary components as a function of frequency and field gives a tremendous amount of information that can be applied to superconductors, topological materials, and quantum magnets. With future advances, time-domain spectroscopic experiments should soon be possible to fields of 60 T or more opening up a new spectroscopic window into magneto-optics phenomena.

## 19. THz electron paramagnetic resonance (EPR) magneto-optical (MO) generalized spectroscopic ellipsometry (GSE) for spin characterization in materials

Mathias Schubert<sup>1,2</sup> and Vanya Darakchieva<sup>2,3</sup>

<sup>1</sup> Department of Electrical and Computer Engineering, University of Nebraska-Lincoln, Lincoln 68588, NE, United States of America

<sup>2</sup> Department of Physics, Chemistry and Biology (IFM), Linköping University, Linköping SE-581 83, Sweden

<sup>3</sup> NanoLund, Lund University, SE-221 00 Lund, Sweden

### Status

We propose the exploration and exploitation of free-space propagation polarized plane wave MO measurement techniques (MO GSE) for detection of EPR in samples with plane parallel interfaces consisting of, for example, wide-band gap (WBG) semiconductors, at ultrahigh frequencies and high magnetic fields, and thereby to establish MO THz-EPR-GSE. In this new approach, multiple significant and potentially paradigm shifting advantages over existing EPR methods emerge which can provide new and significant insight into the fundamental physics of magnetic resonance for WBG semiconductors and many other materials. A significant enhancement in sensitivity of many orders of magnitude towards the detectability and the characterization of spin densities is anticipated by this new approach over traditional (X-band absorbance based) EPR due to the high field conditions and due to the generalized ellipsometry (phase sensitive) EPR technique. Therefore, defect related spin properties in thin layers, and interfaces in thin film heterostructures may be accessible to EPR investigations. Further, the implementation of the concept of MO GSE dispenses with the need of a fixed resonant cavity, while tunable cavities when augmented may further increase the sensitivity to small spin densities. In addition to the g-tensor, the gyromagnetic frequency dependent permittivity tensor of simple and complex spin systems can be reconstructed from the Mueller matrix element information measured in the MO GSE experiment. This information permits to identify directional properties of a spin within its surrounding lattice, for example. We report on MO THz-EPR-GSE instrumentation capable of measuring Mueller matrix EPR data at high magnetic fields ( $-8 \dots +8$  Tesla) and show field and frequency dependent spin resonance of the nitrogen vacancy defect in hexagonal silicon carbide single crystals as example. We propose MO THz-EPR-GSE to improving our understanding of defects and their crystallographic relationships within WBG semiconductors.

### Current and future challenges

Traditional EPR methods exist in multiple variants and establish perhaps one of the most ubiquitous measurement

techniques in science [247]. It is also perhaps the most rewarded scientific field with numerous Nobel prizes based on either experimental and/or theoretical advances related to magnetic resonance and quantum mechanics principles of the electron and the nucleus, for example. Gaining access to electron spin dynamics at THz frequencies is of interest for understanding dynamic nuclear polarization methods and single-molecule magnets for quantum computation and has only recently seen broader interest [248]. The increase in frequency is ultimately tied to the need of increased magnetic fields. Furthermore, EPR methods are widely based on measurement of absorbance, while reflectance-based measurements are rare, as are measurements which determine the full polarization response, i.e. the polarization dependence of the absorbance or reflectance properties. The latter is fully described by a measurement of the Mueller matrix [249], which relates the most general description of light in terms of Stokes vector elements. Sixteen real-valued elements are contained within the Mueller matrix for a given measurement configuration, and can inform about handedness, character (electric, magnetic, magnetoelectric, etc), spatial and temporal dispersion including anisotropy [250], while such appear to be unknown for most EPR experiments. Measurement of Mueller matrix elements, or Jones matrix elements derived therefrom, with a sample immersed into an external magnetic field has traditionally been termed MO generalized ellipsometry (Berger and Pufall [107], Schubert *et al* [251], Ino *et al* [252], and others).

At THz frequencies, MO phenomena gain access to spin transitions. Frequency and time-domain absorbance-based EPR were demonstrated recently, see, e.g. [254–256]. The advantage of high-field EPR are manifold. The increase in spin susceptibility towards its maximum value at  $T = 0$  can be maintained even towards RT in large magnetic fields (e.g. [256]). The increased field means improved energy resolution of the EPR signatures. Deconvolution of subtle resonance lineshapes due to spin entanglements, e.g. with nuclear site magnetization, or electron cloud magnetization coupling permits more accurate assignment and quantification. The use of THz versus traditional, e.g. X band frequencies, permits dramatic improvement in sensitivity to spin volume densities, which we estimate to increase, for example, between 10 GHz and 0.225 THz by approximately 10 000 ([256], appendix F.3.3). The need for a fixed cavity and thus having only a single frequency available to measurement is dispensed with, and frequency scanning EPR is possible. This permits to unambiguously identify, for example, whether a given spin signature is affected by hyper fine structure splitting, anisotropy, and/or zero-field splitting since transitions shift in characteristic ways with changing field and frequency. The interaction of the THz wave with the sample can be described with conventional crystal optics and thereby permits access to the electromagnetic polarization characteristics of a given spin as well as its spatial orientation relative to the external magnetic field direction. Hence, the principle of ellipsometry can be implemented for EPR detection, permitting to characterize the polarization properties of a spin transition.

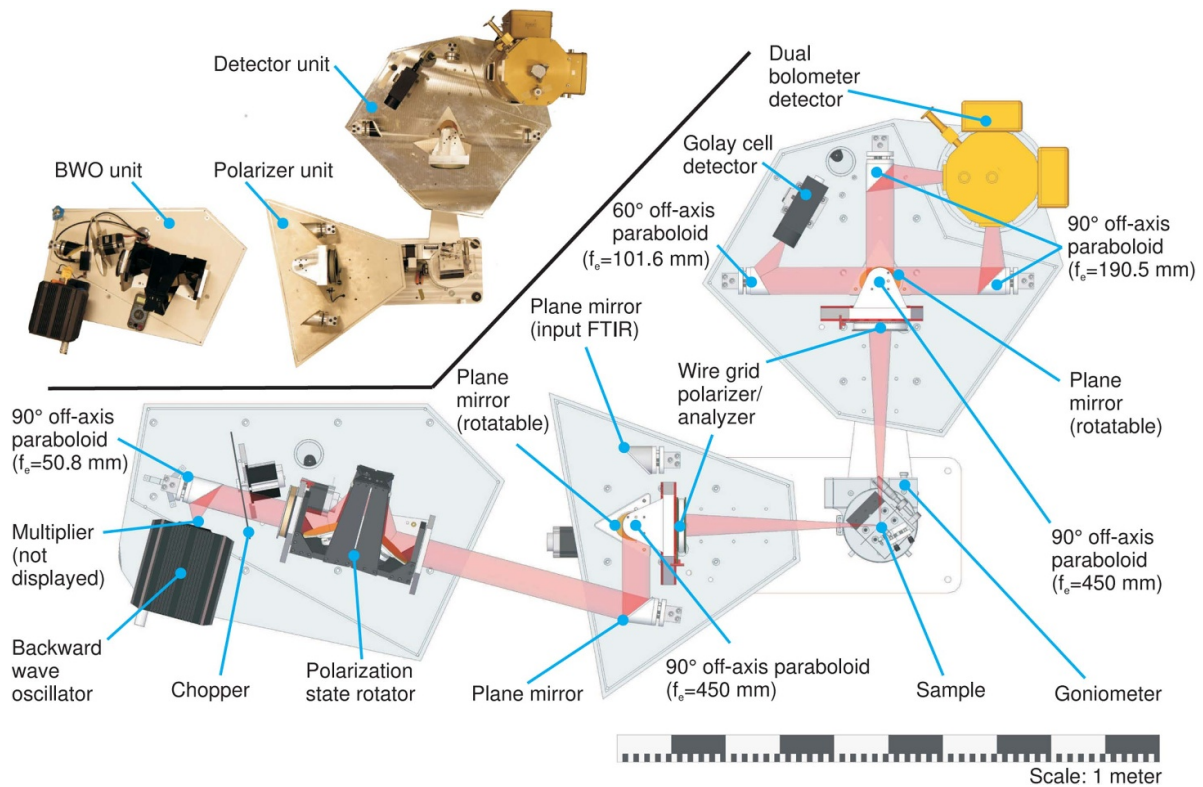


**Figure 31.** THz-EPR-E instrumentation adapted from an optical Hall effect instrumentation at the Terahertz Materials Analysis Center, Lund University. (Top left) Photograph (top view). (Bottom right) To scale drawing of all optical components. Future designs envision use of all-solid-state synthesizer THz source and detector components. © [2018] IEEE. Reprinted, with permission, from [258].

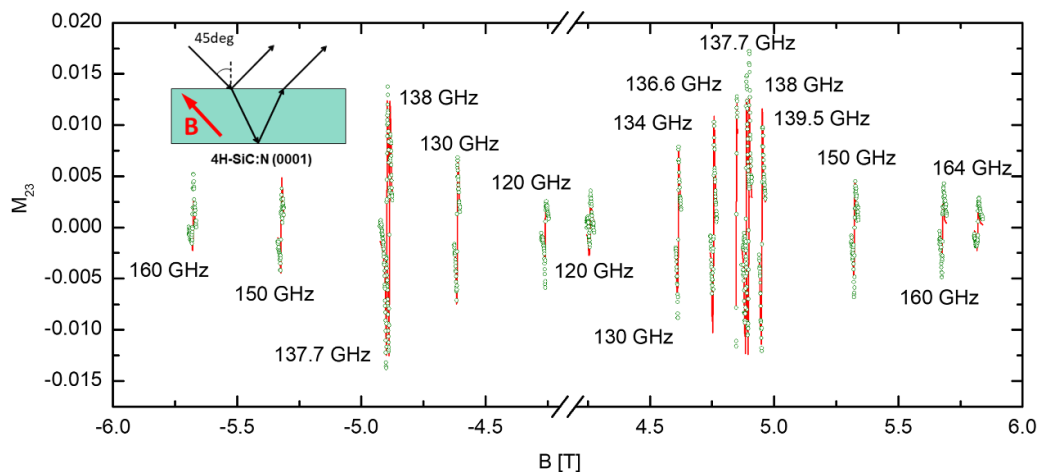


**Figure 32.** THz-EPR-E field scans of reflection Mueller matrix element data  $M_{23}$  at various frequencies of the nitrogen defect in SiC revealing the two (h and k site) hyperfine-structure-split triplet spin transitions at 10 K. The model calculated data are obtained from an ad-hoc solution of the spin dynamics assuming Landau-Level-like transitions in the magnetic susceptibility. The inset depicts the experimental configuration with the orientation of the magnetic field. The varying amplitudes with frequency are due to Fabry–Perot oscillations within the SiC substrate. Note the sign inversion of all signatures with sign inversion of B. Reprinted from [259], with the permission of AIP Publishing.

### Advances in science and technology to meet challenges

A recent review over status and perspectives of high-frequency EPR is given in [255]. The challenges for detecting

polarization resolved THz-EPR require superconducting magnets (fields larger than 4 Tesla) and an apparatus suitable for determining the Mueller matrix elements of a given sample placed within a magnetic field, at varying frequencies in the THz spectral range. Such apparatuses have been



described by our teams recently [257, 258], in part reproduced here in figure 31. The instruments employ free electron oscillator sources with extremely narrow bandwidth ( $\sim 2.5 \dots 25$  kHz depending on instrument configuration) and accessible spectral region of  $\sim 100$  GHz to  $\sim 1.5$  THz. We reproduce here results observed recently for the nitrogen defect in 4H-SiC [259], a spin system well investigated using traditional (X-band) as well as extended (Q-band) EPR techniques [260]. Mueller matrix element data  $M_{23}$ , which correspond to the amount of polarization rotation upon reflection of the THz wave from the silicon carbide substrate, are shown in figure 32 exemplarily for field scans at various frequencies and positive and negative magnetic fields. The model calculated ellipsometry data are obtained by sets of magnetic field and frequency dependent Lorentzian oscillator lineshape functions representing triplet spin transitions at hexagonal and cubic coordinated nitrogen sites (see [259] for further details).

## Concluding remarks

A new and rich set of polarization information on spin properties will become available at THz frequencies measured in high magnetic fields, and which has not been explored thus far. In addition to such high energy information, the full polarization response of spins can be explored by THz MO generalized spectroscopic ellipsometry. The authors foresee a large field of applications for this emerging instrumental approach, for example, in materials with antiferromagnetic order, or semiconductors with defect induced spin systems for quantum technology applications. We also suggest exploring detection of low-density spin systems such as defects in heteroepitaxial structures induced, e.g. by lattice mismatch and differences in thermal expansion coefficients of individual constituents. Such information is highly relevant for improvement of electronic device architectures, for example.



## 20. Giant magneto-optical (MO) Cotton–Mouton (CM) effect in 2D materials

Baofu Ding, Ziyang Huang and Bilu Liu

Shenzhen Geim Graphene Center, Tsinghua-Berkeley Shenzhen Institute and Institute of Materials Research, Tsinghua Shenzhen International Graduate School, Tsinghua University, Shenzhen 518055, People's Republic of China

### Status

The MO effect has received extensive attention from both scientists and technicians, due to its ability for both material characterization and light manipulation in a contactless and non-destructive way. According to the interaction between incident light and functional materials under a magnetic field, the MO interplay is categorized into four main groups, including Zeeman effect, Faraday effect, MOKE, and magneto-birefringence CM effect [261]. Among them, the CM effect, discovered in 1907 by Aimé Cotton and Henri Mouton, can serve as a promising tool to modulate polarization, intensity, and spectrum of incident light via magnetic control in a transmitted manner. When a linearly polarized light propagates through the magneto-birefringent media with the propagation direction perpendicular to the magnetic field, a phase retardation between two orthogonal vector components of the light can generate birefringence, which make them transport at different speeds.

Quantitatively, the CM effect can be described by the expression of  $\Delta n = C\lambda B^2$ , given that the birefringence  $\Delta n$  is proportional to the square of magnetic field  $B$ , where  $C$  and  $\lambda$  are CM coefficient and wavelength of light, respectively. The CM coefficient reflects the sensitivity of functional materials in response to the external magnetic stimulus, and is determined by intrinsic parameters of materials, including their magnetic susceptibility anisotropy, optical anisotropy, and phase-transition concentration, as schematically shown in figure 33 [262].

Despite the CM effect has been studied for more than a century, the CM coefficient, key parameter to evaluate the sensitivity of the effect, is quite low for transparent birefringent media. The practical application of using CM effect to manipulate light requires accurate control of birefringence via external magnetic stimuli in an energy-efficient way. In this regard, the CM coefficient is expected to be as large as possible. It means that the given birefringence of a medium should be induced by a low magnetic field, which can be readily supplied by a permanent magnet and support the portability or even energy-free operation. In principle, all transparent media have CM effect, including gas, water, organic solvent, biological fluid, and liquid crystals (LCs). Unfortunately, most of them have trivial CM effect, i.e. ultralow CM coefficient. Among them, LCs possess relative high CM coefficient and enter the range of  $1\text{--}10\text{ T}^{-2}\text{ m}^{-1}$  due to their large optical anisotropy, enabling the control of the magneto-birefringence

based on the use of an electromagnet to drive LCs [263]. Other media, however, limited by their very small CM coefficient, must be operated in high magnetic field of several or even tens of tesla supplied by high-power and low-temperature superconducting magnets. Such coefficient is not preferred as it cannot meet the condition for real application. It is the relative low coefficient that makes the development of light modulator based on MO CM effect far behind the counterpart based on electro-optic Kerr effect which has been widely used in many optical fields, such as display, smart windows, spatial light modulator, and sensors with an annual global market of >100 billion US\$.

Almost parallelly, tremendous efforts have been devoted to investigating 2D materials since the isolation of graphene in 2004. There are several unique features of 2D materials [264]. Most fundamentally, when making a stable dispersion, 2D materials possessing the largest possible structural anisotropy and resulting anisotropies in optical, magnetic, and electronic properties, among matters in all dimensions. In addition, the big family of 2D materials provide rich chemical and physical properties, and the existence of abundant natural layered minerals facilitate industrial level production of 2D materials at low costs [265–268]. The above features make 2D materials intriguing candidates for practical MO CM applications.

### Current and future challenges

To realize the application of CM-effect based light modulating, large CM coefficient, high saturation birefringence, low optical absorption, and high spatial uniformity are four prerequisites that must be met simultaneously [262]. According to Onsager's theory in LC physics, magnetism and magnetic anisotropy of the functional material in a birefringent medium are two key factors that determine the CM coefficient. Strong magnetism and high magnetic anisotropy of functional materials favour their alignment in a small magnetic field, and give rise to a high CM coefficient. Consequently, some functional materials with the intrinsic ferromagnetism, paramagnetism or superparamagnetism have been explored previously. For instance, sphere-, rod- or disc-like nanoparticles (iron-oxide, iron oxyhydroxide, barium ferrite) with modified surface have been dispersed in solvent and used as functional units in birefringent media [269, 270]. Despite the remarkable improvement in the magnetic sensitivity of these materials, low optical anisotropy, and concentration of iron-oxide nanoparticles in suspension restrict them to meet the condition of high saturation birefringence.

To overcome the limitation, a composite material system consisting of both 2D magnetic nanoparticles and organic LCs is developed and termed as ferronematic LCs [271]. In the presence of a low external magnetic field, these FM 2D nanoparticles, such as barium hexaferrite, can be easily aligned and serve as the micro-motor to drive the adjacent LC molecules to direct parallel to them. Meantime, thanks to their large optical anisotropy and high concentration, the aligned LC molecules

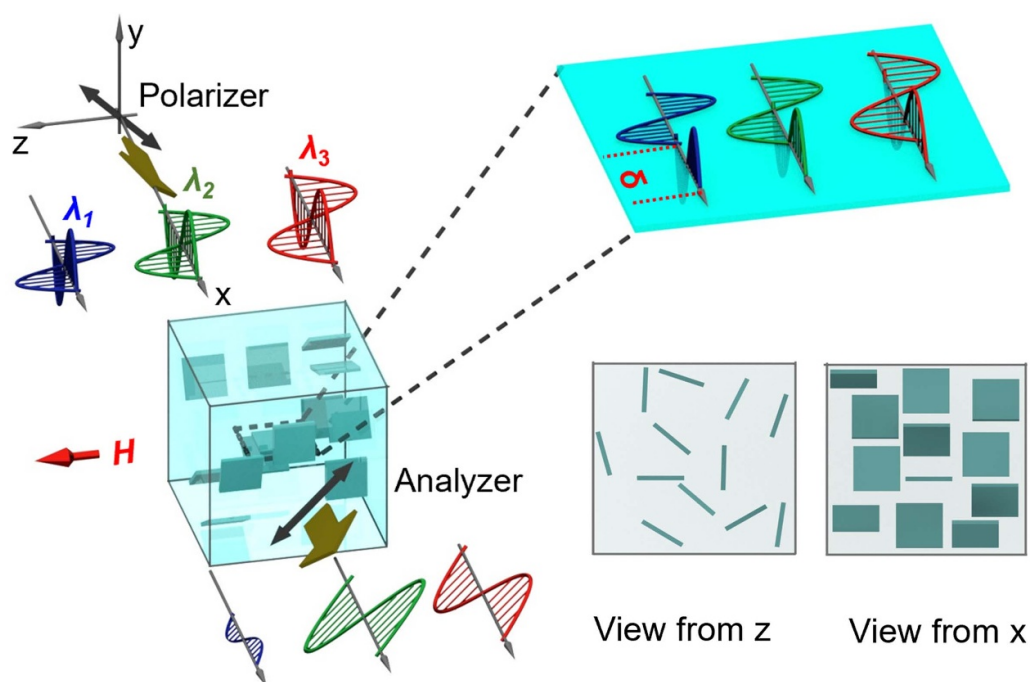


**Figure 33.** Scheme of MO CM effect of 2D materials. In the presence of magnetic field, magnetic 2D materials are aligned parallel or perpendicular to the magnetic flux, giving rise to birefringence of the suspension. The incident linearly polarized light can be decomposed to two polarized components (parallel and perpendicular to magnetic field). After transporting through the suspension, two polarized components have established an in-between phase retardation  $\delta = \frac{2\pi\Delta n d}{\lambda}$ , where  $\Delta n$  the magneto-birefringence,  $d$  the optical path distance,  $\lambda$  the wavelength. When passing through the analyser, optical interference between two components dominates the final intensity of light with wavelength of  $\lambda$ . Reproduced from [262]. CC BY 4.0.

demonstrate high macroscopic saturation birefringence. In this regard, the large saturation birefringence of LCs and high magnetic sensitivity of superparamagnetic/FM materials are effectively combined in the developed composite system. It is worthy to note that in addition to the high magnetic sensitivity and saturation birefringence, the see-through CM based light modulator also requires the high transparency and superior spatial uniformity of the birefringent media. The use of the above materials with strong magnetism usually introduces strong light absorption or scattering, leading to low transparency and depolarization effect, in addition to the problem that their aggregation in the magnetic field make the magneto-birefringence spatially un-uniform. Therefore, it is still challenging to find proper media that can simultaneously satisfy all the four demands.

### Advances in science and technology to meet challenges

Considering the largest structural, magnetic, and optical anisotropies of 2D materials in suspension as well as their surface charges which can enhance dispersion stability [272–274], breakthroughs in the development of CM effect have been made recently in a paramagnetic 2D material with wide band gaps, named 2D cobalt-doped titanium oxide (2D CTO, figures 34(a) and (b)) [262]. A 2D CTO has a wide bandgap of  $>3.5$  eV, and the doping of magnetic element Co increases its magnetism by more than 100 times with negligible decrease of

transparency. The CM coefficient of CTO LC is measured to be  $1400 \text{ T}^{-2} \text{ m}^{-1}$  (figure 34(c)), which is three orders of magnitude larger than other known transparent birefringent media and even comparable with that of opaque suspension consisting of superparamagnetic nanoparticles. Moreover, the 2D CTO nanosheets are sorted in terms of their lateral sizes by a centrifugation method [272]. MO measurements on the monolayer CTO suspension reveal a quadratic dependence of the CM coefficient with lateral size (figure 34(d)) [272]. By introducing the collective behaviour into CTO colloidal system, the CM coefficient is further doubled and reaches a record-high value of  $2700 \text{ T}^{-2} \text{ m}^{-1}$  (figure 34(e)) [274]. High transparency, uniform dispersion, large optical anisotropy, and giant CM effect of CTO dispersion together permit the fabrication of light modulators which work at zero-energy-consumption manner due to the use of permanent magnets. This achievement suggests clear potential of the CM effect toward practical applications in light modulation and other fields. There are many exciting scientific and technological opportunities in this field, including further increase of CM coefficient and device performance, exploitation of other RT FM 2D materials [275], extension of the spectral coverage of the transparent light modulator to the deep/extreme UV or long infrared regimes, device operation at cryogenic or high temperature, etc. For example, a recent work shows that layered minerals like vermiculite has been exfoliated into 2D sheets and possessing sensitive MO CM effect, featuring advantages of low-cost, green production, and fully recyclable in terms of materials and devices [265].

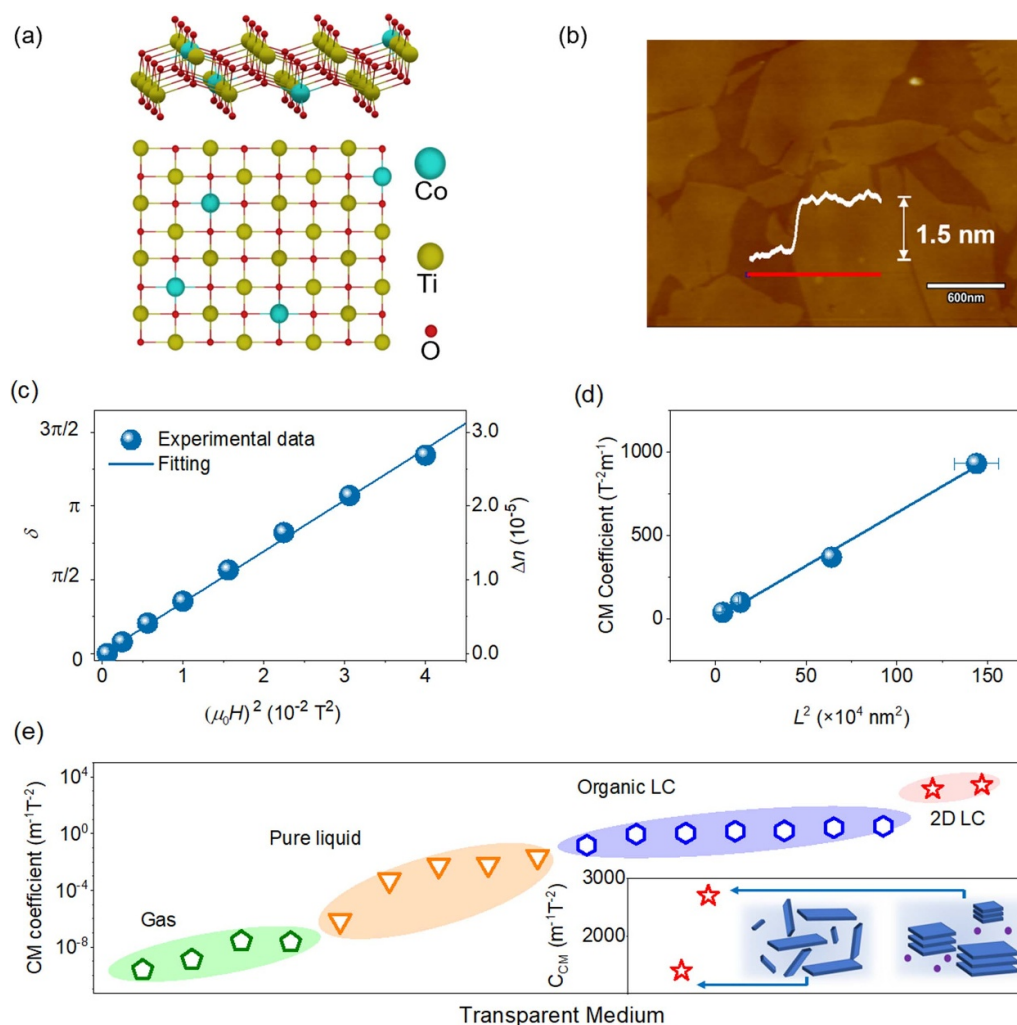


**Figure 34.** Giant MO CM effect of 2D CTO. (a) Atomic structure of 2D CTO. (b) AFM image of 2D CTO. (c) Magnetic-field dependence of the birefringence in the low-field range for 2D CTO LC. Symbols: experimental data; solid line: linear fit. Here, birefringence is proportional to the square of magnetic field. Reproduced from [262]. CC BY 4.0. (d) CM coefficient verse  $L^2$  ( $L$  is the lateral size). The fitting result gives that the CM coefficient has a linear dependence with the square of lateral size of 2D CTO. Reprinted with permission from [272]. Copyright (2021) American Chemical Society. (e) Summary of the CM coefficient obtained so far among all transparent media, including gas, pure solvent, organic LC and 2D CTO LC. Inset shows the comparison of CM coefficient between collective-behaviour dominant and individual-behaviour dominant 2D CTO LC. Reprinted with permission from [274]. Copyright (2021) American Chemical Society.

## Concluding remarks

The development of MO CM effect and the use of 2D materials towards giant CM effect have been discussed. The practical applications of CM effect in light manipulation have been long term hindered by the following reasons, including small CM coefficient induced weak CM effect, small saturation birefringence, low transparency, and/or poor medium uniformity. Several promising strategies and material systems especially 2D materials may overcome these limitations. With continuous developments, the CM effect may hold great promise to

provide an energy-efficient and contactless way for both magnetic material characterization and light manipulation, and further for vast emerging applications, such as interference colour marker, visible chemical/magnetic sensor, continuous phase retarder, flexible magneto-electro-optical device, among many others, just as its counterpart phenomenon, the electro-optical Kerr effect does.

## Data availability statement

No new data were created or analysed in this study.

## Acknowledgments

### 1. Introduction: perspective on recent advances in magneto-optics

*Alexey V Kimel and Anatoly K Zvezdin*

We thank D Afanasiev for critical reading and useful comments. This work was supported by the Dutch Research Council (NWO) and the Russian Science Foundation (RSF, Grant No. 20-42-08002).

### 2. Magneto-optics: quantum mechanical description and predictions

*Sangeeta Sharma and Samuel Shallcross*

Sharma would like to thank DFG for funding through TRR227 (Project A04). Shallcross would like to thank DFG for funding through SH498/4-1. Sharma would also like to thank Dr von Korff Schmising for useful discussions.

### 3. Magneto-optics: electromagnetic theory and modelling

*Nuno de Sousa and Antonio García-Martín*

This work is supported by the Ministerio de Ciencia e Innovación (Grant No. PID2019-109905GA-C22).

### 4. Spectroscopic magneto-optical (MO) characterization

*Georgeta Salvan*

Dr Apoorva Sharma, Dr Shun Okano, and Professor Dr D R T Zahn are thankfully acknowledged for fruitful discussions during the preparation of the manuscript. This work was supported by the Deutsche Forschungsgemeinschaft (DFG) under the project 282193534.

### 5. Higher order magneto-optics effect

*Jaroslav Hamrle and Ondřej Stejskal*

The authors thank Robin Silber, Timo Kuschel and Martin Veis for support, assistance and discussion. This work was supported by Czech Science Foundation (19-13310S) and by OP VVV project MATFUN under Grant CZ.02.1.01/0.0/0.0/15\_003/0000487.

### 6. Kerr microscopy

*Jeffrey McCord*

J M thanks many colleagues for discussions over the last years and in particular wants to thank E Golubeva, R B Holländer, S Jarausch, M Jovičević-Klug, E Lage, B Mozooni, C Müller, M Römer-Stumm, and N O Urs, as well as R Schäfer. Continuous support by the German Science Foundation, especially through their Heisenberg professorship program (DFG MC9/9) and current funding from the Collaborative Research Centre SFB 1261 is highly acknowledged.

### 7. Probing magnons in the frequency domain: Brillouin light scattering (BLS)

*Silvia Tacchi and Giovanni Carlotti*

The authors acknowledge financial support from the Italian Ministry of University and Research through the PRIN-2020 project entitled ‘The Italian factory of micromagnetic modeling and spintronics’, cod. 2020LWPKH7.

### 8. MOKE measurements of spin and orbital currents in nonmagnetic semiconductors and metals

*Pietro Gambardella and Gian Salis*

We acknowledge financial support from the NCCR QSIT and Grant No. 200020\_200465 of the Swiss National Science Foundation.

### 9. Generalized magneto-optical (MO) ellipsometry (GME)

*Andreas Berger*

Work at nanoGUNE was supported by the Spanish Ministry of Science and Innovation under the Maria de Maeztu Units of Excellence Programme (CEX2020-001038-M) and Project No. RTI2018-094881-B-100 (MICINN/FEDER).

### 11. Ultrafast magneto-optics and magneto-acoustics with exchange magnons

*Vasily Temnov, Igor V Bychkov and Leonid Kotov*

Funding from the Agence Nationale de la Recherche (Grant ANR-15-CE24-0032—PPMI-NANO), the Russian Science Foundation (Project No. 21-72-20048) and the Russian Foundation of Basic Research (RFBR 20-07-00466) are gratefully acknowledged.

### 12. Magnetoplasmonics

*Paolo Vavassori and Nicolò Maccaferri*

P V acknowledges support from the Spanish Ministry of Science, Innovation and Universities under the Maria de Maeztu Units of Excellence Programme (CEX2020-001038-M) and the Project RTI2018-094881-B-I00 (MICINN/FEDER). N M acknowledges support from the Luxembourg National Research Fund (Grant No. C19/MS/13624497 ‘ULTRON’), the European Union under the FETOPEN-01-2018-2019-2020 call (Grant No. 964363 ‘ProID’) and the Swedish Research Council (Grant No. 2021-05784).

### 13. All-dielectric magneto-optical metasurfaces (ADMOMSs)

*Daria O Ignatyeva and Vladimir I Belotelov*

This work was financially supported by the Russian Ministry of Science and Higher Education of the Russian Federation, Megagrant Project No. 075-15-2022-1108.



#### 14. Characterization of 3D magnetic nanostructures

*Claire Donnelly and Aurelio Hierro-Rodriguez*

C D acknowledges the support of the Max Planck Society Lise Meitner Excellence Program. A H-R acknowledges the support of the Spanish AEI under project reference PID2019-220104604RB/AEI/10.13039/501100011033. The authors thank Amalio Fernandez Pacheco, Salvador Ferrer, Peter Fischer, Manuel Guizar-Sicairos, Valerio Scagnoli and Charudatta Phatak for fruitful discussions.

#### 15. Magneto-optics with free electron lasers (FELs)

*Iwao Matsuda*

The research was made under the SACLA Basic Development Program 2018–2020. The development was also performed at the facilities of the Synchrotron Radiation Research Organization at the University of Tokyo. The review is based on the XFEL experiments at SACLA with the approval of the Japan Synchrotron Radiation Research Institute (JASRI). The author would like to acknowledge the staff of the SACLA facility, especially Dr Yuya Kubota, Dr Makina Yabashi, Dr Kensuke Tono, and Dr Shigeki Owada.

#### 16. Magneto-optics with light beams carrying orbital angular momentum

*Thierry Ruchon, Mauro Fanciulli and Maurizio Sacchi*

We are very grateful to Matteo Pancaldi (FERMI – Sincrotrone Trieste) and Martin Luttmann (LIDYL, Université Paris Saclay, CEA) for their support and for fruitful discussions. This work was supported by the French ANR under contracts ANR-10-LABX-0039 – PALM (Labex), ANR-11-EQPX0005 – ATTOLAB (Equipex), ANR-21-CE30-0037 – HELIMAG, the Scientific Cooperation Foundation of Paris-Saclay University through the funding of the OPT2X research project (Lidex 2014), by the Ile-de-France region through the Pulse-X project, by the European Union's Horizon 2020 Research and Innovation Programme No. EU-H2020-LASERLAB-EUROPE-654148, and by the Swiss SNSF (project P2ELP2\_181877).

#### 17. Probing spintronics systems using nitrogen-vacancy (NV) centres in diamond

*Hailong Wang and Chunhui Rita Du*

The authors acknowledge the support from Air Force Office of Scientific Research under Award FA9550-21-1-0125.

#### 18. Time-resolved THz polarimetry of quantum materials

*N Peter Armitage*

NPA would like to acknowledge various collaborators whose works are referenced above including I Bozovic, S Crooker, K Post, and S Stemmer. He would also like to acknowledge the contributions of his former student B Cheng and former postdoc A Legros. His recent work on this topic has been supported by ARO MURI W911NF2020166, NSF Grant DMR-1905519, and under the auspices of the Institute for

Quantum Matter, an EFRC funded by the DOE BES under DE-SC0019331.

#### 19. THz EPR magneto-optical (MO) generalized spectroscopic ellipsometry for spin characterization in materials

*Mathias Schubert and Vanya Darakchieva*

We acknowledge support by the National Science Foundation Awards DMR 1808715, OIA-2044049, by Air Force Office of Scientific Research Awards FA9550-18-1-0360, FA9550-19-S-0003, and FA9550-21-1-0259, by the Knut and Alice Wallenbergs Foundation, by the University of Nebraska Foundation and the J A Woollam Foundation, by the Swedish Research Council VR Award No. 2016-00889, the Swedish Foundation for Strategic Research Grant Nos. RIF14-055 and EM16-0024, by the Swedish Governmental Agency for Innovation Systems VINNOVA under the Competence Center Program Grant No. 2016-05190, and by the Swedish Government Strategic Research Area in Materials Science on Functional Materials at Linköping University, Faculty Grant SFO Mat LiU No. 2009-00971.

#### 20. Giant magneto-optical (MO) Cotton–Mouton (CM) effect in 2D materials

*Baofu Ding, Ziyang Huang and Bilu Liu*

We acknowledge support by the National Natural Science Foundation of China (No. 51920105002), the National Science Fund for Distinguished Young Scholars (No. 52125309), the Guangdong Innovative and Entrepreneurial Research Team Program (No. 2017ZT07C341), and the Shenzhen Basic Research Project (Nos. JCYJ20190809180605522 and WDZC20200819095319002).

#### ORCID iDs

Alexey Kimel  <https://orcid.org/0000-0002-0709-042X>  
 Anatoly Zvezdin  <https://orcid.org/0000-0002-6039-780X>  
 Nuno de Sousa  <https://orcid.org/0000-0002-3226-9683>  
 Antonio García-Martín  <https://orcid.org/0000-0002-3248-2708>  
 Georgeta Salvan  <https://orcid.org/0000-0002-2565-9675>  
 Jaroslav Hamrle  <https://orcid.org/0000-0002-8873-3414>  
 Ondřej Stejskal  <https://orcid.org/0000-0002-4235-8612>  
 Jeffrey McCord  <https://orcid.org/0000-0003-0237-6450>  
 Silvia Tacchi  <https://orcid.org/0000-0003-1403-2268>  
 Pietro Gambardella  <https://orcid.org/0000-0003-0031-9217>  
 Markus Münzenberg  <https://orcid.org/0000-0002-1332-5678>  
 Martin Schultze  <https://orcid.org/0000-0003-0438-9255>  
 Vasily Temnov  <https://orcid.org/0000-0003-2708-5916>  
 Nicolò Maccaferri  <https://orcid.org/0000-0002-0143-1510>  
 Daria Ignatyeva  <https://orcid.org/0000-0002-1113-6021>  
 Vladimir Belotelov  <https://orcid.org/0000-0002-6939-4728>  
 Claire Donnelly  <https://orcid.org/0000-0002-9942-2419>  
 Thierry Ruchon  <https://orcid.org/0000-0001-7933-8933>

Mauro Fanciulli  <https://orcid.org/0000-0002-7018-0110>  
 Maurizio Sacchi  <https://orcid.org/0000-0002-3205-0796>  
 Chunhui Rita Du  <https://orcid.org/0000-0001-8063-7711>  
 Hailong Wang  <https://orcid.org/0000-0002-5617-8487>  
 Bilu Liu  <https://orcid.org/0000-0002-7274-5752>  
 Andreas Berger  <https://orcid.org/0000-0001-5865-6609>  
 Paolo Vavassori  <https://orcid.org/0000-0002-4735-6640>

## References

- [1] Fiebig M, Pavlov V V and Pisarev R V 2005 Second-harmonic generation as a tool for studying electronic and magnetic structures of crystals: review *J. Opt. Soc. Am. B* **22** 96–118
- [2] Siegmann H C and Stöhr J 2006 *Magnetism: From Fundamentals to Nanoscale Dynamics* (Berlin: Springer)
- [3] Inoue M, Mitsuteru L, Levy M and Baryshev A V 2003 *Magnetophotonics: From Theory to Applications* (Berlin: Springer)
- [4] Belotelov V I, Doskolovich L L and Zvezdin A K 2007 Extraordinary magneto-optical effects and transmission through metal-dielectric plasmonic systems *Phys. Rev. Lett.* **98** 077401
- [5] Crassee I, Levallois J, Walter A L, Ostler M, Bostwick A, Rotenberg E, Seyller T, van der Marel D and Kuzmenko A B 2011 Giant Faraday rotation in single- and multilayer graphene *Nat. Phys.* **7** 48–51
- [6] Huisman T J, Mikhaylovskiy R V, Rasing T, Kimel A V, Tsukamoto A, de Ronde B, Ma L, Fan W J and Zhou S M 2017 Sub-100-ps dynamics of the anomalous Hall effect at terahertz frequencies *Phys. Rev. B* **95** 094418
- [7] Carva K, Battiato M and Oppeneer P M 2011 Is the controversy over femtosecond magneto-optics really solved? *Nat. Phys.* **7** 665
- [8] Gerasimov M V, Logunov M V, Spirin A V, Nozdin Y N and Tokman I D 2016 Time evolution of domain-wall motion induced by nanosecond laser pulses *Phys. Rev. B* **94** 014434
- [9] Büttner F *et al* 2021 Observation of fluctuation-mediated picosecond nucleation of a topological phase *Nat. Mater.* **20** 30–37
- [10] Can-Ming H 2020 The 2020 roadmap for spin cavitronics *Solid State Phys.* **71** 117–21
- [11] Beaurepaire E, Merle J-C, Daunois A and Bigot J-Y 1996 Ultrafast spin dynamics in ferromagnetic nickel *Phys. Rev. Lett.* **76** 4250–3
- [12] Zhang G P and Hübner W 2000 Laser-induced ultrafast demagnetization in ferromagnetic metals *Phys. Rev. Lett.* **85** 3025
- [13] Krieger K, Dewhurst J K, Elliott P, Sharma S and Gross E K U 2015 Laser-induced demagnetization at ultrashort time scales: predictions of TDDFT *J. Chem. Theory Comput.* **11** 4870
- [14] Stamm C *et al* 2007 Femtosecond modification of electron localization and transfer of angular momentum in nickel *Nat. Mater.* **6** 740–3
- [15] Battiato M, Carva K and Oppeneer P M 2010 Superdiffusive spin transport as a mechanism of ultrafast demagnetization *Phys. Rev. Lett.* **105** 027203
- [16] Hennecke M, Radu I, Abrudan R, Kachel T, Holldack K, Mitzner R, Tsukamoto A and Eisebitt S 2019 Angular momentum flow during ultrafast demagnetization of a ferrimagnet *Phys. Rev. Lett.* **122** 157202
- [17] Schellekens A J, Verhoeven W, Vader T N and Koopmans B 2013 Investigating the contribution of superdiffusive transport to ultrafast demagnetization of ferromagnetic thin films *Appl. Phys. Lett.* **102** 252408
- [18] Dewhurst J K, Elliott P, Shallcross S, Gross E K U and Sharma S 2018 Laser induced inter-site spin transfer *Nano Lett.* **18** 1842
- [19] Dewhurst J, Willems F, Elliott P, Li Q, von Korff Schmising C, Strüber C, Engel D, Eisebitt S and Sharma S 2020 Element specificity of transient extreme ultraviolet magnetic dichroism *Phys. Rev. Lett.* **124** 077203
- [20] de Giovannini U, Hübener H, Sato S A and Rubio A 2020 Direct measurement of electron-phonon coupling with time-resolved ARPES *Phys. Rev. Lett.* **125** 136401
- [21] Juraschek D M, Narang P and Spaldin N A 2020 Phono-magnetic analogs to opto-magnetic effects *Phys. Rev. Res.* **2** 043035
- [22] Yabana K, Sugiyama T, Shinohara Y, Otake T and Bertsch G F 2012 Time-dependent density functional theory for strong electromagnetic fields in crystalline solids *Phys. Rev. B* **85** 045134
- [23] Singh N, Elliott P, Dewhurst J K and Sharma S 2021 Manipulating magnons via ultrafast magnetization modulation *Phys. Rev. B* **103** 134402
- [24] Müller T, Sharma S, Gross E K U and Dewhurst J K 2020 Extending solid-state calculations to ultra-long-range length scales *Phys. Rev. Lett.* **125** 256402
- [25] Oppeneer P M, Mertins H-C, Abramsohn D, Gaupp A, Gudat W, Kuneš J and Schneider C M 2003 Buried antiferromagnetic films investigated by x-ray magneto-optical reflection spectroscopy *Phys. Rev. B* **67** 052401
- [26] Višňovský Š 2018 *Optics in Magnetic Multilayers and Nanostructures* (Boca Raton, FL: CRC Press)
- [27] Mansuripur M 1990 Analysis of multilayer thin-film structures containing magneto-optic and anisotropic media at oblique incidence using  $2 \times 2$  matrices *J. Appl. Phys.* **67** 6466
- [28] García-Martín A, Armelles G and Pereira S 2005 Light transport in photonic crystals composed of magneto-optically active materials *Phys. Rev. B* **71** 205116
- [29] Liscidini M, Gerace D, Andreani L C and Sipe J E 2008 Scattering-matrix analysis of periodically patterned multilayers with asymmetric unit cells and birefringent media *Phys. Rev. B* **77** 035324
- [30] Caballero B, García-Martín A and Cuevas J C 2012 Generalized scattering-matrix approach for magneto-optics in periodically patterned multilayer systems *Phys. Rev. B* **85** 245103
- [31] López-Ortega A, Zapata-Herrera M, Maccaferri N, Pancaldi M, García M, Chuvilín A and Vavassori P 2020 Enhanced magnetic modulation of light polarization exploiting hybridization with multipolar dark plasmons in magnetoplasmonic nanocavities *Light Sci. Appl.* **9** 49
- [32] Abujetas D R, de Sousa N, García-Martín A, Llorens J M and Sánchez-Gil J A 2021 Active angular tuning and switching of Brewster quasi bound states in the continuum in magneto-optic metasurfaces *Nanophotonics* **10** 17
- [33] Smith D A and Stokes K L 2006 Discrete dipole approximation for magneto-optical scattering calculations *Opt. Express* **14** 5746
- [34] de Sousa N, Froufe-Pérez L, Sáenz J J and García-Martín A 2016 Magneto-optical activity in high index dielectric nanoantennas *Sci. Rep.* **6** 30803
- [35] Piechulla P M, Fuhrmann B, Slivina E, Rockstuhl C, Wehrspohn R B and Sprafke A N 2021 Tailored light scattering through hyperuniform disorder in self-organized arrays of high-index nanodisks *Adv. Opt. Mater.* **9** 2100186
- [36] Froufe-Pérez L S, Engel M, Damasceno P F, Müller N, Haberkorn J, Glotzer S C and Scheffold F 2016 Role of

- short-range order and hyperuniformity in the formation of bandgaps in disordered photonic materials *Phys. Rev. Lett.* **117** 053902
- [37] Zvezdin A K and Kotov V A 1997 *Modern Magneto-optics and Magneto-optical Materials* (London: Institute of Physics Pub)
- [38] Mack J, Stillman M J and Kobayashi N 2007 Application of MCD spectroscopy to porphyrinoids *Coord. Chem. Rev.* **251** 429–53
- [39] Herrmann T, Lüdge K, Richter W, Georgarakis K G, Pouloupoulos P, Nünthel R, Lindner J, Wahl M and Esser N 2006 Optical anisotropy and magneto-optical properties of Ni on preoxidized Cu(110) *Phys. Rev. B* **73** 134408
- [40] Birnbaum T, Hahn T, Martin C, Kortus J, Fronk M, Lungwitz F, Zahn D R T and Salvan G 2014 Optical and magneto-optical properties of metal phthalocyanine and metal porphyrin thin films *J. Phys.: Condens. Matter* **26** 104201
- [41] Robaschik P *et al* 2015 Tuning the magneto-optical response of TbPc<sub>2</sub> single molecule magnets by the choice of the substrate *J. Mater. Chem. C* **3** 8039–49
- [42] Salvan G *et al* 2011 Nickel nanoparticles in fullerene matrix fabricated by co-evaporation: structural, magnetic, and magneto-optical properties *Appl. Phys. A* **103** 433–8
- [43] Li W, Fronk M, Albrecht M, Franke M, Zahn D R T and Salvan G 2014 Field-dependent magneto-optical Kerr effect spectroscopy applied to the magnetic component diagnosis of a rubrene/Ni system *Opt. Express* **22** 18454
- [44] Hamrle J, Ferré J, Nývlt M and Višňovský Š 2002 In-depth resolution of the magneto-optical Kerr effect in ferromagnetic multilayers *Phys. Rev. B* **66** 224423
- [45] Brozyniak A, Mendirek G, Hohage M, Navarro-Quezada A and Zeppenfeld P 2021 *In situ* electromagnet with active cooling for real-time magneto-optic Kerr effect spectroscopy *Rev. Sci. Instrum.* **92** 025105
- [46] Kim D, Oh Y-W, Kim J U, Lee S, Baucour A, Shin J, Kim K-J, Park B-G and Seo M-K 2020 Extreme anti-reflection enhanced magneto-optic Kerr effect microscopy *Nat. Commun.* **11** 5937
- [47] Loughran T H J, Keatley P S, Hendry E, Barnes W L and Hicken R J 2018 Enhancing the magneto-optical Kerr effect through the use of a plasmonic antenna *Opt. Express* **26** 4738–50
- [48] Koopmans B, Koopmans B, Santos P V, Santos P V and Cardona M 1998 Microscopic reflection difference spectroscopy on semiconductor nanostructures *Phys. Status Solidi a* **170** 307–15
- [49] Ferre J and Gehring G A 1984 Linear optical birefringence of magnetic crystals *Rep. Prog. Phys.* **47** 513–611
- [50] Višňovský Š 1986 Magneto-optical permittivity tensor in crystals *Czech. J. Phys. B* **36** 1424–33
- [51] Silber R *et al* 2019 Quadratic magneto-optic Kerr effect spectroscopy of Fe epitaxial films on MgO(001) substrates *Phys. Rev. B* **100** 064403
- [52] Sepúlveda B, Huttel Y, Martínez Boubeta C, Cebollada A and Armelles G 2003 Linear and quadratic magneto-optical Kerr effects in continuous and granular ultrathin monocrystalline Fe films *Phys. Rev. B* **68** 064401
- [53] Silber R, Král D, Stejskal O, Kubota T, Ando Y, Pištora J, Veis M, Hamrle J and Kuschel T 2020 Scaling of quadratic and linear magneto-optic Kerr effect spectra with L<sub>21</sub> ordering of Co<sub>2</sub>MnSi Heusler compound *Appl. Phys. Lett.* **116** 262401
- [54] Hamrle J, Blomeier S, Gaier O, Hillebrands B, Schneider H, Jakob G, Postava K and Felser C 2007 Huge quadratic magneto-optical Kerr effect and magnetization reversal in the Co<sub>2</sub>FeSi Heusler compound *J. Phys. D: Appl. Phys.* **40** 1563–9
- [55] Hamrle J, Ferré J, Jamet J P, Repain V, Baudot G and Rousset S 2003 Vicinal interface sensitive magneto-optical Kerr effect: application to Co/Au(322) *Phys. Rev. B* **67** 155411
- [56] Hamrlová J, Hamrle J, Postava K and Pištora J 2013 Quadratic-in-magnetization permittivity and conductivity tensor in cubic crystals *Phys. Status Solidi b* **250** 2194–205
- [57] Eremenko V V, Yu G L, Kharchenko N K and Naumenko V M 1992 *Magneto-Optics and Spectroscopy of Antiferromagnets* (Berlin: Springer)
- [58] Saidl V *et al* 2017 Optical determination of the Néel vector in a CuMnAs thin-film antiferromagnet *Nat. Photon.* **11** 91–96
- [59] Zhao H C *et al* 2021 Large ultrafast-modulated Voigt effect in noncollinear antiferromagnet Mn<sub>3</sub>Sn *Nat. Commun.* **12** 5266
- [60] Tzschaschel C, Satoh T and Fiebig M 2020 Efficient spin excitation via ultrafast damping-like torques in antiferromagnets *Nat. Commun.* **11** 6142
- [61] Stejskal O, Veis M and Hamrle J 2021 Band structure analysis of the magneto-optical effect in bcc Fe *Sci. Rep.* **11** 21026
- [62] Petukhov A V, Rasing T, Katayama T, Nakajima N and Suzuki Y 1998 Anisotropic third-order magneto-optical Kerr effect *J. Appl. Phys.* **83** 6742–4
- [63] Gaerner M, Silber R, Peters T, Hamrle J and Kuschel T 2022 Cubic magneto-optic Kerr effect in Ni(111) thin films with and without twinning (arxiv:2205.08298)
- [64] McCord J 2015 Progress in magnetic domain observation by advanced magneto-optical microscopy *J. Phys. D: Appl. Phys.* **48** 333001
- [65] Schäfer R and McCord J 2021 Magneto-optical microscopy *Magnetic Measurement Techniques for Materials Characterization* (Cham: Springer) ch Y, pp 171–229
- [66] Hubert A and Schäfer R 1998 *Magnetic Domains: The Analysis of Magnetic Microstructures* 1st edn (Berlin: Springer)
- [67] von Hofe T, Urs N O, Mozooni B, Jansen T, Kirchhof C, Bürgler D, Quandt E and McCord J 2013 Dual wavelength magneto-optical imaging of magnetic thin films *Appl. Phys. Lett.* **103** 142410
- [68] Soldatov I V and Schäfer R 2017 Selective sensitivity in Kerr microscopy *Rev. Sci. Instrum.* **88** 073701
- [69] Holländer R B, Müller C, Lohmann M, Mozooni B and McCord J 2017 Component selection in time-resolved magneto-optical wide-field imaging for the investigation of magnetic microstructures *J. Magn. Magn. Mater.* **432** 283–90
- [70] Steinbach F, Schick D, von Korff Schmising C, Yao K, Borchert M, Engel W D and Eisebitt S 2021 Wide-field magneto-optical microscope to access quantitative magnetization dynamics with femtosecond temporal and sub-micrometer spatial resolution *J. Appl. Phys.* **130** 083905
- [71] Soldatov I V and Schäfer R 2017 Advances in quantitative Kerr microscopy *Phys. Rev. B* **95** 014426
- [72] Schäfer R, Oppeneer P M, Ognev A V, Samardak A S and Soldatov I V 2021 Analyzer-free, intensity-based, wide-field magneto-optical microscopy *Appl. Phys. Rev.* **8** 031402
- [73] Higo T *et al* 2018 Large magneto-optical Kerr effect and imaging of magnetic octupole domains in an antiferromagnetic metal *Nat. Photon.* **12** 73–78
- [74] Soldatov I V, Jiang W, Te Velthuis S G E, Hoffmann A and Schäfer R 2018 Size analysis of sub-resolution objects by Kerr microscopy *Appl. Phys. Lett.* **112** 262404
- [75] Lage E, Mattheis R and McCord J 2019 Stochasticity of domain wall pinning in curved ferromagnetic nanowires



- investigated by high-resolution Kerr microscopy *J. Magn. Magn. Mater.* **487** 165273
- [76] Streubel R, Fischer P, Kronast F, Kravchuk V P, Sheka D D, Gaididei Y, Schmidt O G and Makarov D 2016 Magnetism in curved geometries *J. Phys. D: Appl. Phys.* **49** 363001
- [77] Xu J *et al* 2019 Imaging antiferromagnetic domains in nickel oxide thin films by optical birefringence effect *Phys. Rev. B* **100** 134413
- [78] Brillouin L 1922 Diffusion de la lumière et des rayons X par un corps transparent homogène (Light and x-rays scattering by a homogeneous transparent body) *Ann. Phys.* **9** 88–122
- [79] Giovannini L, Zivieri R, Gubbiotti G, Carlotti G, Pareti L and Turilli G 2001 Theory of Brillouin cross section for scattering from magnetic multilayers: second-order magneto-optic effect in Ni/Cu bilayers and trilayers *Phys. Rev. B* **63** 104405
- [80] Sandercock J R 1982 *Light Scattering in Solids III* ed M Cardona and G Güntherodt (Berlin: Springer) pp 173–206
- [81] Nembach H T, Shaw J M, Weiler M, Jué E and Silva T J 2015 Linear relation between Heisenberg exchange and interfacial Dzyaloshinskii–Moriya interaction in metal films *Nat. Phys.* **11** 825–9
- [82] Kuepferling M *et al* 2020 Measuring interfacial Dzyaloshinskii–Moriya interaction in ultra-thin films (arXiv:2009.11830)
- [83] Tacchi S, Gubbiotti G, Madami M and Carlotti G 2017 Brillouin light scattering studies of 2D magnonic crystals *J. Phys.: Condens. Matter* **29** 073001
- [84] Pirro P, Vasyuchka V I, Serga A A and Hillebrands B 2021 Advances in coherent magnonics *Nat. Rev. Mater.* **6** 1114–35
- [85] Chumak A V, Vasyuchka V I, Serga A A and Hillebrands B 2015 Magnon spintronics *Nat. Phys.* **11** 453–61
- [86] Sebastian T, Schultheiss K, Obry B, Hillebrands B and Schultheiss H 2015 Micro-focused Brillouin light scattering: imaging spin waves at the nanoscale *Front. Phys.* **3** 35
- [87] Demokritov S O, Demidov V E, Dzyapko O, Melkov G A, Serga A A, Hillebrands B and Slavin A N 2006 Bose-Einstein condensation of quasi-equilibrium magnons at room temperature under pumping *Nature* **443** 430
- [88] THATec Innovation 2022 (available at: <https://thatec-innovation.com/>) (Accessed 8 September 2022)
- [89] Jersch J, Demidov V E, Fuchs H, Rott K, Krzysieczko P, Münchenberger J, Reiss G and Demokritov S O 2010 Mapping of localized spin-wave excitations by near-field Brillouin light scattering *Appl. Phys. Lett.* **97** 152502
- [90] Maksymov I S 2015 Magneto-plasmonics and resonant interaction of light with dynamic magnetisation in metallic and all-magneto-dielectric nanostructures *Nanomaterials* **5** 577–613
- [91] Scarponi F *et al* 2017 High-performance versatile setup for simultaneous Brillouin–Raman microspectroscopy *Phys. Rev. X* **7** 031015
- [92] Kato Y K, Myers R C, Gossard A C and Awschalom D D 2004 Observation of the spin Hall effect in semiconductors *Science* **306** 1910
- [93] Stern N, Ghosh S, Xiang G, Zhu M, Samarth N and Awschalom D 2006 Current-induced polarization and the spin Hall effect at room temperature *Phys. Rev. Lett.* **97** 126603
- [94] Stamm C, Murer C, Berritta M, Feng J, Gabureac M, Oppeneer P and Gambardella P 2017 Magneto-optical detection of the spin Hall effect in Pt and W thin films *Phys. Rev. Lett.* **119** 087203
- [95] Manchon A, Železný J, Miron I, Jungwirth T, Sinova J, Thiaville A, Garello K and Gambardella P 2019 Current-induced spin-orbit torques in ferromagnetic and antiferromagnetic systems *Rev. Mod. Phys.* **91** 035004
- [96] Walser M P, Reichl C, Wegscheider W and Salis G 2012 Direct mapping of the formation of a persistent spin helix *Nat. Phys.* **8** 757
- [97] Zucchetti C *et al* 2018 Tuning spin-charge interconversion with quantum confinement in ultrathin bismuth films *Phys. Rev. B* **98** 184418
- [98] Puebla J, Auvray F, Xu M, Rana B, Albouy A, Tsai H, Kondou K, Tatara G and Otani Y 2017 Direct optical observation of spin accumulation at nonmagnetic metal/oxide interface *Appl. Phys. Lett.* **111** 092402
- [99] Crooker S A, Furis M, Lou X, Adelman C, Smith D L, Palmström C J and Crowell P A 2005 Imaging spin transport in lateral ferromagnet/semiconductor structures *Science* **309** 2191
- [100] Altmann P, Hernandez F, Ferreira G, Kohda M, Reichl C, Wegscheider W and Salis G 2016 Current-controlled spin precession of quasistationary electrons in a cubic spin orbit field *Phys. Rev. Lett.* **116** 196802
- [101] Oestreich M, Romer M, Haug R J and Hagele D 2005 Spin noise spectroscopy in GaAs *Phys. Rev. Lett.* **95** 216603
- [102] Mak K F, Xiao D and Shan J 2018 Light-valley interactions in 2D semiconductors *Nat. Photon.* **12** 451
- [103] Go D, Jo D, Kim C and Lee H-W 2018 Intrinsic spin and orbital Hall effects from orbital texture *Phys. Rev. Lett.* **121** 086602
- [104] Salis G and Moser M 2005 Faraday-rotation spectrum of electron spins in microcavity-embedded GaAs quantum wells *Phys. Rev. B* **72** 115325
- [105] Poshakinskiy A V and Tarasenko S A 2015 Spatiotemporal spin fluctuations caused by spin-orbit-coupled Brownian motion *Phys. Rev. B* **92** 045308
- [106] Salemi L, Berritta M and Oppeneer P M 2021 Quantitative comparison of electrically induced spin and orbital polarizations in heavy-metal/3d-metal bilayers *Phys. Rev. Mater.* **5** 074407
- [107] Berger A and Pufall M R 1997 Generalized magneto-optical ellipsometry *Appl. Phys. Lett.* **71** 965–7
- [108] Neuber G, Rauer R, Kunze J, Korn T, Pels C, Meier G, Merkt U, Bäckström J and Rübhausen M 2003 Temperature-dependent spectral generalized magneto-optical ellipsometry *Appl. Phys. Lett.* **83** 4509–11
- [109] Mok K, Du N and Schmidt H 2011 Vector-magneto-optical generalized ellipsometry *Rev. Sci. Instrum.* **82** 033112
- [110] Berger A and Pufall M R 1999 Quantitative vector magnetometry using generalized magnetooptical ellipsometry *J. Appl. Phys.* **85** 4583–5
- [111] Oblak E, Riego P, Garcia-Manso A, Martínez-de-Guereñu A, Arizti F, Artetxe I and Berger A 2020 Ultrasensitive transverse magneto-optical Kerr effect measurements using an effective ellipsometric detection scheme *J. Phys. D: Appl. Phys.* **53** 205001
- [112] Arregi J A, González-Díaz J B, Idigoras O and Berger A 2015 Strain induced magneto-optical anisotropy in epitaxial hcp Co-films *Phys. Rev. B* **92** 184405
- [113] Weber R, Martín Valderrama C, Fallarino L and Berger A 2020 Dependence of the magneto-optical signal on the Co layer thickness asymmetry in Co/Pt/Co films *Phys. Rev. B* **102** 214434
- [114] Martín Valderrama C, Quintana M, Martínez-de-Guereñu A, Yamauchi T, Hamada Y, Kurokawa Y, Yuasa H and Berger A 2021 Insertion layer magnetism detection and analysis using transverse magneto-optical Kerr effect (T-MOKE) ellipsometry *J. Appl. Phys.* **54** 435002
- [115] Riego P, Velez S, Gomez-Perez J M, Arregi J A, Hueso L E, Casanova F and Berger A 2016 Absence of detectable current-induced magneto-optical Kerr effects in Pt, Ta, and W *Appl. Phys. Lett.* **109** 172402



- [116] Arregi J A, Gonzalez-Diaz J B, Bergaretxe E, Idigoras O, Unsal T and Berger A 2012 Study of generalized magneto-optical ellipsometry measurement reliability *J. Appl. Phys.* **111** 103912
- [117] Visnovsky Š 1986 Magneto-optical ellipsometry *Czech. J. Phys. B* **36** 625–50
- [118] Zak J, Moog E R, Liu C and Bader S D 1991 Magneto-optics of multilayers with arbitrary magnetization directions *Phys. Rev. B* **43** 6423–9
- [119] Schubert M 1998 Generalized ellipsometry and complex optical systems *Thin Solid Films* **313–314** 323–32
- [120] You C-Y and Shin S-C 1998 Generalized analytic formulae for magneto-optical Kerr effects *J. Appl. Phys.* **84** 541–6
- [121] Kirilyuk A, Kimel A V and Rasing T 2010 Ultrafast optical manipulation of magnetic order *Rev. Mod. Phys.* **82** 2731–84
- [122] Koopmans B, van Kampen M, Kohlhepp J T and de Jonge W J M 2000 Ultrafast magneto-optics in nickel: magnetism or optics? *Phys. Rev. Lett.* **85** 844–7
- [123] Walowski J and Münzenberg M 2016 Perspective: ultrafast magnetism and THz spintronics *J. Appl. Phys.* **120** 140901
- [124] Kampfrath T *et al* 2013 Terahertz spin current pulses controlled by magnetic heterostructures *Nat. Nanotechnol.* **8** 256–60
- [125] Kimel A V, Kirilyuk A, Usachev P A, Pisarev R V, Balbashov A M and Rasing T 2005 Ultrafast non-thermal control of magnetization by instantaneous photomagnetic pulses *Nature* **435** 655–7
- [126] Berritta M, Mondal R, Carva K and Oppeneer P M 2016 *Ab initio* theory of coherent laser-induced magnetization in metals *Phys. Rev. Lett.* **117** 137203
- [127] Bigot J-Y, Vomir M and Beaurepaire E 2009 Coherent ultrafast magnetism induced by femtosecond laser pulses *Nat. Phys.* **5** 515–20
- [128] Siegrist F *et al* 2019 Light-wave dynamic control of magnetism *Nature* **571** 240–4
- [129] Meineke C *et al* 2022 Scalable high-repetition-rate sub-half-cycle terahertz pulses from spatially indirect interband transitions *Light Sci. Appl.* **11** 151
- [130] Seifert T *et al* 2016 Efficient metallic spintronic emitters of ultrabroadband terahertz radiation *Nat. Photon.* **10** 483–8
- [131] Vedmedenko E Y *et al* 2020 The 2020 magnetism roadmap *J. Phys. D: Appl. Phys.* **53** 453001
- [132] Back C *et al* 2020 The 2020 skyrmionics roadmap *J. Phys. D: Appl. Phys.* **53** 363001
- [133] van Kampen M, Jozsa C, Kohlhepp J T, LeClair P, Lagae L, de Jonge W J M and Koopmans B 2002 All-optical probe of coherent spin waves *Phys. Rev. Lett.* **88** 227201
- [134] Salikhov R *et al* 2019 Gilbert damping in NiFeGd compounds: ferromagnetic resonance versus time-resolved spectroscopy *Phys. Rev. B* **99** 104412
- [135] Razdolski I, Alekhin A, Ilin N, Meyburg J P, Roddatis V, Diesing D, Bovensiepen U and Melnikov A 2017 Nanoscale interface confinement of ultrafast spin transfer torque driving non-uniform spin dynamics *Nat. Commun.* **8** 15007
- [136] Deb M, Popova E, Zeuschner S P, Hehn M, Keller N, Mangin S, Malinowski G and Bargheer M 2021 Generation of spin waves via spin-phonon interaction in a buried dielectric thin film *Phys. Rev. B* **103** 024411
- [137] Bombeck M *et al* 2012 Excitation of spin waves in ferromagnetic (Ga,Mn)As layers by picosecond strain pulses *Phys. Rev. B* **85** 195324
- [138] Ciomei M-C, Rubi M and Wegrowe J-E 2011 Magnetization dynamics in the inertial regime: nutation predicted at short time scales *Phys. Rev. B* **83** 020410(R)
- [139] Neeraj K *et al* 2021 Inertial spin dynamics in ferromagnets *Nat. Phys.* **17** 245–51
- [140] Lomonosov A M, Temnov V V and Wegrowe J-E 2021 Anatomy of inertial magnons in ferromagnetic nanostructures *Phys. Rev. B* **104** 054425
- [141] Vlasov V S, Lomonosov A M, Golov A V, Kotov L N, Besse V, Alekhin A, Kuzmin D A, Bychkov I V and Temnov V V 2020 Magnetization switching in bistable nanomagnets by picosecond pulses of surface acoustic waves *Phys. Rev. B* **101** 024425
- [142] Besse V, Golov A V, Vlasov V S, Alekhin A, Kuzmin D, Bychkov I V, Kotov L N and Temnov V V 2020 Generation of exchange magnons in thin ferromagnetic films by ultrashort acoustic pulses *J. Magn. Magn. Mater.* **502** 166320
- [143] Kim J-W and Bigot J-Y 2017 Magnetization precession induced by picosecond acoustic pulses in a freestanding film acting as an acoustic cavity *Phys. Rev. B* **95** 144422
- [144] Huynh A, Perrin B and Lemaître A 2015 Semiconductor superlattices: a tool for terahertz acoustics *Ultrasonics* **56** 66–79
- [145] Janušonis J, Chang C L, Jansma T, Gatilova A, Vlasov V S, Lomonosov A M, Temnov V V and Tobey R I 2016 Ultrafast magnetoelastic probing of surface acoustic transients *Phys. Rev. B* **94** 024415
- [146] Chang C L, Lomonosov A M, Janušonis J, Vlasov V S, Temnov V V and Tobey R I 2017 Parametric frequency mixing in a magnetoelastically driven linear ferromagnetic-resonance oscillator *Phys. Rev. B* **95** 060409(R)
- [147] Kraimia M, Kuszewski P, Duquesne J-Y, Lemaître A, Margaillan F, Gourdon C and Thevenard L 2020 Time- and space-resolved nonlinear magnetoacoustic dynamics *Phys. Rev. B* **101** 144425
- [148] Maccaferri N *et al* 2013 Tuning the magneto-optical response of nanosize ferromagnetic Ni disks using the phase of localized plasmons *Phys. Rev. Lett.* **111** 167401
- [149] Maccaferri N, Inchausti X, García-Martín A, Cuevas J C, Tripathy D, Adeyeye A O and Vavassori P 2015 Resonant enhancement of magneto-optical activity induced by surface plasmon polariton modes coupling in 2D magnetoplasmonic crystals *ACS Photonics* **2** 1769–79
- [150] Maccaferri N, Bergamini L, Pancaldi M, Schmidt M K, Kataja M, van Dijken S, Zabala N, Aizpurua J and Vavassori P 2016 Anisotropic nanoantenna-based magnetoplasmonic crystals for highly enhanced and tunable magneto-optical activity *Nano Lett.* **16** 2533–42
- [151] Kuttruff J *et al* 2021 Magneto-optical activity in nonmagnetic hyperbolic nanoparticles *Phys. Rev. Lett.* **127** 217402
- [152] Khurgin J B 2017 Replacing noble metals with alternative materials in plasmonics and metamaterials: how good an idea? *Phil. Trans. R. Soc. A* **375** 20160068
- [153] West P R, Ishii S, Naik G V, Emami N K, Shalaev V M and Boltasseva A 2010 Searching for better plasmonic materials *Laser Photonics Rev.* **4** 795–808
- [154] Kuttruff J, Garoli D, Allerbeck J, Krahne R, de Luca A, Brida D, Caligiuri V and Maccaferri N 2020 Ultrafast all-optical switching enabled by epsilon-near-zero-tailored absorption in metal-insulator nanocavities *Commun. Phys.* **3** 114
- [155] Novikov I A, Kiryanov M A, Nurgalieva P K, Frolov A, Popov V V P, Dolgova T V and Fedyanin A A 2020 Ultrafast magneto-optics in nickel magnetoplasmonic crystals *Nano Lett.* **20** 8615–9
- [156] Mishra K, Ciuculkaite A, Zapata-Herrera M, Vavassori P, Kapaklis V, Rasing T, Dmitriev A, Kimel A and Kirilyuk A 2021 Ultrafast demagnetization in a ferrimagnet under electromagnetic field funneling *Nanoscale* **13** 19367–75
- [157] Bin-Alam M S *et al* 2021 Ultra-high-Q resonances in plasmonic metasurfaces *Nat. Commun.* **12** 974

- [158] Freire-Fernández F, Mansell R and van Dijken S 2020 Magnetoplasmonic properties of perpendicularly magnetized [Co/Pt]<sub>N</sub> nanodots *Phys. Rev. B* **101** 054416
- [159] Freire-Fernández F, Cuerda J, Daskalakis K S, Perumbilavil S, Martikainen J-P, Arjas K, Törmä P and van Dijken S 2022 Magnetic on-off switching of a plasmonic laser *Nat. Photon.* **16** 27–32
- [160] de la Torre A, Kennes D M, Claassen M, Gerber S, McIver J W and Sentef M A 2021 Colloquium: nonthermal pathways to ultrafast control in quantum materials *Rev. Mod. Phys.* **93** 041002
- [161] Bai B, Tervo J and Turunen J 2006 Polarization conversion in resonant magneto-optic gratings *New J. Phys.* **8** 205
- [162] Gamet E, Varghese B, Verrier I and Royer F 2017 Enhancement of magneto-optical effects by a single 1D all dielectric resonant grating *J. Phys. D: Appl. Phys.* **50** 495105
- [163] Voronov A A, Karki D, Ignatyeva D O, Kozhaev M A, Levy M and Belotelov V I 2020 Magneto-optics of subwavelength all-dielectric gratings *Opt. Express* **28** 17988–96
- [164] Ignatyeva D O, Karki D, Voronov A A, Kozhaev M A, Krichevsky D M, Chernov A I, Levy M and Belotelov V 2020 All-dielectric magnetic metasurface for advanced light control in dual polarizations combined with high-Q resonances *Nat. Commun.* **11** 5487
- [165] Bsawmaii L, Gamet E, Royer F, Neveu S and Jamon D 2020 Longitudinal magneto-optical effect enhancement with high transmission through a 1D all-dielectric resonant guided mode grating *Opt. Express* **28** 8436–44
- [166] Royer F, Varghese B, Gamet E, Neveu S, Jourlin Y and Jamon D 2020 Enhancement of both Faraday and Kerr effects with an all-dielectric grating based on a magneto-optical nanocomposite material *ACS Omega* **5** 2886–92
- [167] Zimnyakova P E, Ignatyeva D O, Karki D, Voronov A A, Shaposhnikov A N, Berzhansky V N, Levy M and Belotelov V I 2022 Two-dimensional array of iron-garnet nanocylinders supporting localized and lattice modes for the broadband boosted magneto-optics *Nanophotonics* **11** 119–27
- [168] Ignatyeva D O, Knyazev G A, Kalish A N, Chernov A I and Belotelov V I 2021 Vector magneto-optical magnetometer based on resonant all-dielectric gratings with highly anisotropic iron garnet films *J. Appl. Phys.* **54** 295001
- [169] Chernov A I, Kozhaev M A, Ignatyeva D O, Beginin E N, Sadovnikov A V, Voronov A A, Karki D, Levy M and Belotelov V I 2020 All-dielectric nanophotonics enables tunable excitation of the exchange spin waves *Nano Lett.* **20** 5259–66
- [170] Xia S *et al* 2022 Circular displacement current induced anomalous magneto-optical effects in high index Mie resonators *Laser Photonics Rev.* **16** 2200067
- [171] Bsawmaii L, Gamet E, Neveu S, Jamon D and Royer F 2022 Magnetic nanocomposite films with photo-patterned 1D grating on top enable giant magneto-optical intensity effects *Opt. Mater. Express* **12** 513–23
- [172] Christofi A, Kawaguchi Y, Alù A and Khanikaev A B 2018 Giant enhancement of Faraday rotation due to electromagnetically induced transparency in all-dielectric magneto-optical metasurfaces *Opt. Lett.* **43** 1838–41
- [173] Barsukova M G, Shorokhov A S, Musorin A I, Neshev D N, Kivshar Y S and Fedyanin A A 2017 Magneto-optical response enhanced by Mie resonances in nanoantennas *ACS Photonics* **4** 2390–5
- [174] Rizal C, Manera M G, Ignatyeva D O, Mejía-Salazar J R, Rella R, Belotelov V I, Pineider F and Maccaferri N 2021 Magnetophotonics for sensing and magnetometry toward industrial applications *J. Appl. Phys.* **130** 230901
- [175] Fernández-Pacheco A, Streubel R, Fruchart O, Hertel R, Fischer P and Cowburn R 2017 Three-dimensional nanomagnetism *Nat. Commun.* **8** 15756
- [176] Hertel R 2016 Ultrafast domain wall dynamics in magnetic nanotubes and nanowires *J. Phys. D: Appl. Phys.* **28** 483002
- [177] Sutcliffe P 2017 Skyrmion knots in frustrated magnets *Phys. Rev. Lett.* **118** 247203
- [178] Williams G *et al* 2018 Two-photon lithography for 3D magnetic nanostructure fabrication *Nano Res.* **11** 845
- [179] de Teresa J M, Fernández-Pacheco A, Córdoba R, Serrano-Ramón L, Sangiao S and Ibarra M R 2016 Review of magnetic nanostructures grown by focused electron beam induced deposition (FEBID) *J. Phys. D: Appl. Phys.* **49** 243003
- [180] Sheka D D 2021 A perspective on curvilinear magnetism *Appl. Phys. Lett.* **118** 230502
- [181] Sanz-Hernandez D *et al* 2020 Artificial double-helix for geometrical control of magnetic chirality *ACS Nano* **14** 8084
- [182] Parkin S, Hayashi M and Thomas L 2008 Magnetic domain-wall racetrack memory *Science* **320** 190
- [183] Donnelly C, Guizar-Sicairos M, Scagnoli V, Gliga S, Holler M, Raabe J and Heyderman L J 2017 Three-dimensional magnetization structures revealed with x-ray vector nanotomography *Nature* **547** 328
- [184] Hierro-Rodríguez A, Quirós C, Sorrentino A, Alvarez-Prado L M, Martín J I, Alameda J M, McVitie S, Pereiro E, Vélez M and Ferrer S 2020 Revealing 3D magnetization of thin films with soft x-ray tomography: magnetic singularities and topological charges *Nat. Commun.* **11** 6382
- [185] Donnelly C *et al* 2020 Time-resolved imaging of three-dimensional nanoscale magnetization dynamics *Nat. Nanotechnol.* **15** 356
- [186] Seki S, Suzuki M, Ishibashi M, Takagi R, Khanh N D, Shiota Y, Shibata K, Koshibae W, Tokura Y and Ono T 2022 Direct visualization of the three-dimensional shape of skyrmion strings in a noncentrosymmetric magnet *Nat. Mater.* **21** 181
- [187] Donnelly C, Metlov K L, Scagnoli V, Guizar-Sicairos M, Holler M, Bingham N S, Raabe J, Heyderman L J, Cooper N R and Gliga S 2021 Experimental observation of vortex rings in a bulk magnet *Nat. Phys.* **17** 316
- [188] Donnelly C *et al* 2022 Complex free-space magnetic field nanotextures induced by three-dimensional magnetic nanostructures *Nat. Nanotechnol.* **17** 136–42
- [189] Jungwirth T, Sinova J, Manchon A, Martí X, Wunderlich J and Felser C 2018 The multiple directions of antiferromagnetic spintronics *Nat. Phys.* **14** 200
- [190] Donnelly C, Gliga S, Scagnoli V, Holler M, Raabe J, Heyderman L J and Guizar-Sicairos M 2018 Tomographic reconstruction of a three-dimensional magnetization vector field *New J. Phys.* **20** 083009
- [191] Witte K *et al* 2020 From 2D STXM to 3D imaging: soft x-ray laminography of thin specimens *Nano Lett.* **20** 1305
- [192] Pellegrini C 2020 The development of XFELs *Nat. Rev. Phys.* **2** 330
- [193] Huang N, Deng H, Liu B, Wang D and Zhao Z 2021 Features and futures of x-ray free-electron lasers *Innovation* **2** 100097
- [194] Matsuda I and Kubota Y 2021 Recent progress in spectroscopies using soft x-ray free-electron lasers *Chem. Lett.* **50** 1336–44
- [195] Lovesey S W and Collins S P 1996 *X-Ray Scattering and Absorption by Magnetic Materials* (London: Oxford Press)
- [196] Mertins H-C, Valencia S, Gaupp A, Gudat W, Oppeneer P M and Schneider C M 2005 Magneto-optical polarization spectroscopy with soft x-rays *Appl. Phys. A* **80** 1011

- [197] Kubota Y *et al* 2017 Determination of the element-specific complex permittivity using a soft x-ray phase modulator *Phys. Rev. B* **96** 214417
- [198] Yamamoto K *et al* 2020 Element-selectively tracking ultrafast demagnetization process in Co/Pt multilayer thin films by the resonant magneto-optical Kerr effect *Appl. Phys. Lett.* **116** 172406
- [199] von Korff Schmising C *et al* 2020 Element-specific magnetization dynamics of complex magnetic systems probed by ultrafast magneto-optical spectroscopy *Appl. Sci.* **10** 7580
- [200] Möller C, Probst H, Otto J, Stroh K, Mahn C, Steil S, Moshnyaga V, Jansen G S M, Steil D and Mathias S 2021 Ultrafast element-resolved magneto-optics using a fiber-laser-driven extreme ultraviolet light source *Rev. Sci. Instrum.* **92** 065107
- [201] Müller L *et al* 2013 Ultrafast dynamics of magnetic domain structures probed by coherent free-electron laser light *Synchrotron Radiat. News* **26** 27
- [202] Yamamoto S *et al* 2018 Element selectivity in second-harmonic generation of GaFeO<sub>3</sub> by a soft-x-ray free-electron laser *Phys. Rev. Lett.* **120** 223902
- [203] Lam R K *et al* 2018 *Phys. Rev. Lett.* **120** 023901
- [204] Uzundal C B *et al* 2021 Polarization-resolved extreme ultraviolet second harmonic generation from LiNbO<sub>3</sub> *Phys. Rev. Lett.* **127** 237402
- [205] Yaji K *et al* 2016 High-resolution three-dimensional spin- and angle-resolved photoelectron spectrometer using vacuum ultraviolet laser light *Rev. Sci. Instrum.* **87** 053111
- [206] Fanciulli M *et al* 2020 Spin, time, and angle resolved photoemission spectroscopy on WTe<sub>2</sub> *Phys. Rev. Res.* **2** 013261
- [207] Bliokh K Y and Nori F 2015 Transverse and longitudinal angular momenta of light *Phys. Rep.* **592** 1
- [208] Forbes K A and Andrews D L 2021 Orbital angular momentum of twisted light: chirality and optical activity *J. Phys. Photon.* **3** 022007
- [209] Shen Y *et al* 2019 Optical vortices 30 years on: OAM manipulation from topological charge to multiple singularities *Light Sci. Appl.* **8** 90
- [210] van Veenendaal M and McNulty I 2007 Prediction of strong dichroism induced by x-rays carrying orbital momentum *Phys. Rev. Lett.* **98** 157401
- [211] Mathevet R, de Lesegno B V, Pruvost L and Rikken G L J A 2013 Negative experimental evidence for magneto-orbital dichroism *Opt. Express* **21** 3941
- [212] van Veenendaal M 2015 Interaction between x-ray and magnetic vortices *Phys. Rev. B* **92** 245116
- [213] Sirenko A, Marsik P, Bernhard C, Stanislavchuk T, Kiryukhin V and Cheong S-W 2019 Terahertz vortex beam as a spectroscopic probe of magnetic excitations *Phys. Rev. Lett.* **122** 237401
- [214] Sirenko A, Marsik P, Bugnon L, Soulier M, Bernhard C, Stanislavchuk T, Xu X and Cheong S-W 2021 Total angular momentum dichroism of the terahertz vortex beams at the antiferromagnetic resonances *Phys. Rev. Lett.* **126** 157401
- [215] Woods J S *et al* 2021 Switchable x-ray orbital angular momentum from an artificial spin ice *Phys. Rev. Lett.* **126** 117201
- [216] Fanciulli M, Bresteau D, Vimal M, Luttmann M, Sacchi M and Ruchon T 2021 Electromagnetic theory of helicoidal dichroism in reflection from magnetic structures *Phys. Rev. A* **103** 013501
- [217] Fanciulli M *et al* 2022 Observation of magnetic helicoidal dichroism with extreme ultraviolet light vortices *Phys. Rev. Lett.* **128** 077401
- [218] Généaux R, Camper A, Auguste T, Gobert O, Caillat J, Taïeb R and Ruchon T 2016 Synthesis and characterization of attosecond light vortices in the extreme ultraviolet *Nat. Commun.* **7** 12583
- [219] Ribič P R *et al* 2017 Extreme-ultraviolet vortices from a free-electron laser *Phys. Rev. X* **7** 031036
- [220] Degen C L, Reinhard F and Cappellaro P 2017 Quantum sensing *Rev. Mod. Phys.* **89** 035002
- [221] Gross I *et al* 2017 Real-space imaging of non-collinear antiferromagnetic order with a single-spin magnetometer *Nature* **549** 252–6
- [222] McCullian B A, Thabt A M, Gray B A, Melendez A L, Wolf M S, Safonov V L, Pelekhov D V, Bhallamudi V P, Page M R and Hammel P C 2020 Broadband multi-magnon relaxometry using a quantum spin sensor for high frequency ferromagnetic dynamics sensing *Nat. Commun.* **11** 5229
- [223] Du C *et al* 2017 Control and local measurement of the spin chemical potential in a magnetic insulator *Science* **357** 195–8
- [224] Wang H *et al* 2022 Noninvasive measurements of spin transport properties of an antiferromagnetic insulator *Sci. Adv.* **8** 8562
- [225] Scholten S C, Healey A J, Robertson I O, Abrahams G J, Broadway D A and Tetienne J-P 2021 Widefield quantum microscopy with nitrogen-vacancy centers in diamond: strengths, limitations, and prospects *J. Appl. Phys.* **130** 150902
- [226] Maletinsky P, Hong S, Grinolds M S, Hausmann B, Lukin M D, Walsworth R L, Loncar M and Yacoby A 2012 A robust scanning diamond sensor for nanoscale imaging with single nitrogen-vacancy centres *Nat. Nanotechnol.* **7** 320–4
- [227] Pelliccione M, Jenkins A, Ovarthaiyapong P, Reetz C, Emmanouilidou E, Ni N and Bleszynski Jayich A C 2016 Scanned probe imaging of nanoscale magnetism at cryogenic temperatures with a single-spin quantum sensor *Nat. Nanotechnol.* **11** 700–5
- [228] Dolde F, Jakobi I, Naydenov B, Zhao N, Pezzagna S, Trautmann C, Meijer J, Neumann P, Jelezko F and Wrachtrup J 2013 Room-temperature entanglement between single defect spins in diamond *Nat. Phys.* **9** 139–43
- [229] Awschalom D D, Hanson R, Wrachtrup J and Zhou B B 2018 Quantum technologies with optically interfaced solid-state spins *Nat. Photon.* **12** 516–27
- [230] Awschalom D D *et al* 2021 Quantum engineering with hybrid magnonic systems and materials (invited paper) *IEEE Trans. Quantum Eng.* **2** 1–36
- [231] Huang M *et al* 2021 Wide field imaging of van der Waals ferromagnet Fe<sub>3</sub>GeTe<sub>2</sub> by spin defects in hexagonal boron nitride (arXiv:2112.13570)
- [232] Healey A J *et al* 2021 Quantum microscopy with van der Waals heterostructures (arXiv:2112.03488)
- [233] Stepanov V, Cho F H, Abeywardana C and Takahashi S 2015 High-frequency and high-field optically detected magnetic resonance of nitrogen-vacancy centers in diamond *Appl. Phys. Lett.* **106** 063111
- [234] MacQuarrie E R, Otten M, Gray S K and Fuchs G D 2017 Cooling a mechanical resonator with nitrogen-vacancy centres using a room temperature excited state spin-strain interaction *Nat. Commun.* **8** 14358
- [235] Armitage N P 2014 Constraints on Jones transmission matrices from time-reversal invariance and discrete spatial symmetries *Phys. Rev. B* **90** 035135
- [236] Morris C M, Valdés Aguilar R, Stier A V and Peter Armitage N 2012 Polarization modulation time-domain terahertz polarimetry *Opt. Express* **20** 12303–17
- [237] Cheng B, Taylor P, Folkes P, Rong C and Armitage N P 2019 Magnetoterahertz response and faraday rotation from massive Dirac fermions in the topological



- crystalline insulator  $\text{Pb}_{0.5}\text{Sn}_{0.5}\text{Te}$  *Phys. Rev. Lett.* **122** 097401
- [238] Cheng B, Schumann T, Wang Y, Zhang X, Barbalas D, Stemmer S and Peter Armitage N 2020 A large effective phonon magnetic moment in a Dirac semimetal *Nano Lett.* **20** 5991–6
- [239] Noe G T, Zhang Q, Lee J, Kato E, Woods G L, Nojiri H and Kono J 2014 Rapid scanning terahertz time-domain magnetospectroscopy with a table-top repetitive pulsed magnet *Appl. Opt.* **53** 5850–5
- [240] Dietz R, Vieweg N, Puppe T, Zach A, Globisch B, Göbel T, Leisching P and Schell M 2014 All fiber-coupled THz-TDS system with kHz measurement rate based on electronically controlled optical sampling *Opt. Lett.* **39** 6482–5
- [241] Post K W *et al* 2021 Observation of cyclotron resonance and measurement of the hole mass in optimally doped  $\text{La}_{2-x}\text{Sr}_x\text{CuO}_4$  *Phys. Rev. B* **103** 134515
- [242] Laurita N J, Luo Y, hu R, Wu M, Cheong S-W, Tchernyshyov O and Armitage N P 2017 Asymmetric splitting of an antiferromagnetic resonance via quartic exchange interactions in multiferroic hexagonal  $\text{HoMnO}_3$  *Phys. Rev. Lett.* **119** 227601
- [243] Legros A, Zhang S-S, Bai X, Zhang H, Dun Z, Adam Phelan W, Batista C D, Mourigal M and Armitage N P 2021 Observation of 4- and 6-magnon bound-states in the spin-anisotropic frustrated antiferromagnet  $\text{FeI}_2$  *Phys. Rev. Lett.* **127** 267201
- [244] Tagay Z and Armitage N P 2022 *Opt. Express* submitted
- [245] Xia J, Maeno Y, Beyersdorf P T, Fejer M M and Kapitulnik A 2006 High resolution polar Kerr effect measurements of  $\text{Sr}_2\text{RuO}_4$ : evidence for broken time-reversal symmetry in the superconducting state *Phys. Rev. Lett.* **97** 167002
- [246] Xia J *et al* 2008 Polar Kerr-effect measurements of the high-temperature  $\text{YBaCu}_3\text{O}_{6+x}$  superconductor: evidence for broken symmetry near the pseudogap temperature *Phys. Rev. Lett.* **100** 127002
- [247] Zavoisky E 1945 Spin-magnetic resonance in paramagnetics *Fiz. Zh.* **9** 211
- [248] Neugebauer P *et al* 2018 Ultra-broadband EPR spectroscopy in field and frequency domains *Phys. Chem. Chem. Phys.* **20** 15528–34
- [249] Mueller H 1943 Memorandum on the polarization optics of the photoelastic shutter *Report of the OSRD Project OEMsr-576 2* (Massachusetts Institute of Technology)
- [250] Fujiwara H 2007 *Spectroscopic Ellipsometry* (New York: Wiley)
- [251] Schubert M, Hofmann T and Herzinger C M 2003 Generalized far-infrared magneto-optic ellipsometry for semiconductor layer structures: determination of free-carrier effective mass, mobility and concentration parameters in n-type GaAs *J. Opt. Soc. Am. A* **20** 347–56
- [252] Ino Y, Shimano R, Svirko Y and Kuwata-Gonokami M 2004 Terahertz time domain magneto-optical ellipsometry in reflection geometry *Phys. Rev. B* **8** 155101
- [253] Ohmichi E, Fujimoto T, Minato K and Ohta H 2020 Terahertz electron paramagnetic resonance spectroscopy using continuous-wave frequency-tunable photomixers based on photoconductive antennae *Appl. Phys. Lett.* **116** 051101
- [254] Kozuki K, Nagashima T and Hangyo M 2011 Measurement of electron paramagnetic resonance using terahertz time-domain spectroscopy *Opt. Express* **19** 24950–6
- [255] Sojka A, Sedivy M, Laguta O, Marko A, Santana V T and Neugebauer P 2021 High-frequency EPR: current state and perspectives *Electron Paramagnetic Resonance* vol 27 (London: The Royal Society of Chemistry) pp 214–52
- [256] Poole C P 1983 *Electron Spin Resonance: A Comprehensive Treatise on Experimental Techniques* (New York: Wiley)
- [257] Kühne P, Herzinger C M, Schubert M, Woollam J A and Hofmann T 2014 An integrated mid-infrared, far-infrared and terahertz optical Hall effect instrument *Rev. Sci. Instrum.* **2014** 071301
- [258] Kühne P, Armakavicius N, Stanishev V, Herzinger M, Schubert M and Darakchieva V 2018 Advanced terahertz frequency-domain ellipsometry instrumentation for *in situ* and *ex situ* applications *IEEE Trans. Terahertz Sci. Technol.* **8** 257
- [259] Schubert M *et al* 2022 Terahertz electron paramagnetic resonance generalized spectroscopic ellipsometry: the magnetic response of the nitrogen defect in 4H-SiC *Appl. Phys. Lett.* **120** 102101
- [260] Greulich-Weber S 1997 EPR and ENDOR investigations of shallow impurities in SiC polytypes *Phys. Status Solidi a* **162** 95
- [261] Lan T, Ding B and Liu B 2020 Magneto-optic effect of two-dimensional materials and related applications *Nano Select* **1** 298–310
- [262] Ding B, Kuang W, Pan Y, Grigorieva I V, Geim A K, Liu B and Cheng H-M 2020 Giant magneto-birefringence effect and tuneable colouration of 2D crystal suspensions *Nat. Commun.* **11** 3725
- [263] Blachnik N, Kneppel H and Schneider F 2000 Cotton–Mouton constants and pretransitional phenomena in the isotropic phase of liquid crystals *Liq. Cryst.* **27** 1219–27
- [264] Chaves A *et al* 2020 Bandgap engineering of two-dimensional semiconductor materials *npj 2D Mater. Appl.* **4** 29
- [265] Huang Z *et al* 2022 2D functional minerals as sustainable materials for magneto-optics *Adv. Mater.* **34** 2110464
- [266] Zhang C, Tan J Y, Pan Y, Cai X, Zou X, Cheng H-M and Liu B L 2020 Mass production of two-dimensional materials by intermediate-assisted grinding exfoliation *Nat. Sci. Rev.* **7** 324–32
- [267] Zhang C, Luo Y T, Tan J Y, Yu Q M, Yang F N, Zhang Z Y, Yang L S, Cheng H-M and Liu B L 2020 High-throughput production of cheap mineral-based two-dimensional electrocatalysts for high-current-density hydrogen evolution *Nat. Commun.* **11** 3724
- [268] Yang L S *et al* 2021 Glue-assisted grinding exfoliation of large-size 2D materials for insulating thermal conduction and large-current-density hydrogen evolution *Mater. Today* **51** 145–54
- [269] Shuai M *et al* 2016 Spontaneous liquid crystal and ferromagnetic ordering of colloidal magnetic nanoplates *Nat. Commun.* **7** 10394
- [270] Wang M, He L, Zorba S and Yin Y 2014 Magnetically actuated liquid crystals *Nano Lett.* **14** 3966–71
- [271] Mertelj A, Lisjak D, Drofenik M and Čopič M 2013 Ferromagnetism in suspensions of magnetic platelets in liquid crystal *Nature* **504** 237
- [272] Ding B, Pan Y, Zhang Z, Lan T, Huang Z, Lu B, Liu B and Cheng H-M 2021 Largely tunable magneto-coloration of monolayer 2D materials via size tailoring *ACS Nano* **15** 9445–52
- [273] Zhang S, Pelligra C I, Keskar G, Majewski P W, Ren F, Pfefferle L D and Osuji C O 2011 Liquid crystalline order and magnetocrystalline anisotropy in magnetically doped semiconducting ZnO nanowires *ACS Nano* **5** 8357–64
- [274] Lan T, Ding B, Huang Z, Bian F, Pan Y, Cheng H-M and Liu B 2021 Collective behavior induced highly sensitive magneto-optic effect in 2D inorganic liquid crystals *J. Am. Chem. Soc.* **143** 12886–93
- [275] Burch K S, Mandrus D and Park J-G 2018 Magnetism in two-dimensional van der Waals materials *Nature* **563** 47–52